Faculté des Bioingénieurs

Extraction and purification of volatile fatty acids

Présenté par Alexis Struyf

Promoteur(s) : Prof. Patrick Gerin (UCL/ELI/ELIM)
Guillaume Castel (UCL/ELI/ELIM)

Lecteurs : Prof. Iwona Cybulska (UCL/ELI/ELIM)
Prof. Nicolas Velings (CERISIC)

Mémoire de fin d'études présenté en vue de l'obtention
du diplôme de **Bioingénieur : chimie et bio-industries**

Année académique 2017-2018

Acknowledgment

I would like to thank the Pr. Patrick Gerin, co-promotor of thesis, for the continuous support given during the entire year, for the numerous corrections and revisions that were realized, and for all the advices and all the time invested to help to achieve this work.

I would also like to express all my gratitude to Guillaume Castel, co-promotor and supervisor, for his encouragements, motivation, help and support given from the beginning to the end of the year. Guillaume was initially working on the extraction of VFAs and has integrated me in the project, investing also a lot of time and energy for me.

I also express all my gratitude for all the GEBI members, and especially the ones that have contributed to the good realization of experiments. Thomas Nicolay, Hélène Dailly, and Matthieu Leclercq were always there when I was confronted to a problem and needed their help.

To Iwona Cybulska and Nicolas Velings, thank you for accepting to read this document and take part of the jury, I sincerely hope that reading it will be interesting and rewarding.

Last but not least, I am very grateful to all my friends and family that have showed interest for my thesis and that have given me motivation to realize a work of quality, specially Aurélie and Antoine.

Thank you all,

Alexis

Table of contents

Abbreviation list

AAB	Acetic acid bacteria
AD	Anaerobic digestion
DVB	Divinylbenzene
HAc	Acetic acid
HBu	Butyric acid
HX	Mineral acid
ILs	Ionic liquids
LA	Lactic acid
LAB	Lactic acid bacteria
MS	Model solution
PLA	Polylactic acid
Q^+	Quaternary ammonium
R	Resin
S	Styrene
TPA	Terephthalic acid
VFA	Volatile fatty acid
WLP	Wood–Ljungdahl pathway

List of tables

List of figures

1. Introduction

Because of the rising concerns on the reduction of easily recoverable petroleum resources over the next decades and the increasing awareness of the need for more sustainable processes in industry, significant attention is now given in both academia and industry for the production of bio-based chemicals (Reyhanitash and al., 2015). Important progress has already been made to obtain carboxylic acids from other sources than petrochemistry, but there are still some major limits of cost and purity of the final products (Murali et al., 2017).

Lignocellulosic biomass derived from agriculture and forestry, such as agro-industrial residues, forest-industrial residues, energy crops, or municipal solid waste, is the most abundant bioresource to consider as feedstock for biorefineries (Volynets et al., 2017). In general, complex biomass contains polysaccharides, proteins, lipids and aromatic components. Major components of lignocellulosic biomass are cellulose, hemicellulose, and lignin. The percentage of these components differs considering the source but is usually 33 - 55% cellulose with 13 - 33% hemicellulose and 13 - 32% lignin by dry weight. This lignocellulosic biomass can be broken down into smaller molecules and some of them can have high values.

Several routes have been developed for the conversion of lignocellulosic biomass to valuable chemicals, such as thermochemical and biochemical processes (Murali et al., 2017). With the last route, that relies on enzymes and microorganisms, it is possible to obtain a large variety of products with more specificity and less costs. If fermentation of sugars into alcohols like ethanol or butanol is already well known, fermentation of complex biomass into volatile fatty acids is still a novel stage of research, and a lot of importance is given to the recovery of the products with an environmental-friendly, sustainable and economically viable technology.

Separation of volatile fatty acids (VFAs) from fermented broths is challenging, due to low VFA concentrations in ion-rich solutions (Reyhanitash et al., 2017). Consequently, separation capacity and selectivity with traditional solvents and adsorbents are both compromised. Adsorption enables the separation of substances from dilute and complex solutions, so adsorption processes are retaining a lot of attention. After performing adsorption, the target compounds have to be desorbed from the adsorbent to complete the recovery process and regenerate the adsorbent. One of the possible ways of recovering the volatile fatty acids produced during fermentation with an adsorption and desorption cycle is by using ion exchange resins (Rebecchi et al., 2016).

The challenge of this thesis is to contribute to the development a new approach for an ion exchange process that enables the recovery of a concentrated and purified solution of volatile fatty acids from a fermentation broth with the difficulty of keeping a

low economical cost and an environment-friendly technology. Since the two predominant VFA species in the fermentation broths are acetic and butyric acid, the approach focused on these two species and most of the information from the state of art also relies on these two carboxylic acids.

2. State of the art

2.1 Volatile fatty acids: an overview

Carboxylic acids are a group of aliphatic mono- and di-carboxylic acids that include organic acids such as formic, acetic, propionic, butyric, valeric, caproic, lactic, succinic, fumaric, citric, gluconic, ascorbic, etc (Murali et al., 2017). Carboxylic acids are conventionally produced from fossil oil and have significant applications in the chemical, pharmaceutical, food, and fuel industries. Interestingly, some carboxylic acids have already met the biochemical production at industrial scale, while others are still in the research status, as indicated in Table 2-1.

Table 2-1: Carboxylic acids of commercial interest obtained by fermentation or biotransformation of renewable resources (López-Garzón and Straathof, 2014).

Molecular formula	Carboxylic acid	Status biochemical production	Main application
$C_2H_4O_2$	Acetic	Industrial	Vinegar
$C_3H_4O_2$	Acrylic	Research	Polymers
$C_3H_6O_2$	Pyruvic	Research	Chemicals
$C_3H_6O_2$	Propionic	Design stage	Chemicals
$C_3H_6O_3$	D/L-Lactic	Industrial	Food, polymers
$C_3H_6O_3$	3-Hydroxy-propionic	Research	Polymers
$C_4H_4O_4$	Fumaric	Formerly industrial	Food, polymers
$C_4H_6O_4$	Succinic	Industrial	Polymers, chemicals
$C_4H_6O_5$	L-Malic	Research	Chemicals
$C_4H_8O_2$	Butyric	Design stage	Chemicals
$C_5H_6O_4$	Itaconic	Industrial	Polymers
$C_5H_8O_4$	Glutaric	Research	Polymers
$C_6H_4O_5$	2,5-Furan-dicarboxylic	Research	Polymers
$C_6H_8O_7$	Citric	Industrial	Food
$C_6H_{10}O_4$	Adipic	Design stage	Polymers
$C_6H_{10}O_7$	2-Keto-L-gulonic	Industrial	Vitamin C precursor
$C_6H_{12}O_7$	D-Gluconic	Industrial	Food

Volatile fatty acids (referred as “VFAs” in this thesis) are the mono-carboxylic acids that have between 1 and 6 carbons, they have relatively high volatility compared to the other carboxylic acids (Bhatia and Yang, 2017). The main VFAs include acetic acid, propionic acid, butyric acid, isobutyric acid and isovaleric acid. The commercial production of VFAs strongly relies on chemical synthesis that uses non-renewable petroleum as source material, but these petroleum-based pathways are not sustainable.

As an alternative, VFAs can be produced via microbial fermentation starting from a large diversity of carbon sources as raw material (Bhatia and Yang, 2017). During the last decades, researchers have studied different processes to produce VFAs through microbial fermentation. The easiest approaches are based on the use of pure sugars like glucose or xylose that enable higher productivity and minimum side products, but there are also disadvantages such as a higher cost for the raw materials. In contrast,

lignocellulosic biomass is a highly abundant and available carbon source that can also be fermented to VFAs, by adding a step of pretreatment of the complex biomass.

Nevertheless, the focus of this thesis will be primarily on two of the short-chain carboxylic acids, acetic and butyric acid, which are predominantly produced as reaction intermediates in the microbial conversion of sugars. Other predominant carboxylic acids produced during microbial conversion are propionic acid and lactic acid (Murali et al., 2017).

2.2 Acetic and butyric acid

2.1.1 Physico-chemical properties

Acetic acid ($C_2H_4O_2$, Figure 2-1A) or ethanoic acid is a colorless and volatile liquid at ambient temperature (Burdock, 1997). Its solubility in water is unlimited, and its dissociation constant at 25 °C is 1.845×10^{-5} mole/liter (Zeitsch, 2000).

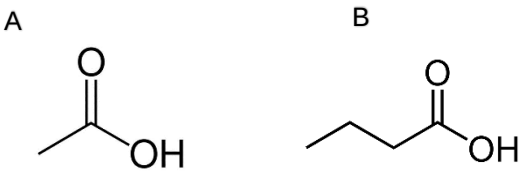

Figure 2-1 : (A) Molecule of acetic acid (Anonymous, 2017) and (B) butyric acid (Jang et al., 2014)

Butyric acid ($C_4H_8O_2$, Figure 2-1B) is a saturated four-carbon carboxylic acid, a colorless liquid soluble in water, ethanol and ether (Burdock, 1997). The general physico-chemical of the two VFAs can be found in Table 2-2.

Table 2-2: Physico-chemical properties of acetic and butyric acid

Molecule	Molecular weight [g/mol][(a)]	Specific density[(a)]	Melting point [°C][(b)]	Boiling point at 1 atm [°C][(b)]	pk_a value[(b)]
Acetic acid	60.05	1.049	17	118	4.75
Butyric acid	88.10	0.960	-8	163	4.81

[(a)](Burdock, 1997)

[(b)](López-Garzón and Straathof, 2014)

2.1.2 Chemical routes of production

<u>Acetic acid</u>

The most widely accepted route for the chemical synthesis of acetic acid is the methanol carbonylation called Monsanto process as it covers 65 % of global acetic acid manufacturing processes (Ehsanipour et al., 2016). In the presence of a rhodium iodide-based catalyst, methanol reacts with carbon monoxide to produce acetic acid

in the temperature and pressure ranges of 150- 200°C and 30-50 bar, respectively (Pal and Nayak, 2017). Acetaldehyde oxidation is another process of acetic acid production where acetaldehyde derived from petroleum is oxidized to acetic acid in the presence of a metal catalysts like cobalt or chromium, at 150°C and 55 bar. Acetic acid production routes can also start from other petroleum-derived stocks such as butane or ethylene. A scheme of the different pathways is illustrated in Figure 2-2.

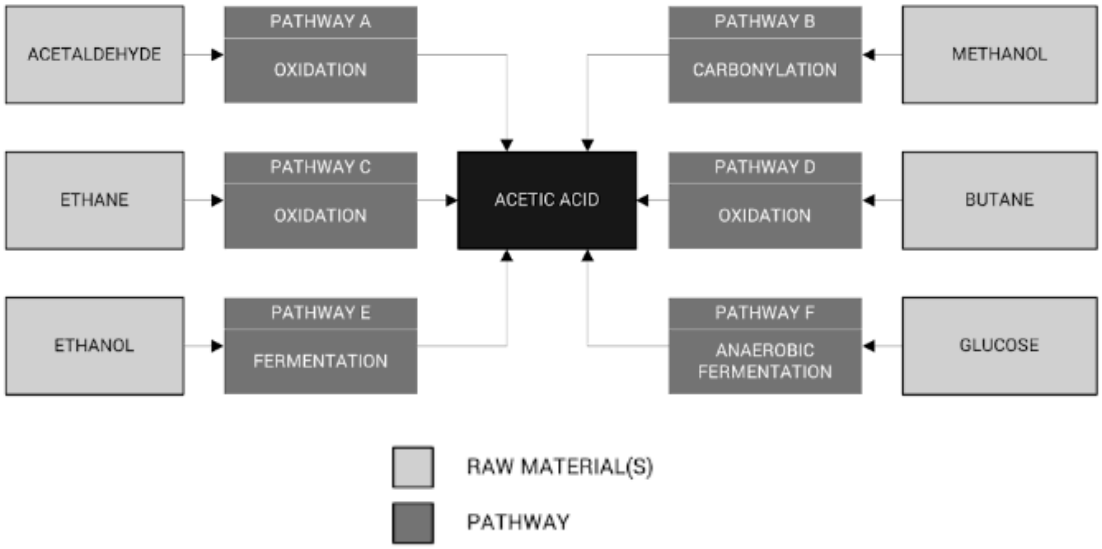

Figure 2-2 : Main acetic acid production pathways (Anonymous, 2017).

Butyric acid

Butyric acid is produced through the oxidation of butyraldehyde, obtained from propylene which is derived from crude oil (Dwidar et al., 2012). For the moment, the chemical production of butyric acid is preferred mainly because of its lower production cost and the availability of the starting materials. Nevertheless, biological routes are gaining in importance because there is a growing demand for organic and natural products, and the price of crude oil needed for chemical synthesis tends to increase with time (Jha et al., 2014).

2.1.3 Biological routes of production

Acetic acid

Aerobic pathway - Ethanol oxidation

The aerobic pathway is used by acetic acid bacteria (AAB), well known for their ability to oxidize ethanol as substrate to acetic acid in neutral and acidic media (Vidra and Németh, 2017). This pathway makes them important to the vinegar industry, since it has been estimated that 10% of the world acetic acid production is manufactured by bacterial fermentation for making vinegar. Acetic acid has been produced from ethanol

as vinegar since ancient times by the oxidation of wine and beer. In the specific case of vinegar production used in food industry, the VFA does not have to be recovered from the fermentation broth (López-Garzón and Straathof, 2014). Starting from simple sugars, there is thus a two-stage fermentation process to produce vinegar, consisting in alcoholic and acetic fermentation. Alcoholic fermentation is carried out under anaerobic conditions and proceeds rapidly, usually depleting most sugars within the first 3 weeks. Fermentable sugars are converted into ethanol by the action of yeasts (Reaction 2-1), normally strains of *Saccharomyces cerevisiae* (Vidra and Németh, 2017):

$C_6H_{12}O_6 \rightarrow 2CO_2 + 2CH_3CH_2OH$ Reaction 2-1

In the acetic fermentation that follows, the AAB can further oxidize ethanol into acetic acid (Figure 2-3). The second fermentation is carried out under aerobic conditions, as mentioned in Reaction 2-2. Ethanol is oxidized to acetaldehyde by alcohol dehydrogenase and then aldehyde dehydrogenase oxidizes it to acetic acid (Vidra and Németh, 2017):

$2\ CH_3CH_2OH + O_2 \rightarrow 2\ CH_3COOH + 2\ H_2O$ Reaction 2-2

The overall theoretical yield is 0.67 gram of acetic acid per gram glucose. Complete aeration and strict control of the oxygen concentration during fermentation are important to maximize yields and keep the bacteria viable (Cheryan et al., 1997). Some important organisms used for this process are aerobic bacteria belonging to genera such as *Acetobacter* and *Gluconacetobacter* (Baumann and Westermann, 2016). AAB are able to produce very high concentrations of acetic acid, some strains can easily produce more than 50 and up to 150 g/L of acetic acid, corresponding to 0.83M and 2.49M respectively (Raspor and Goranovič, 2008).

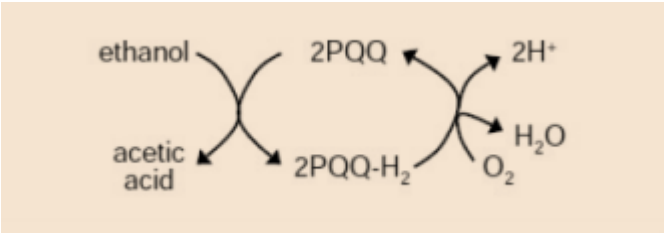

Figure 2-3 : The formation of acetic acid from ethanol by AAB. PQQ: pyrroloquinoline (Vidra and Németh, 2017).

Anaerobic pathway

During the 1980s, an alternative for biological production of acetic acid emerged with anaerobic fermentation using *Clostridia* (Murali et al., 2017). The group of acetogens produce the acid from organic matter, with the main mechanism of synthesis called the Wood–Ljungdahl pathway (WLP). During homoacetogenesis, acetate is the only

fermentation product. Most of the bacteria's known today to be homoacetogens belong to the genera *Clostridium* (*C. aceticum, C. thermoaceticum, C. formicoaceticum)* and *Acetobacterium*. Some of these organisms can convert glucose and xylose, as well as some other hexoses and pentoses, almost quantitatively to acetic acid (Cheryan et al., 1997):

$C_6H_{12}O_6 \rightarrow 3\ CH_3COOH$ Reaction 2-3

$2\ C_5H_{10}O_5 \rightarrow 5\ CH_3COOH$ Reaction 2-4

Homoacetate fermentation provides the highest known ATP gain for glucose fermentations of more than 4.3 ATP/mol glucose in the case of *Acetobacterium woodii,* as shown in Figure 2-4 (Schuchmann and Müller, 2016). One mole of glucose is oxidized in 2 moles of pyruvate, generating ATP. Pyruvate is then decarboxylated in CO_2 and acetyl-CoA, further converted in acetate:

$C_6H_{12}O_6 + 4\ ADP + 4\ Pi \rightarrow 2\ CH_3COOH + 2\ CO_2 + 4\ ATP + 2\ H_2O + 8\ [H]$

The high ATP yield reached is only possible because the redox balance is maintained by subsequent reduction of released CO_2 to a third mole of acetate by the WLP according to (Schuchmann and Müller, 2016):

$2\ CO_2 + 8\ [H] \rightarrow CH_3COOH + 2\ H_2O$ Reaction 2-5

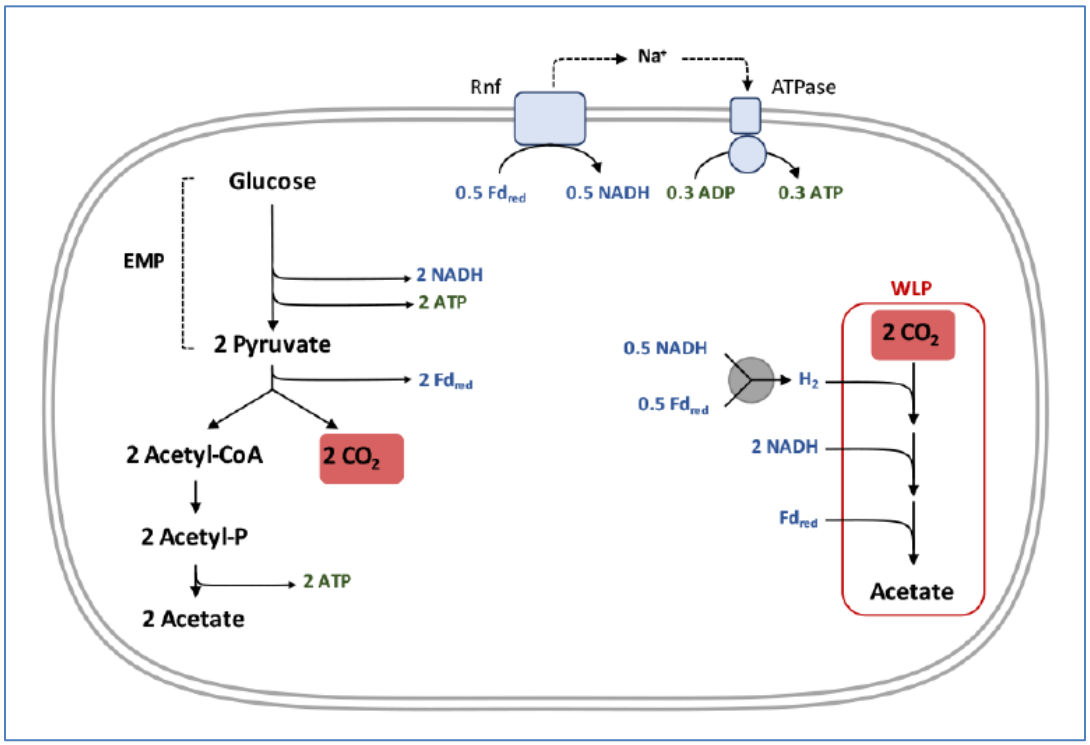

Figure 2-4: Carbohydrate metabolism of A. woodii. Fd_{red}: ferredoxin reduced by 2 electrons (Schuchmann and Müller, 2016).

This reaction allows the complete oxidation of one mole of glucose to three moles of acetate (Schuchmann and Müller, 2016). Otherwise, the redox balance must be maintained by reduction of other molecules such as pyruvate to ethanol or lactate which is not coupled to ATP synthesis. Coupling this reaction to the synthesis of even more ATP leads to a very energy-efficient fermentation.

Butyric acid

Although the chemical synthesis is dominant regarding commercial production, butyric acid from biological origin is preferred by consumers for further uses in foodstuff additives and pharmaceutical products (Jha et al., 2014). A large part of the bacterial strains which are able to produce butyric acid can be found in wastewater, excess sludge, soil, contaminated dairy and food products, meat, and animal digestive systems. Some common strains used in industry are *C. tyrobutyricum*, *C. acetobutylicum*, and *C. thermobutyricum*. Concentrations of 62,8 g/L could be reached experimentally with the strain *C. tyrobutyricum* CIP 1–776 in a fedbatch reactor with glucose as sugar source (Dwidar et al., 2012). Butyric acid production starts with the metabolism of glucose to pyruvate through the Embden–Mayerhof–Parnas (EMP) pathway followed by conversion to acetyl-CoA and then to acetoacetyl-CoA through a thiolase reaction (Zhu and Yang, 2004). The butyryl CoA produced from acetoacetyl-CoA is then converted to butyryl phosphate by phosphotransbutyrylase and then converted to butyrate by butyrate kinase. A simplified view of the pathway is illustrated in Figure 2-5. Around 3.3 ATP/mole glucose are generated during butyric acid fermentation as carried out by strictly anaerobic clostridia such as *C. pasteurianum* leading to end products acetate, butyrate, CO_2 and H_2 (Schuchmann and Müller, 2016).

The mentioned clostridial strains that can produce butyric acid usually do not possess cellulolytic enzymes and have a lesser ability to use cellulose as substrate (Murali et al., 2017). For that reason, cellulosic substrates need a pretreatment and enzymatic hydrolysis to split biomass into simple sugars for butyric acid production. Butyric acid can be derivatized in a bio-fuel with high potential but its production through fermentation of biomass has been regarded as very complex and hard to control (Jha et al., 2014). The fermentation process is limited by some constraints: the strains used are confronted to self-inhibitory effect of end products and produce other acids that are very hard to separate.

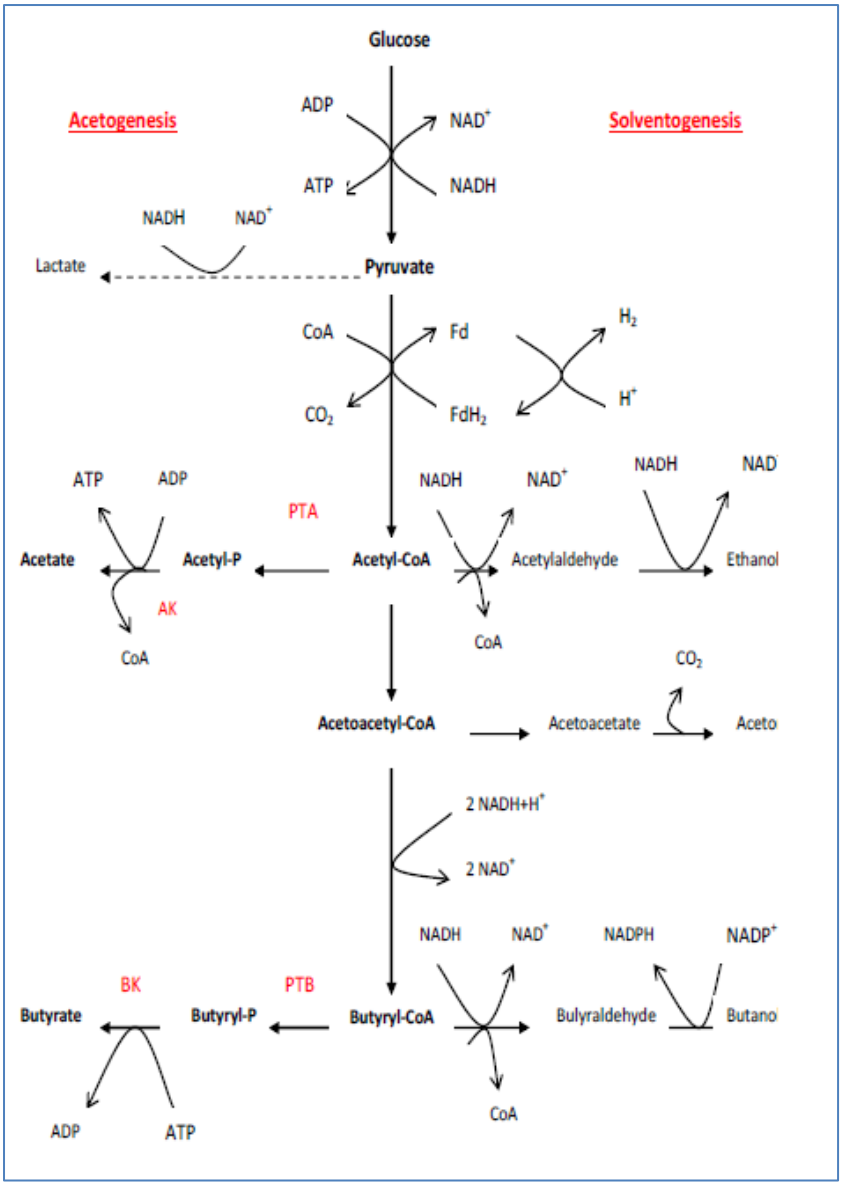

Figure 2-5 : Pathways for butyrate and acetate fermentation. Stoichiometry is not indicated (Jha et al., 2014).

In all cases, using pure strains to produce carboxylic acids usually allows a good knowledge and control of the biochemical pathways implicated in the production and easy genetic engineering (Murali et al., 2017). But there is a risk of contamination during the culture, which implies formation of not desired products. It must also be kept in mind that starting with complex substrates for carboxylic acid production, there can be molecules like aromatic or phenolic compounds that inhibit some microbial strains.

Mixed VFA production from cost-effective carbon sources

Compared with pure culture-based industrial biotechnology, mixed microbial biotechnology does not require sterilization, has a high adaptive capacity, can use

mixed substrates thanks to microbial diversity and it is possible to operate it as a continuous process (Coma et al., 2017).

Anaerobic digestion (AD) is a sequential biochemical process in which the complex organic components present in organic compounds, such as polysaccharides, proteins, and lipids, are hydrolyzed, broken down, and fermented into intermediate products that are later oxido-reduced into methane and carbon dioxide (Silva et al., 2013). AD is a process with three steps: hydrolysis, acidogenesis and methanogenesis, the two last steps being fermentative pathways. While the acidogenesis leads to the production of intermediate products, mostly VFAs, the following methanogenesis results in the consumption of these intermediates into stable gaseous end products, mainly methane and carbon dioxide.

The intermediate metabolites such as volatile fatty acids (Figure 2-6) can be valuable and compete economically with the methane and carbon dioxide end-products (Silva et al., 2013). The wide range of organic acids and other molecules that can be obtained during an anaerobic digestion will depend on the raw material composition and operational conditions, which will control the equilibrium between different organisms and determine the final microbial community. It is important to note that in all microbial fermentations where organic carbon is both the electron donor and acceptor for the redox reactions, methane presents the lowest Gibbs energy change and thus it is the homogeneous end-product generated irrespective of the substrate (Coma et al., 2017). Consequently, to avoid methane production and enhance carboxylic acid accumulation in mixed microbial technology, methane production must be inhibited by working at suboptimal AD conditions.

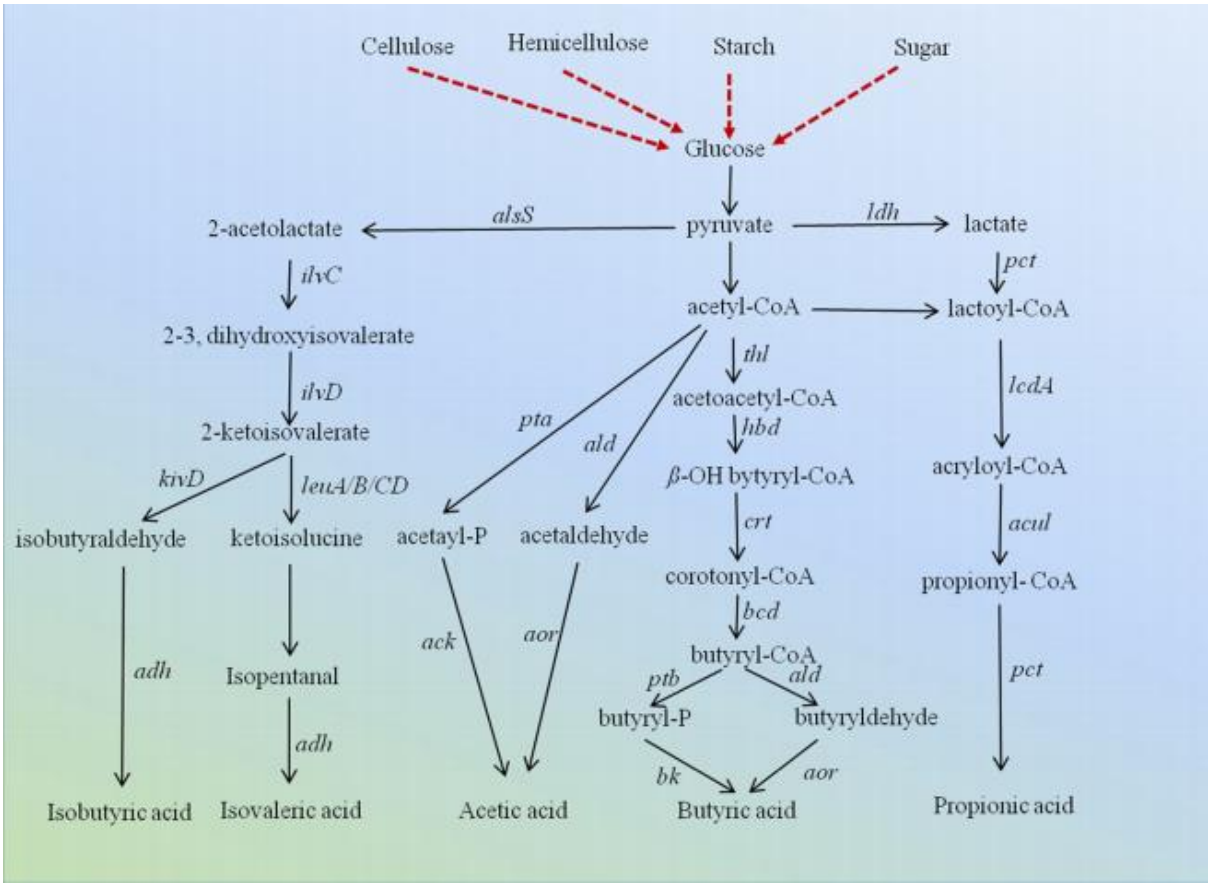

Figure 2-6 : Scheme of various possible metabolic pathways for VFAs (acetic acid, propionic acid, butyric acid, isobutyric acid, and isovaleric acid). The multistep pathway is presented with dotted lines and the single step reaction with simple arrows. For enzyme names, refer to Annex 1 (Bhatia and Yang, 2017).

Various wastes can be used as cost-effective carbon sources for VFA production: municipal sludge is produced in high quantities and has an interesting chemical oxygen demand (14,8 - 23 g/L) making it suitable for VFA production (Bhatia and Yang, 2017). Food waste is another carbon-rich cheap material but its separation from other wastes like plastic and glass is sometimes complicated. Liquid waste issued from agriculture, food and paper industry are also raw materials possible for VFA production, as studied in a research (Bengtsson et al., 2008) on acidogenic fermentation of four different industrial wastewaters (cheese whey permeate and three pulp and paper mill effluents). In batch experiments, these fermented substrates resulted in significant VFA production and two of the wastewaters, cheese whey permeate and a paper mill effluent, were found to have nearly 100% fermentable fractions of the soluble organic matter.

2.1.3 Uses

Acetic acid has a diversity of uses, it finds applications in the food industry as vinegar and in several food preparations, but the major use of acetic acid is in the oxidative production of vinyl acetate monomer (VAM) catalyzed by palladium (de Bruyn, 1999):

$CH_3COOH + CH_2{=}CH_2 + ½\ O_2 \rightarrow CH_3COOCH{=}CH_2 + H_2O$ Reaction 2-6

Vinyl acetate monomers can be used for further polymerization to produce polyvinyl acetate (PVA), which is used in several plastics, paints and adhesives. The condensation reaction of acetic acid produces acetic anhydride, a typical acetylation agent, which is subsequently used to produce cellulose acetate, used in synthetic textiles (Pal and Nayak, 2017). Acetic acid is used as a solvent in the production of terephthalic acid (TPA), mainly used for the manufacture of polyethylene terephthalate (PET) for packaging fibers, clothing, plastic bottles, and films (Baumann and Westermann, 2016). Glacial acetic acid is a good polar protic solvent which is frequently used to recrystallize organic compounds during purification processes (Pal and Nayak, 2017). Acetic acid can be derived in esters such as ethyl acetate, n-butyl acetate, isobutyl acetate, and propyl acetate which are frequently used as solvents for inks, paints and coatings. Other applications for acetic acid include use as an etching agent, as a component in the manufacturing of hydrophobic and hydrophilic papers in polymer industries (Murali et al., 2017).

Butyric acid has some significant applications in food and flavors because its ester derivatives are generally aromatic and they increase fruit fragrance (Baumann and Westermann, 2016). In pharmaceuticals, it is used as a component in several anti-cancer drugs and other therapeutic treatments (Murali et al., 2017). In the chemical industry, butyric acid mainly finds uses in the production of cellulose acetate butyrate plastics (Dwidar et al., 2012). Butyrate and its derivatives are extensively used as solvent, diluents, plasticizer, fiber, and raw materials (Jha et al., 2014).

Butyric acid can be converted in butanol, which also offers some strong perspectives as a biofuel more efficient than ethanol since it has a higher energy content, lower volatility, and does not readily absorb moisture. It is known that the higher the number of reduced carbon atoms, the more energy is contained. Thus, because reduced carbon atoms of butanol double that of ethanol, butanol contains more energy compared to ethanol, resulting in an energy density of 26.9 MJ/kg for ethanol and 33.1 MJ/kg for butanol (Jha et al., 2014; Ndaba et al., 2015). Even if butanol is more hydrocarbon-like in its properties, it still lags far behind ethanol in terms of commercial production (Serras-Pereira et al., 2013).

2.1.4 Market and value

According to 2015 market research, the market price of acetic acid varies within US $1200 and $1600 per ton in different countries (Pal and Nayak, 2017). Global demand of virgin acetic acid market stands at 13 million tons in 2015 which is forecasted to extend approximately to 18 million tons by 2020, showing a compound annual growth rate of around 5%. According to other authors, the growth will be driven mainly by the Chinese market with a rapid expansion in production facilities and a future

consumption growth of acetic acid is expected to be around 7% per year (Baumann and Westermann, 2016).

In 2014, a market research valued the butyric acid market at $124.6 million (Murali et al., 2017), and its price was estimated to be between $1800 and $1900 per ton, depending on the purity and quantity (Baumann and Westermann, 2016). The annual production of this acid is around 50 thousand tons (Bhatia and Yang, 2017).

2.3 Recovery of volatile fatty acids produced by fermentation

For industrial production, various recovery principles and configurations are used, because the fermentation conditions and physical properties of specific carboxylic acids differ (López-Garzón and Straathof, 2014). After removing cells from the fermentation broth, the aqueous carboxylic acid or carboxylate solution contains numerous impurities such as sugars and salts remaining from the fermentation feed, fermentation by-products such as proteins and undesired carboxylic acids, and debris derived from the cell lysis and/or decay. In many recovery strategies, the bulk of the impurities can be removed by selectively transferring the product to another phase. So, there are different methods for the recovery of VFAs from aqueous solutions, but most of these methods have some disadvantages, such as the recovery of other products or extra process steps (Rocha et al., 2017).

Existing conventional processes for recovery of organic acids from fermentation broths (Figure 2-7) include stripping, adsorption, electrodialysis, direct distillation, solvent extraction, evaporation, chromatographic methods, ultrafiltration, reverse osmosis, and drying (Eda et al., 2017). Some of these processes allow in-situ product removal, what can be seen as an advantage because it prolongs the time before the fermentation stops due to inhibiting product concentrations. Removing the undissociated carboxylic acid can reduce the consumption of pH-controlling base and the associated inorganic salt accumulation (López-Garzón and Straathof, 2014).

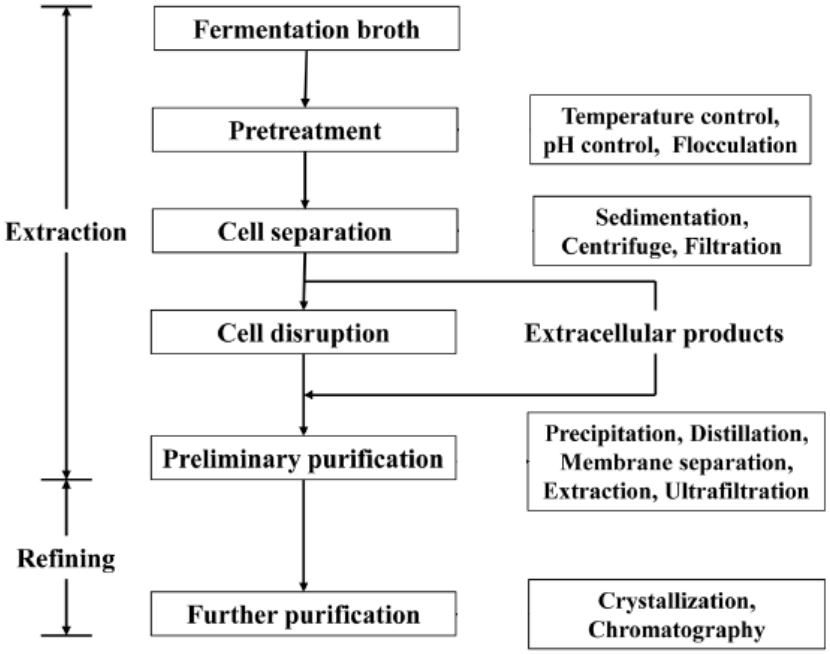

Figure 2-7 : General flow of separation of organic acids from fermentation broth. The flow is valid for organic acids that are extracellular products (Li et al., 2016).

As an example to illustrate the complexity of the fermentation broths, fermented wastewaters are not ideal aqueous solutions and typically contain significant amounts of various dissolved salts (Reyhanitash et al., 2016). Na^+, K^+, $H_2PO_4^-/HPO_4^{2-}$, Cl^- and SO_4^{2-} are the most common ions originating from the dissolved salts present in fermented wastewater. As seen in Table 2-3, the VFA concentrations are expected to be between 2.5 and 10 g/L.

Table 2-3: Typical composition of fermented wastewater (Reyhanitash et al., 2016).

Component	Chemical formula	Concentration (g/L)	pK_a
Acetic acid	CH_3COOH	2.5–10	4.76
Propionic acid	CH_3CH_2COOH	2.5–10	4.88
Butyric acid	$CH_3(CH_2)_2COOH$	2.5–10	4.82
Lactic acid	$CH_3CH(OH)COOH$	2.5–10	3.86
Sodium	Na^+	1–5	
Potassium	K^+	1–5	
Chloride	Cl^-	1–10	
Phosphate	$H_2PO_4^-/HPO_4^{2-}$	1–10	
Sulfate	SO_4^{2-}	1–10	
Sulfide	S^{2-}	0.3	
Magnesium	Mg^{2+}	0.3	
Calcium	Ca^{2+}	0.3	
Ammonium	NH_4^+	0.1	
Trace elements (e.g. cobalt, nickel and iron)	Co, Fe, Ni (ionic forms)	10^{-4}	
Inert COD (e.g. humic acid and fulvic acid)		1	
Microbes			

Difficulty in isolating and concentrating butyric acid from anaerobic fermentation broth is considered as one of the major problems for butyrate production (Jha et al., 2014). Two processes, solvent extraction and distillation, are extensively applied to separate butyric acid from other byproducts like acetic acid, but toxicity of the solvent in

extraction and huge energy consumption in distillation are limiting the efficiency of these processes.

Generally, the recovery of carboxylic acids including VFAs can be seen as a procedure containing multiple steps (Table 2-4) that can be considered as a primary recovery of extraction and a secondary step of refining (Li et al., 2016). For each of these steps, a few processes will be described below with more detail.

Primary Recovery	Concentration	Purification (Regeneration)	Salt co-produced
Carboxylate precipitation	Water evaporation	Protonation with H_2SO_4	$CaSO_4$
		Ketonization	$CaCO_3$
Protonation with H_2SO_4 or CO_2	Extraction with tertiary amine	Thermal decomposition	$CaCO_3$
		Esterification	$CaCO_3$
	Adsorption	Desorption e.g. with MeOH	$CaSO_4$ or $CaCO_3$
Monopolar electrodialysis	Bipolar electrodialysis	Water removal/ nanofiltration	NaOH
Membrane electrolysis	Extraction	Esterification	none
Protonation with cation exchange resin	Desorption with HCl	Precipitation or water evaporation (Regeneration by thermal decomposition of $MgCl_2$)	$MgCl_2$
Anion exchange resin	Desorption with NaCl or H_2SO_4	Water evaporation or crystallization	NaCl or Na_2SO_4
	Desorption with MeOH (EtOH) + H_2SO_4	Esterification	Na_2SO_4 or $CaSO_4$
	Alkylation	Distillation	$NaHCO_3$

Table 2-4: Reported schemes for the recovery of carboxylates from fermentation broth at pH > pKa (Cabrera-Rodríguez et al., 2017)

2.3.1 Primary recovery processes

Liquid-liquid extraction

In liquid-liquid extraction, the carboxylic acid is recovered by transfer to a suitable solvent (Reyhanitash et al., 2016; Rocha et al., 2017). It is one of the most applied affinity separation techniques and the extraction performance depends strongly on the characteristics of the extractant, with a proper choice of solvent, it can enable effective recovery of VFAs from dilute solutions in an energy efficient manner. Classical extractants (alcohols, ketones, aliphatic, aromatic, etc.) give low distribution coefficients, resulting in the poor extraction efficiency of carboxylic acids (Eda et al., 2017). In contrast, the use of amines or organo-phosphoric compounds as extractants

yields higher efficiency with better distribution coefficients compared to classical extractants.

Reactive extraction is another type of liquid-liquid extraction (Li et al., 2016). For easier extraction, the VFA can sometimes be converted into another compound with a better distribution coefficient. This type of extraction is easily operated by controlling the pH value of the two phases. The processes implicated include hydrolysis, complexation, dissociation, and ion association in two phases, and finally phase equilibrium. For organic acid recovery, the most used extractants are phosphorous solvents and aliphatic amines. Among the aliphatic amines, long chain aliphatic primary, secondary, and tertiary amines are distinguished (Eda et al., 2017). The primary amines are characterized by a high solubility in the aqueous phase, while the secondary amines offer the highest VFA distribution coefficients but tend to form amides in the downstream regeneration by distillation. The tertiary amines offer advantages over the other extractants on the grounds of their lower cost and generally higher equilibrium distribution coefficient K_D. Acid-amine complex stability is affected by the basicity of the amine, which can be altered using various diluents.

In the recent extraction literature, ionic liquids (ILs) have also been reported for extraction of VFAs, and some have been noticed to be better than conventional solvents in terms of extraction efficiency from idealized aqueous solutions containing only acids and water (Reyhanitash et al., 2016). ILs exist as molten salts at ambient temperature and consist entirely of ions, usually a charge–stabilized organic cation and an inorganic or organic anion (Tonova, 2017). A study concluded that phosphonium-based ILs are better extractants than the traditional organic solvents for recovery of short chain organic acids from aqueous dilute solutions. They succeeded to obtain higher distribution coefficients as compared to most traditional solvents by using phosphonium-based ionic liquids for the extraction of low concentrated lactic acid solutions, and obtained an extraction efficiency of 98,4% with a two-step extraction (Oliveira et al., 2012). Other searchers (Andersen et al., 2016) proposed an IL-mediated esterification for reactive extraction of low-value VFA from dilute aqueous streams. The ionic liquid was composed of a trihexyl(tetradecyl)phosphonium cation ($[P_{666,14}]^+$) and a mixed chloride and bis(trifluoromethylsulfonyl)imide anion that showed good extraction and esterification properties. The extracted acetic acid was reacted with ethanol to produce ethyl acetate, this product was then recovered by evaporation as shown in Figure 2-8.

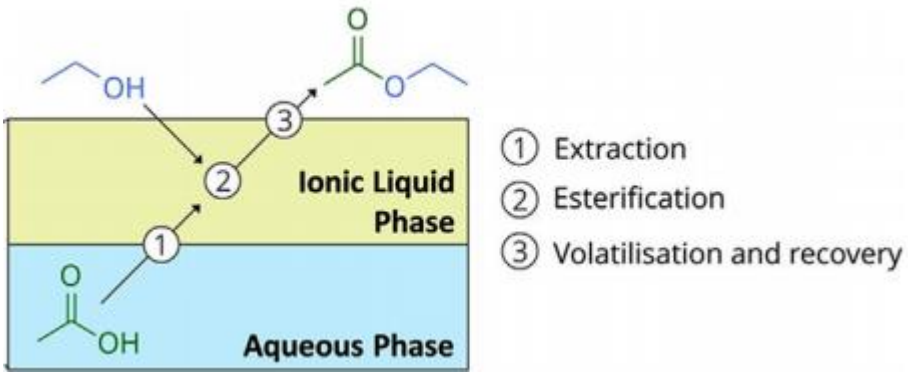

Figure 2-8: Ionic liquid-driven esterification process scheme (Andersen et al., 2016)

In a study, a solvent extraction with ionic liquids ($[P_{666,14}]$[Phos] and trioctylamine) was used to recover acetic acid from fermented wastewater (Reyhanitash et al., 2015). CO_2 was investigated for its potential to acidify fermentation broths so that the volatile fatty acids are in their protonated form instead of being in dissociated form. CO_2 was applied in pressures up to 40 bar to enhance the efficiency of extraction. It was demonstrated that there is an increase in extractability of HAc, expressed as HAc distribution ($D = [HAc]_{solvent}/[HAc]_{aqueous}$), when the CO_2 pressure was increased.

Electrodialysis

An important technology that allows in situ product recovery of carboxylic acids is electrodialysis, by using an electrical field to facilitate ionic transport towards electrodes for optimal acid removal (Murali et al., 2017). Some electrodialysis processes have been tested for acid recovery including conventional electrodialysis (Figure 2-9): electro-metathesis, electro-ion substitution, electro-deionization, and bipolar membrane electrodialysis. Electrodialysis can result in high acid purity and a study refers the possibility of removing up to 99% of acetic and butyric acid from sucrose-fed fermentation broths (Jones et al., 2015). But one of the most limiting factors for using electrodialysis at industrial scale is electricity consumption, as it can result in high processing costs. Hábová et al. (2004) indicated that the power requirements for lactic acid separation using electrodialysis can vary from 0.21 to 0.71 kWh/kg acid produced under optimized conditions for maximum lactate recovery.

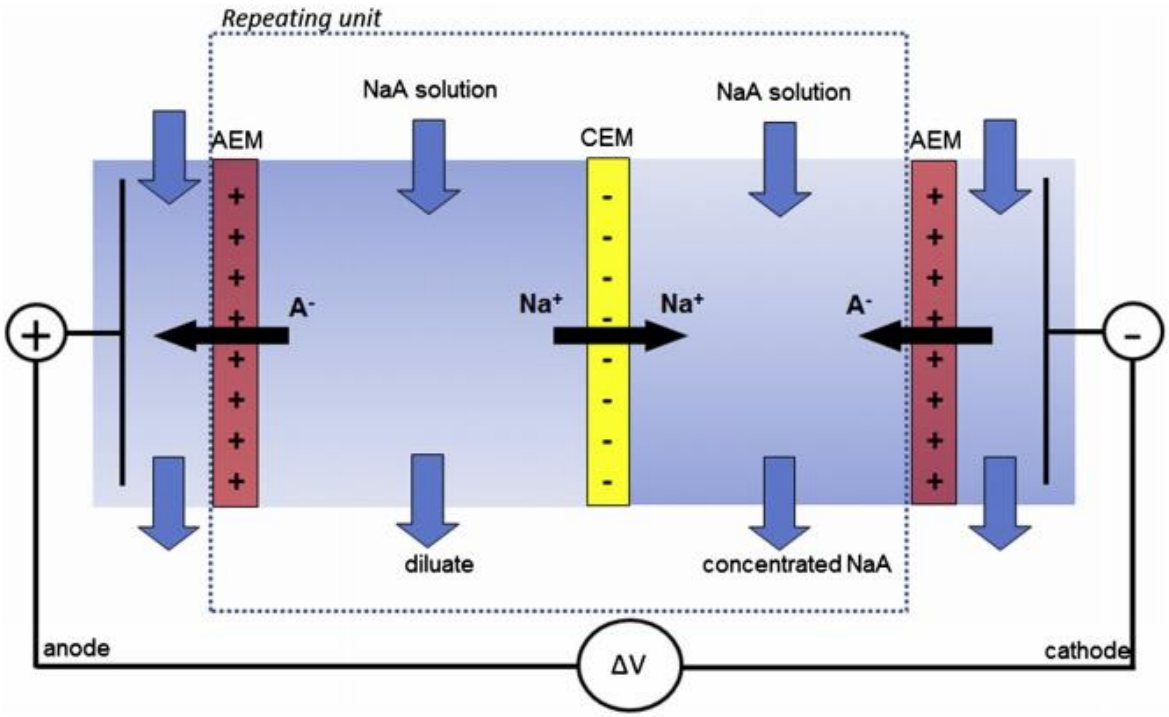

Figure 2-9 : Principle of common electrodialysis in a two-compartment configuration, using as example the concentration of a sodium carboxylate (NaA) solution. CEM: cation exchange membrane, AEM: anion exchange membrane (López-Garzón and Straathof, 2014).

Although the applicability of this technique has been demonstrated for several carboxylates, there are still difficulties for its widespread use (López-Garzón and Straathof, 2014). The cost of the membranes needs to be reduced in order to broaden its application. Improving antifouling characteristics and increasing selectivity for co-ions are the main application-related optimization goals.

Adsorption

The power of adsorption stems from the possibility of designing the surface chemistry of the sorbent to selectively recover target molecules (Kalyanpur, 2002). One of the main advantages of adsorption operations over extraction is the effortlessness of the auxiliary phase removal. Solid adsorbents confined in columns are easily handled in comparison to liquid–liquid systems in which phase separation might require either large equipment or energy demanding operations. This aspect also has consequences in the material consumption as a difficult phase separation causes solvent losses. One of the disadvantage is that adsorbents are susceptible to fouling which may limit the operational lifetime of the material, causing the necessity to renew the adsorption material periodically (López-Garzón and Straathof, 2014).

The adsorbents relevant to the recovery of carboxylic acids and carboxylates can be classified according to their electronic properties in ionic and non-ionic materials and more thoroughly by their functionality and support structure (López-Garzón and

Straathof, 2014). Ionic materials, also known as ion exchangers, have the ability to adsorb carboxylic species. Water-insoluble amine, ammonium and related bases are used in this purpose. Weak anion exchangers become charged over a limited pH range and otherwise are not able to exchange anions whereas strong anion exchangers exchange anions over a broad pH range. It must be kept in mind that weak anion exchangers do not actually perform anion exchange during the capture process, instead, an overall exchange is complete when the carboxylic acid is desorbed. An entire section is dedicated to the ion exchange resins (p21).

2.3.3 Final purification

Final VFA purification requires either distillation or crystallization, usually involving evaporation of water (López-Garzón and Straathof, 2014).

Distillation and evaporation

Distillation is a method of separating a mixture based on differences in volatility of the components (Li et al., 2016). Even if other techniques are available to separate organic acids from fermentation broths, distillation remains an important alternative technology, especially in the final refining. Since all VFAs have a boiling point higher than water (Yalkowsky et al., 2010), the distillation of a VFA-water mixture will cause the water to be the first compound to vaporize. Water has a high latent heat of vaporization, so distillation of VFAs is only economically attractive as a final step of purification, after the VFAs in aqueous phase have already been concentrated (Gangadwala et al., 2008; Rocha et al., 2017). Even then, purification is complicated because of a tangent pinch of the water end in the x-y diagram, what means high reflux ratio of high number of column stages to get pure products.

In the case of recovery of acetic acid, water is more volatile than acetic acid and relative volatility of water to acetic acid is very low. In a mixture with a the range of 1-30% of acetic acid in water, relative volatility is very close to one (Padhiyar and Thakore, 2013). Although acetic acid and water do not form an azeotrope, it is necessary to have a large number of equilibrium stages and a very high reflux ratio to obtain glacial grade acid by simple distillation (Patil and Kulkarni, 2014).

According to Berg and Yeh (1987), propionic acid recovery from an aqueous solution cannot be done by conventional rectification because propanoic acid boiling at 141.4°C forms a minimum azeotrope with water boiling at 99.1°C and containing 82.2 %wt. water. Thus, it is impossible to separate completely propanoic acid from water by rectification because as soon as the minimum azeotrope composition is attained, no further change in composition will occur. They suggest that acid amides (such as dimethylformamide or acetamide), either alone or admixed with other organic compounds, will effectively negate the propanoic acid - water minimum azeotrope and

permit the separation of pure water from propanoic acid by rectification when employed as the agent in extractive distillation.

2.3.4 Example of a well-controlled purification process: lactic acid

Overview of the compound

Lactic acid ($C_3H_6O_3$, Figure 2-10) is a carboxylic acid that has two enantiomers: L-(+)-lactic acid, the biological form, and D-(−)-lactic acid (Komesu et al., 2017b). It finds uses in a wide variety of applications like pharmaceutical products, pH regulation, food additive, and pesticide. Lactic acid (LA) is also the monomer used for polymerization into polylactic acid (PLA), a polymer that has the potential to provide a new biodegradable product platform to compete with hydrocarbon-based thermoplastics. PLA can be an alternative for food packaging including rigid containers, shrink wrap and short shelf-life trays, as well as mulch films and rubbish bags. The exploitation of full PLA potential, however, depends largely on how cost-effectively LA can be produced with high levels of purity required for polymerization. The major technology barrier in cost-effective production of high-purity biologically-produced lactic acid is its recovery and purification.

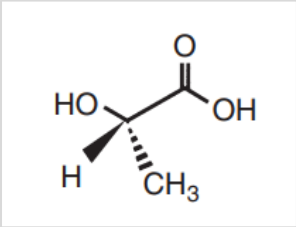

Figure 2-10: Molecule of lactic acid (Miller et al., 2011).

Bacterial fermentation

Nowadays, bacterial fermentation is preferred to chemical synthesis and about 90% of world production is obtained by fermentative pathways (Komesu et al., 2017a). An optically pure L-(+)- or D-(−)-lactic acid can be obtained by the microbial fermentative method, contrarily to chemical synthesis that always yields a racemic mixture of DL-lactic acid from petroleum resources. Carbohydrate sources including whey, starchy materials and glycerol can be used for fermentation into LA. Lactic acid bacteria (LAB) are facultative anaerobic bacteria and they can produce lactic acid with high yield and high productivity (Wang et al., 2015). Common LAB species belong to the genera *Lactobacillus, Lactococcus,* or *Pediococcus*. Some strains can produce lactic acid from a high concentration of xylose via the pentose phosphate pathway which yields 5 mol of lactic acid from 3 mol of xylose. In other words, the theoretical yield is close to 100%, and few by-products are formed through fermentation by these strains.

Purification process

For purification of LA, precipitation, solvent extraction, adsorption, direct distillation, and electrodialysis are conventionally adopted (Sun et al., 2006). However, much of these purification procedures are difficult because of the low volatility of LA (122 ◦C at 1661.73 Pa), high affinity for water and its tendency to self-polymerize.

The most economical recovery technology is the precipitation process (Miller et al., 2011). The fermentation broth is heated to approximately 70 ºC to kill bacteria; cells are then separated from the broth by centrifugation or filtration (Jantasee et al., 2017). The lactic acid is usually in form of calcium lactate because the most widely practiced method of controlling pH in industrial fermentation is with lime ($Ca(OH)_2$). The fermentation broth containing calcium lactate is acidified with H_2SO_4 to form the undissociated lactic acid and calcium sulfate, which is a low-value byproduct. The $CaSO_4$ is then removed by filtration or centrifugation and the final result of this process is a clarified lactic acid broth. The purification of lactic acid by the precipitation consumes high amounts of acid, and it produces one-half mole of gypsum ($CaSO_4 \cdot H_2O$) per mole of lactic acid, equivalent to 0.96 kg of gypsum/kg of lactic acid (Eggeman and Verser, 2005).

Further purification is required to produce either a food-grade product or, at even higher purity, polymer-grade lactic acid (Miller et al., 2011). Unit operations typically include resin beds (cation, anion) to remove unwanted ions and colorants are removed from the solution with activated carbon. Finally, a unit operation with high separation power is needed to produce food- and especially polymer-grade lactic acid. Examples include chromatography, ester formation and hydrolysis, and subsequent distillation and hydrolysis, or solvent extraction. The choice of the technology is driven by end-product purity needs and capital cost considerations.

2.4 Ion exchange resins

Ion exchange is defined as a reversible interchange of ions between a solid, the ion exchange material, and a solution in which there is no permanent change in the structure of the solid. Most ion exchange resins consist of a cross-linked polymer matrix with ion-active sites relatively uniformly distributed in the structure. The ion exchange materials, the resins, are usually sold as spheres or granules with a specific size and uniformity, depending on the application. They have a polydisperse and gaussian size distribution usually between 0.3 and 1.2 mm, or a monodisperse size distribution.

2.4.1 Types of anion exchange resins

Carboxylic acids can be separated from a fermentation broth by using anion exchange resins. When unprotonated, the carboxyl group has a negative charge that allows ionic bonding with positively charged functional groups on the anion exchange resin, and other materials are removed by washing the resin with water (Ponnampalam, 1999).

Weak base resins

Weak base resins do not contain exchangeable ionic sites and function as acid adsorbents. These resins are capable of adsorbing strong acids with a high capacity and are readily regenerated with caustic soda.

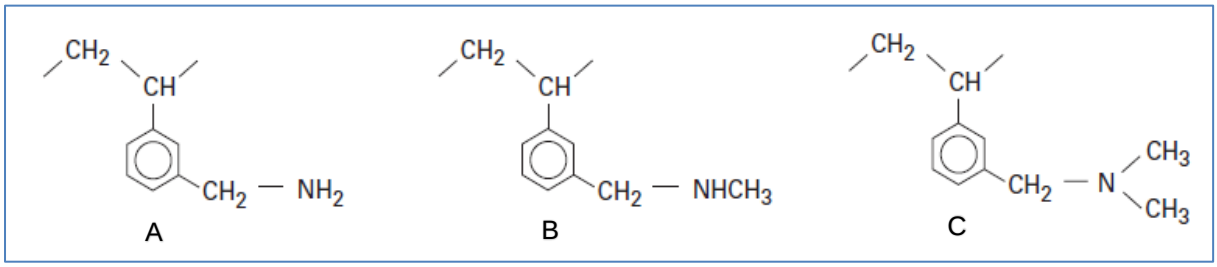

Figure 2-11: Weak base styrenic anion exchange resins. The functional group is (A) a primary amine (B) a secondary amine or (C) a tertiary amine (De Dardel, 2015).

The weak base group can be for example pyridine, imidazole, or a primary/ secondary/tertiary amine function grafted on the polymer matrix, as shown in Figure 2-11 (López-Garzón and Straathof, 2014). If an acid HA is adsorbed on the resin R, sodium hydroxide can be used to desorb the acid. The resin is regenerated after the desorption step and the cycle can be resumed like:

Adsorption: $HA_{aquous\ phase} + R \rightarrow RH^+A^-$ + aqueous phase Reaction 2-7

Desorption: $RH^+A^- + NaOH \rightarrow R + NaA + H_2O$ Reaction 2-8

In this reaction cycle, the adsorption capacity is strongly influenced by the pH since a decrease in pH increases the protons available to enable ion pairing between the soluble acid and the amine (López-Garzón and Straathof, 2014). In a simplified acid-base interaction, the first step reduces the acid concentration in the aqueous phase. During the desorption, an acid salt is formed equimolarly to water. Another stoichiometry is possible depending on the acid structure and valence.

The use of smaller volume of more concentrated desorbant will cause the recovery of a more concentrated carboxylate solution (López-Garzón and Straathof, 2014). Desorption with NaOH releases a carboxylate salt form (NaA), as indicated in reaction 2-8. For recovery of the carboxylic acid, other additional steps must be included. One of the possibilities is to pass the carboxylate salt solution through a cation exchanger in hydrogen form (Vaccari et al., 1993).

Desorption with a mineral acid (HX) allows the recovery of the carboxylic acid instead of a carboxylate. In that case, a regeneration step of the resin must be included:

Adsorption: $HA_{aquous\ phase} + R \rightarrow RH^+A^-$ + aqueous phase Reaction 2-9

Desorption: $RH^+A^- + HX \rightarrow RH^+X^- + HA$ Reaction 2-10

Regeneration: $RH^+X^- + NaOH \rightarrow R + H_2O + NaX$ Reaction 2-11

The mineral acid must be strong enough to displace the carboxylic acid adsorbed on the resin. Mineral acids with a pK_a value lower than the carboxylic acid are expected to establish a stronger interaction with the basic group from the resin, but other characteristics also determine the efficiency of the desorption. Affinity of a resin for an ion is linked to the dimension of the hydrated ion (De Dardel, 2015; López-Garzón and Straathof, 2014).

Strong base resins

Strong base resins are functionalized with a quaternized amine (López-Garzón and Straathof, 2014). This functional group is permanently charged and has a negative counterion to maintain the electroneutrality. One common anion is the hydroxide ion (Q^+OH^-). When carboxylates are absorbed by ion pairing, the counterion (OH^-) is released:

Adsoprtion: $HA + Q^+OH^- \rightarrow Q^+A^- + H_2O$ Reaction 2-12

Desorption: $Q^+A^- + NaOH \rightarrow Q^+OH^- + NaA$ Reaction 2-13

Because the interaction between Q^+ and the carboxylate A^- is much stronger compared to the other amine groups, the reaction 2-13 will need a more concentrated base to be effective (López-Garzón and Straathof, 2014). Strong base resins are commercially available under two different types.

The type 1 resins are quaternary ammonium products, where the functional group, a quaternary trimethylammonium chloride (Figure 2-12A), is the most basic available and it has the greatest affinity for the weak acids such as silicic acid and carbonic acid (Harland, 1994). However, the efficiency of regeneration of the resin to the hydroxide form is a little bit lower (Wheaton and Lefevre, 2000). Type 1 resins are also more stable chemically compared to type 2 so they are privileged for high temperature applications.

Type 2 resins (Figure 2-12B) are obtained by the reaction of the styrene-DVB copolymer with dimethylethanolamine (Wheaton and Lefevre, 2000). This quaternary ammonium has lower basicity than that of the type 1 resin, but it is high enough to

remove the weak acid anions for most applications. The regeneration efficiency of a type 2 resin is considerably better than that of type 1.

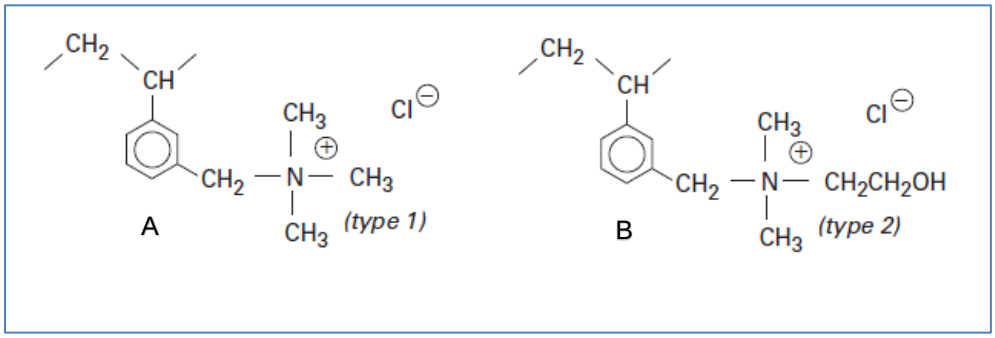

Figure 2-12: Strong basic styrenic anion exchange resin. (A) Type 1 resin has a trimethylammonium chloride group, whereas (B) has a type 2 functional group (De Dardel, 2015).

Nonionic materials

When considering a solution with protonated carboxylic acids, adsorption without ion-exchange is possible because other types of interactions are also responsible for adsorption, like hydrophobic interactions (López-Garzón and Straathof, 2014). In these types of interactions, the polarity of the target molecule is important and it is expected that nonionic resins show low capacities and affinities for short chain carboxylic acids. Nonionic materials for recovery of undissociated acids are still in an early stage of development.

2.4.2 Structure of the resin

Synthesis

To confer ion exchange properties, the host polymer structure must allow diffusion of hydrated ions (Harland, 1994). Modern organic ion exchange resins are synthesized by polymerization mechanisms. A polymerization is induced between monomers containing vinyl double bonds ($-CH=CH_2$), one of the monomers contains two or more vinyl double bonds to permit crosslinking. Crosslinking is essential because otherwise the polymerization would produce linear polymers and the derived ion exchange material would be soluble. Two common polymer matrices are styrenic and acrylic exchange resins.

Styrenic resins are produced by copolymerization of styrene with divinylbenzene (Figure 2-13), the reaction is initiated by a benzoyl peroxide catalyst. This reaction is exothermic and produced in an aqueous phase, where the monomers are immiscibly dispersed as spherical droplets, resulting in small beads of copolymer being formed. The amplitude of crosslinking is determined by the proportion of crosslinking agent (

DVB) and has a strong impact on mechanical and chemical behavior of the derived exchange material (Harland, 1994).

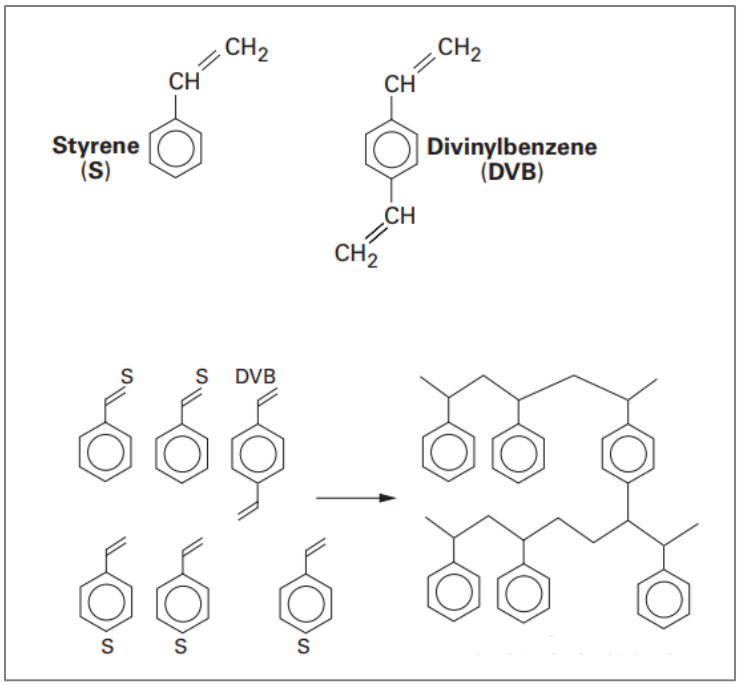

Figure 2-13: Copolymerization of styrene (S) with divinylbenzene (DVB) produces a crosslinked polystyrene-divinylbenzene matrix (De Dardel, 2015).

Acrylic exchange resins are produced with acrylic monomers and DVB. It is one of the alternatives that has been most widely exploited (Harland, 1994). In the same way as styrenic exchangers, a copolymerization between the monomers leads to a reticulated structure. Various derivatives of propenoic acid can be used as monomers, including acrylonitriles and acrylic esters. An example of a copolymerization between methyl acrylate and DVB is illustrated in Figure 2-14.

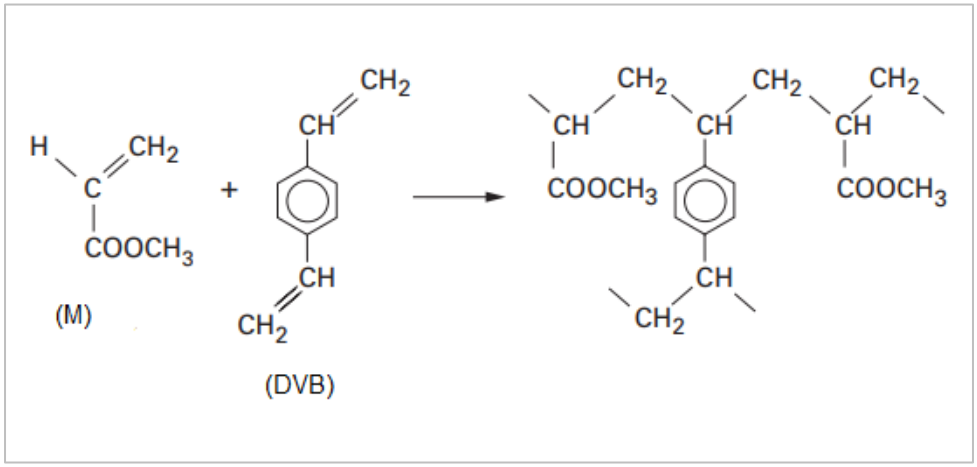

Figure 2-14: Copolymerization of methyl acrylate (M) with divinylbenzene (DVB) produces a crosslinked polymethyl-acrylate matrix (De Dardel, 2015).

Physical structure

Resins can be found with two different structure types (Zaganiaris, 2011). The first type is a gel with a homogenous structure nonporous, composed of a continuous polymeric phase. In the second type, the beads are called macroreticulated or microporous. These beads are heterogenous, they consist in interconnected macropores surrounded by gel-type microbeads. A representation is given in Figure 2-15. Macroreticular resins contain a significant fractional void volume and there are characteristic pore size distributions for each of the macroreticular resins, while conventional gel resins have no significant pore structure (Kun and Kunin, 1967).

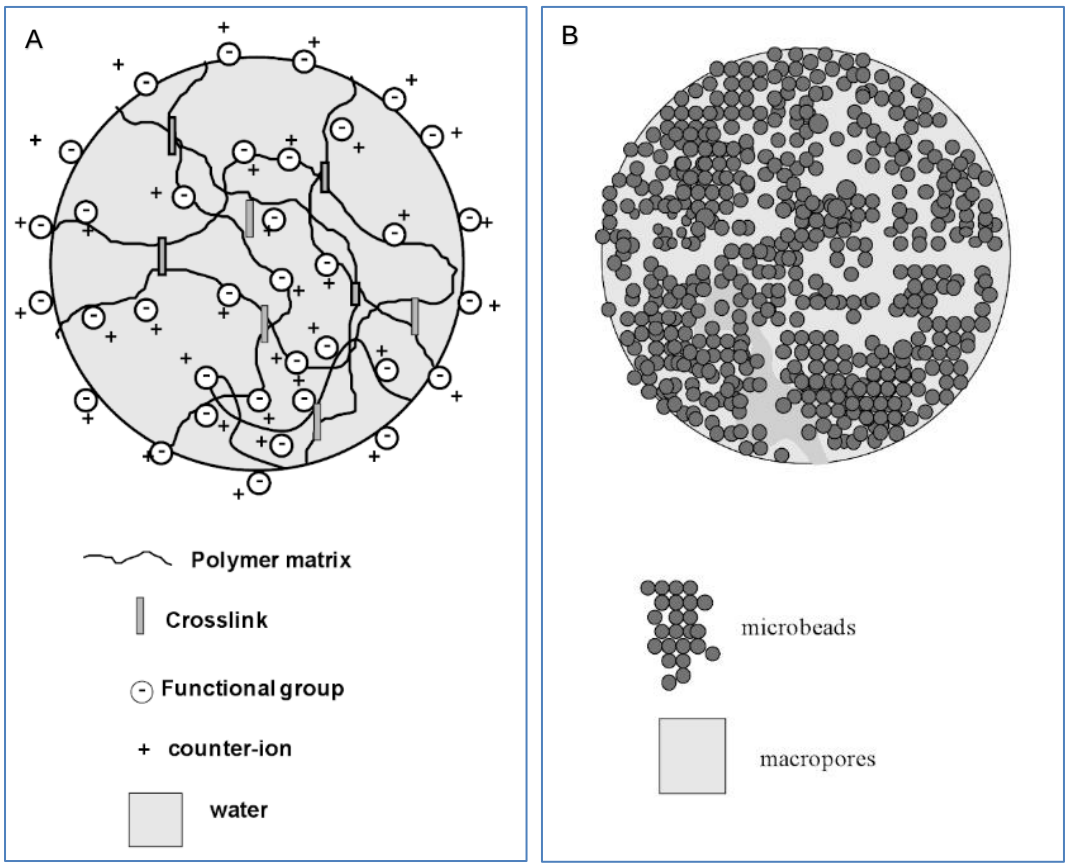

Figure 2-15: Schematic representation of (A) a gel-type bead and (B) a microporous-type bead (Zaganiaris, 2011).

2.4.3 Properties

Capacity

The capacity of a resin can be expressed in a few different ways (Wheaton and Lefevre, 2000). Total capacity is the total number of sites available for exchange. This capacity can be expressed on a dry weight, a wet weight or wet apparent volume. Operating capacity is the useful capacity of a resin in a certain column and under certain circumstances and conditions.

Selectivity

By definition, the ion exchange reactions are reversible. In the case of a monovalent exchange between an anion VFA^- and a hydroxide OH^- on a strong base resin (Q^+), the reaction is (De Dardel, 2015):

$$Q^+OH^- + VFA^- \leftrightharpoons Q^+VFA^- + OH^-$$

The law of mass action gives:

$$\frac{[\overline{VFA^-}]}{[\overline{OH^-}]}\frac{\overline{\gamma}_{VFA}}{\overline{\gamma}_{OH}} = K\,\frac{[VFA^-]}{[OH^-]}\frac{\gamma_{VFA}}{\gamma_{OH}}$$

The terms $[VFA^-]$ and $[OH^-]$ are the equivalent concentrations of the ions in the liquid, and the terms with a line are in the solid phase (De Dardel, 2015). γ_{VFA} and γ_{OH} are the corresponding activity coefficients. In a first approximation, we consider that the activity coefficients are similar in the solid and aqueous phase, so a simplification gives:

$$K_{OH^-}^{VFA^-} = \frac{[\overline{VFA^-}]}{[\overline{OH^-}]}\frac{[OH^-]}{[VFA^-]}$$

$K_{OH^-}^{VFA^-}$ is the selectivity coefficient for the exchange VFA^-/OH^- (De Dardel, 2015).

Stability

Ion exchange resins can undergo chemical degradation (Wheaton and Lefevre, 2000). Chemical degradation happens in the presence of strong oxidants like chromic or nitric acid. Oxygen and chlorine can also degrade the resin when catalyzed by other

minerals. These oxidative conditions induce oxidation of the polymer matrix, and can break the crosslinks, leading to the resin deformation and softening.

The resins are also sensitive to high temperatures (De Dardel, 2015). Anion exchange resins are subjected to Hoffmann degradation reactions, that transforms the quaternary ammoniums into tertiary amines (Figure 2-16) or even degrades the entire active group. The type 1 strong basic resin is more stable than the type 2 and can keep full efficiency during more than 5 years at ambient temperature. The degradation becomes observable at 50°C or more. Type 2 is more sensitive to temperature because of the ethanol group that weakens the bond between the ethanol and the quaternized amine. These resins will lose 50% of their strong base groups in 5 years at ambient temperature. The fact that the quaternary amines are degraded in tertiary amines causes the resins to still be functional owing to the tertiary groups, weakly basic, that are still able to adsorb acids.

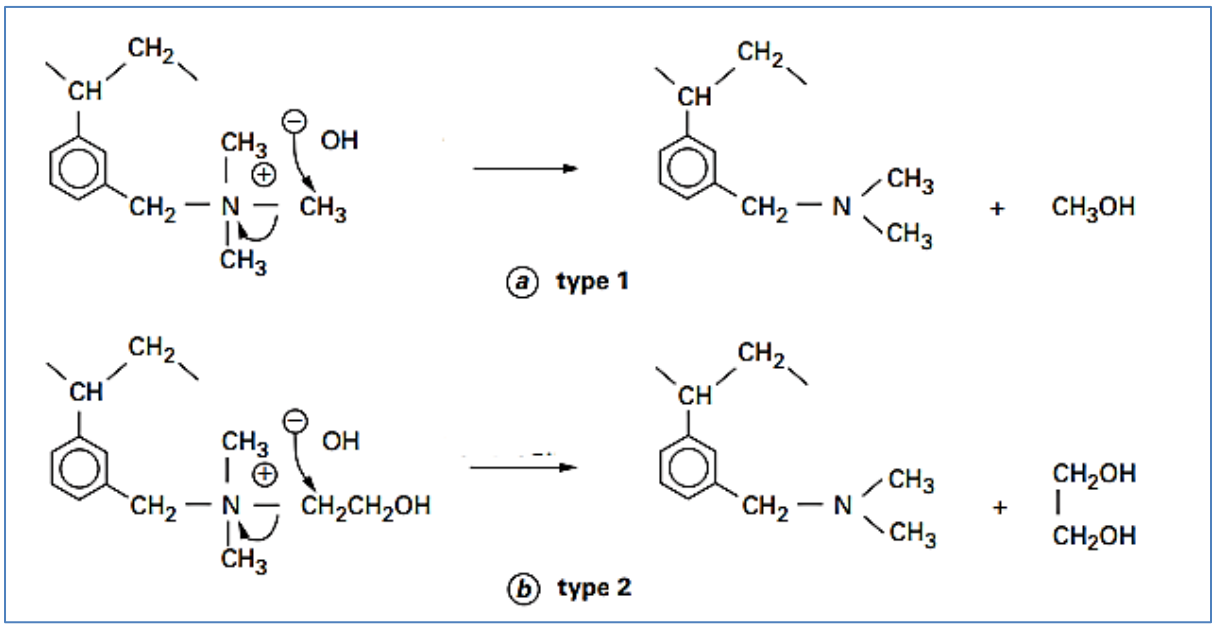

Figure 2-16: Hoffmann degradation reactions for type 1 and type 2 strong basic resins at high temperature (De Dardel, 2015).

For water treatment, ion exchange resins can work efficiently during years, sometimes up to 20, without losing their chemical and physical properties (De Dardel, 2015).

Kinetics

Kinetics determine at what speed the ion exchange takes place (Zaganiaris, 2011). This speed is related with the diffusion through the film of solution in close contact with the beads called the Nernst film, and diffusion in the porosity of the resin. If a strong base resin loaded in the OH^- form is in contact with a VFA solution, an exchange can happen between OH^- and VFA^-. As it can be supposed that the VFA^- transfer from the solution to the Nerst film is instantaneous due to the agitation, the overall ion exchange

rate is determined by the VFA^- diffusion through the film and diffusion inside the resin particle. If one of the two phenomena is slow compared to the other, it will be determinant for the exchange. In the resin, part of the space is occupied by the polymer matrix, so the ions can only diffuse in the space occupied by water. For that reason, the diffusion coefficient $\underline{D}_{VFA^-}$ is smaller in the resin than in the solution.

2.4.4 Ion exchange unit operations

In batch processes, the whole solution is mixed with the resin and the mixture is agitated until equilibrium is reached (Zaganiaris, 2011). The exchanges will be dependent of selectivity coefficients of the ions present in the solution.

In column operations, the solution containing the target ions passes through a column containing the resin (Zaganiaris, 2011). In the process of single bed column operation, the solution flows through a fixed resin bed.

2.5 Recovery of VFAs using ion exchange resins

2.5.1 Research and development

For carboxylic acid recovery, it is most common to use resins that have tertiary or quaternized amines as functional groups (Murali et al., 2017). The acids can then be removed with a caustic elution, and a further step of acidification followed with evaporation allows the obtaining of the purified acids.

Using an Amberlyst A21 resin (weakly basic), it was possible to recover volatile fatty acids from an acidogenic digestion process fed with grape pomace (Rebecchi et al., 2016). Basified ethanol allowed a complete desorption of all the adsorbed VFAs under their salt form. The solvent was recovered by evaporation, with negligible losses of the desorbed VFAs. With this process, the production of a highly concentrated water solution of the recovered VFAs is possible.

A research (Yousuf et al., 2016) investigated the recovery of carboxylic acids produced during dark fermentation of food waste. They concluded that it was possible to remove 74% of the carboxylic acids produced with a resin Amberlite IRA67 (weak base). The pH was an important parameter for adsorption and a pH below the pK_a of the carboxylic acids was beneficial. However, this study lacked in further investigating the efficient methods for desorbing the acids.

Even if lactic acid is not a VFA, it deserves attention because of the numerous similarities concerning production and recovery. According to Roque (1994), lactic acid fermentation is usually led under pH between 4.5 and 6, producing lactate salts. For recovery, a strong-base ion exchanger appears to be the obvious choice because it adsorbs lactates. Recovering lactate from the sorbent, however, requires a stronger

desorbent. For example, if NaOH is used, the product is sodium lactate. But, if the desired product is the acid, further processing is necessary. Weak-base adsorbents, on the other hand, adsorb only protonated lactic acid; therefore, they are not effective at pHs where only lactates are present. The advantage of weak-base sorbents is that the protonated lactic acid adsorbed is easily recovered by using alcohols like methanol and ethanol. An acid product is recovered after evaporating the alcohol.

2.5.2 Use of CO_2 for VFA recovery

CO_2 deserves a special discussion because of recycling and integration options, its nontoxicity, its low price, and its availability at production sites (López-Garzón and Straathof, 2014). The pK_a values of carbonic acid (H_2CO_3) are 6.3 and 10.3. The apparent pK_a of CO_2 depends on the equilibrium of the reaction:

$$H_2O + CO_2 \leftrightharpoons H_2CO_3$$

In an aqueous system, the achievable pH depends on the partial pressure of CO_2. The pH value is 3.72 for 1 bar CO_2 and 3.42 for 10 bar CO_2 (López-Garzón and Straathof, 2014). This allows some extent of protonation of carboxylic acids, if their pK_a is high.

A study (Cabrera-Rodríguez et al., 2017) proposed an alternative for the recovery of carboxylates produced by fermentations at pH values above the pK_a of the carboxylic acid. In their approach, the aqueous carboxylate anion is recovered using an anion exchange material followed by desorption and esterification with CO_2-expanded methanol[1]. An ester yield of 1.03 ± 0.07 mol methyl acetate/acetate$_{adsorbed}$ was obtained for the combined desorption-esterification at 5 bar of CO_2 and 60 °C. The desorption reaction is thought to be:

$$Q^+Ac^- + MeOH + CO_2 \leftrightharpoons Q^+HCO_3^- + MeAc$$

But, to our knowledge, CO_2 has never been investigated for its use to directly desorb VFAs in their acid form from ion exchange materials.

[1] CO_2-expanded methanol (cxMeOH) consists of pressurized gaseous CO_2 dissolved in methanol. When compressed CO_2 dissolves in methanol, the solvent expands in volume and decreases in polarity (Paudel, 2015).

3. Aim of the thesis

The principal aim of this thesis is to contribute to the development of a method that allows to extract and purify volatile fatty acids that are produced during fermentation of complex biomass, using as less chemicals as possible, in an energy-efficient and economically viable way. More specifically, this work contributes to the experimentation and analysis of the use of anion exchange resins as a recovery process of dilute VFAs in aqueous phase. We initiated the investigation by using a model solution containing only acetic and butyric acid in demineralized water. The first part of this thesis investigated the adsorption properties of different types of ion exchange resins and the impact of the model solution pH on the adsorption. A second part of the research was dedicated to the investigation of novel methods for desorbing the adsorbed VFAs, with a specific focus on desorption processes with CO_2, naturally produced during fermentation.

4. Materials and methods

4.1 Resins

All resins used were kindly provided by Purolite and Mitsubitchi Chemicals. The samples were resins in the form of spherical beads. The table 4-1 summarizes the three resins selected during the experiments and their properties.

Table 4-1: Resins used for experiments

Resin reference	Resin type	Structure	Functional group
Purolite SGA 550	Strong base (type 1)	Crosslinked styrene-divinyl benzene gel	Quaternary ammonium
Purolite A103Splus	Weak base	Macroporous polystyrene crosslinked with divinyl benzene	Tertiary amine
Mitsubitchi Chemical Sepabeads SP207	Non-ionic	Modified polystyrene/divinylbenzene	Bromine

For simplification, the resins will be further referred as their resin type: “strong base”, ”weak base” and “non-ionic”.

4.2 Model solution

The model solutions, of a total volume of 100mL, contained 8mmol of acetic acid (UCB, Belgium) and 8mmol of butyric acid (Sigma Aldrich, USA).

4.3 Experiments

Each experiment was driven with a new sample of resin, first by conditioning it, then adsorbing the VFAs from the model solution on the resin, followed by a desorption step, multiple or single.

4.1.1 Conditioning the resin and adsorption of the VFAs

For each experiment, a glass column was filled with 10 grams of resin. The column was a glass chromatography column with a volume of 16 mL (Econo-Column® Chromatography Columns, 1.0 × 20 cm, Bio-rad).

The resin was then conditioned by recirculating at 0.4mL/s 100 mL of 1M NaOH with a peristaltic pump (Reglo digital ISM833C, Ismatec). The NaOH solution was prepared from sodium hydroxide pellets (VWR, USA). The resin was rinsed for approximately 5

minutes by eluting distilled water at 0.4mL/s, until pH of the outgoing water was neutral. The pH was measured with pH-indicator strips (MColorpHast, Merck KGaA, Germany).

Adsorption was performed with a model solution (MS). The MS was recirculated through the column during the adsorption step, as indicated in figure 4-1. After a time of adsorption depending on resin type, the excess solution was drained and 50 mL of demineralized water were flushed through the column to rinse any residual not adsorbed VFA.

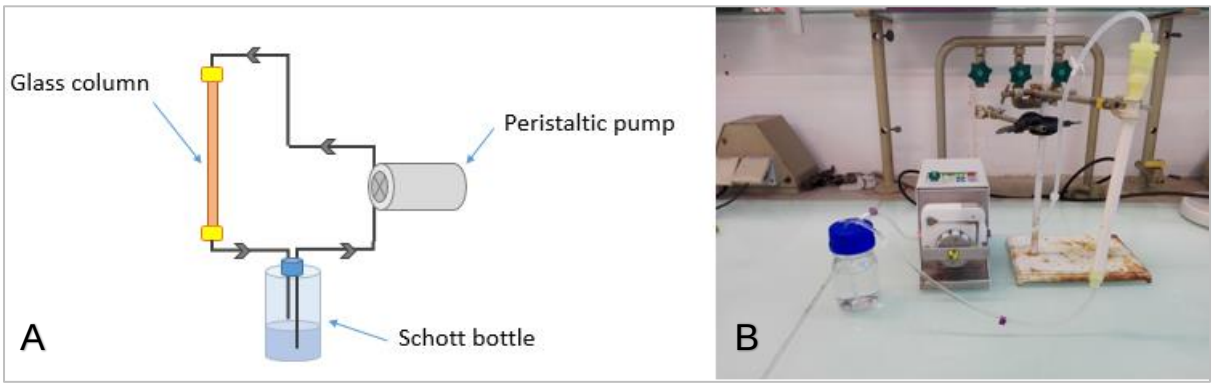

Figure 4-1: (A) Setup used for the conditioning of the resin and the adsorption of volatile fatty acids. (B) Picture of the setup.

4.1.2 Desorption of the VFAs

Various novel methods for desorbing the VFAs were tested with different designs and apparatus.

Thermal desorption: design T1

Thermal desorption was performed on the non-ionic resins. The assembly is similar to a distillation (Figure 4-2). A still pot containing 10 grams of loaded resins and approximately 20 mL of demineralized water was immersed in paraffin oil at 110°C and connected to a condenser, were condensed vapors could flow in a recipient containing 80 mL of sodium hydroxide at 1M. The final volume was adjusted to 100 mL with water that was used to wash the residual VFAs in the condenser. The liquid used to refrigerate was water, cooled down to 4°C with a refrigerator device (VWR® Refrigerated Circulating Baths, 89202-980, United States). Thermal desorption was performed for 2 hours.

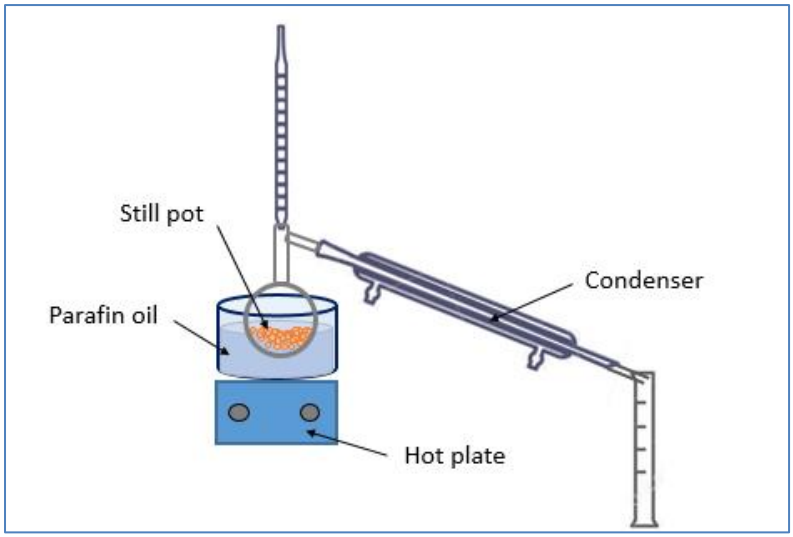

Figure 4-2: Scheme of thermal desorption using design T1

Thermal desorption: design T2

In this design (Figure 4-3), a CO_2 flow (Air liquide, Belgium) was used as gas vector to carry the vapors of VFAs out of the column. A flow of 12,5 mL/min of CO_2 was brought via a stainless tube through the column heated inside an oven. The oven (oven Memmert RW) was kept at 120°C. The exhaust CO_2 flow was cooled down through a stainless-steel coil immersed in crushed ice. The flow then bubbled in a 50mL of 1M NaOH to trap uncondensed VFA.

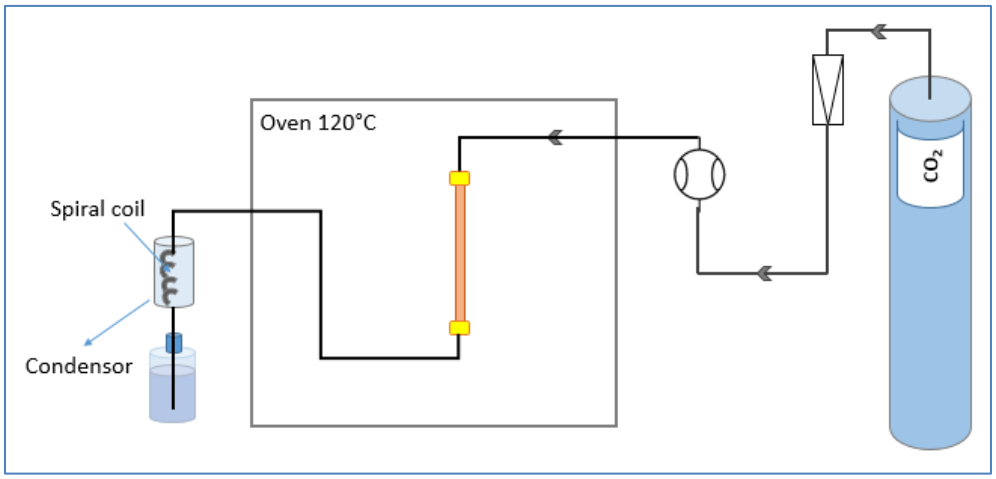

Figure 4-3: Scheme of thermal desorption using design T2.

CO_2 desorption: design C1

For the desorption with CO_2, the first tests (figure 4-4) were realized in an oven Memmert RW maintained at 60°C. The CO_2 gas flows at the rate of 5 mL/min through a spiral coil in a 2L scotch bottle containing approximately 1500 mL of water to heat and saturate the gas with water vapor. The warm and humidified CO_2 flow than leaves

the bottle by another opening and then passes through the glass column charged with resin, ending in a 1-liter solution of 1M NaOH.

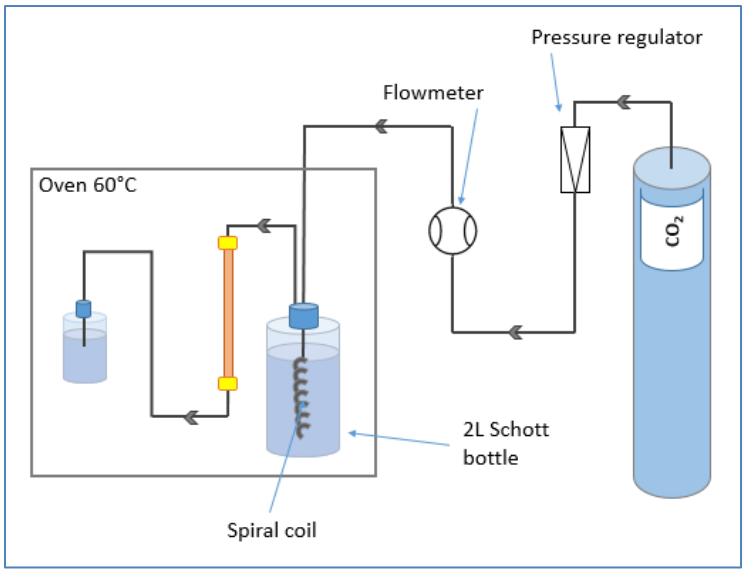

Figure 4-4: Scheme of CO_2 desorption using an oven, design C1.

CO_2 desorption: design C2

The experimental design (figure 4-5) consisted in suspending the resin in water and bubbling the CO_2 in the water/resin suspension, the CO_2 being carried through a tube to the bottom of the glass tube. The exhaust vapors were trapped in a 100 mL 1M sodium hydroxide solution.

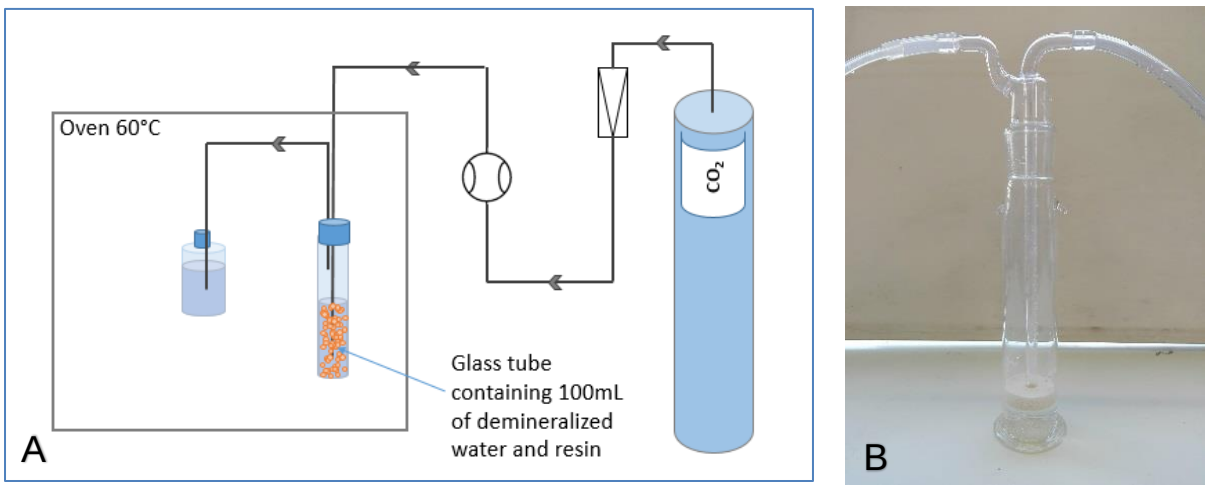

Figure 4-5: (A) Scheme of CO_2 desorption using immerged resin, design C2. (B) Close-up of the glass recipient with the dipping tube and resins in suspension.

CO_2 desorption: design C3

The resin was suspended in 100 mL of water in a stainless steel container of 350 mL crafted in UCL laboratories (Figure 4-6). CO_2 was first flushed for 2 minutes through a

plunging tube to enable evacuation of the air inside the container. Then, the outlet valve was closed and pressure was progressively increased to reach 3 bars. CO_2 pressure was maintained for various times. During these times, the container was periodically agitated manually. The aqueous solution could then be recovered by opening the 3-way valve, since the pressure inside the container pushed the liquid out via the plunging tube that had a sintered glass at the end, disabling the passage of the resin particles.

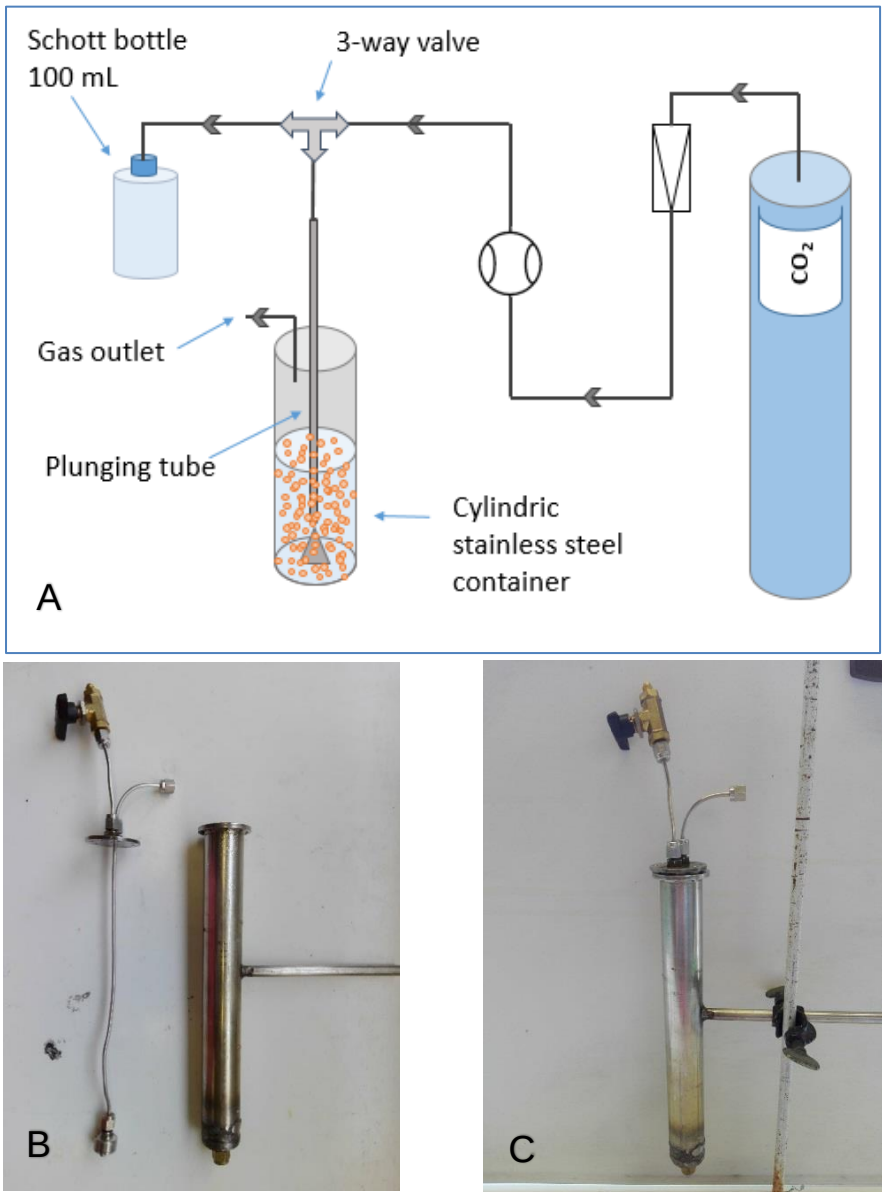

Figure 4-6: (A) Scheme of CO_2 desorption using design C3. Cylindric inox recipient (B) unassembled and (C) assembled.

CO_2 desorption: design C4

Other tests were proceeded with a pressure reactor of about 300 mL (4560 mini reactor, Parr Instrument company, USA) containing 10 grams of resins suspended in 100 mL of demineralized water. The experimental setup is illustrated in figure 4-7. The

controller was a Parr 4848 reactor controller (Parr Instrument company, USA). Before starting to raise temperature and pressure, CO_2 was flushed for 2 minutes to remove the air contained in the reactor. After the flush, the temperature was slowly increased until reaching the desired value. At that point, the CO_2 pressure was risen and the stirrer was set at 200 rpm. After one hour of water-resin equilibration, the aqueous phase inside the Parr reactor was removed by the liquid outlet. 1 mL of the aqueous phase was taken for further HPLC analysis.

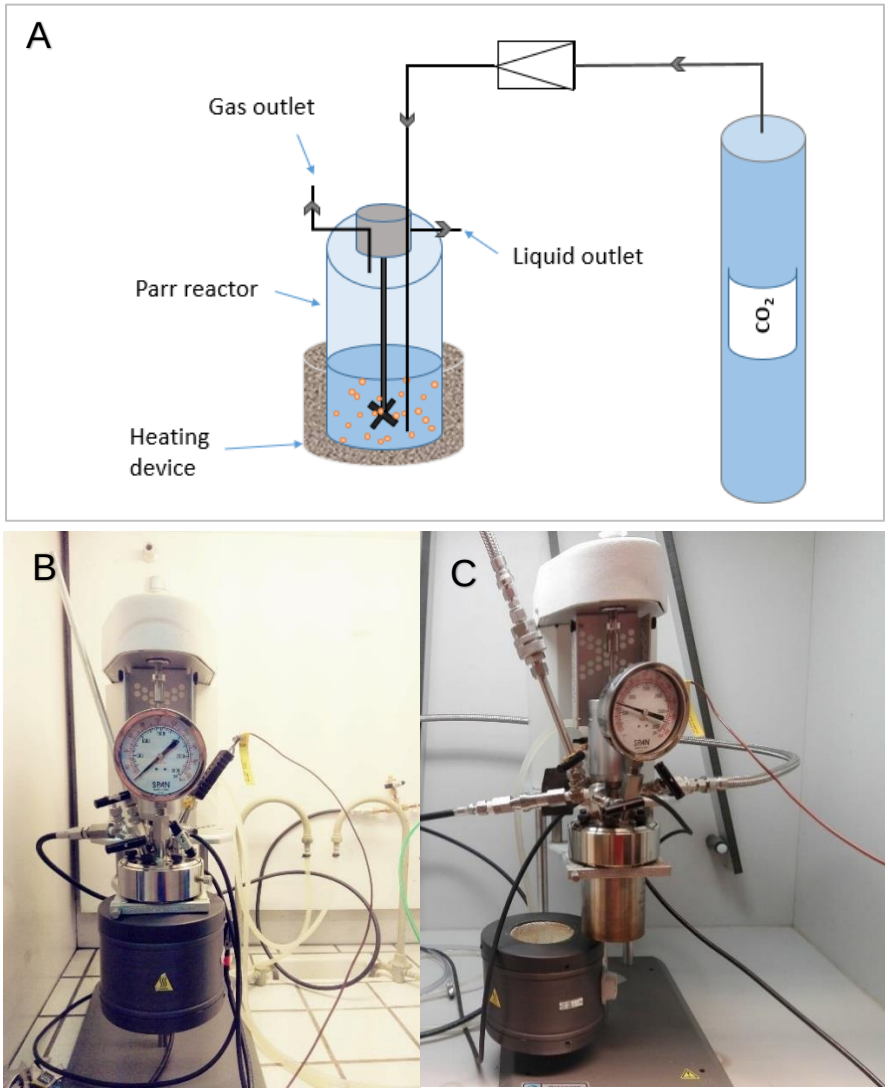

Figure 4-7: Parr reactor. (A) Scheme of desorption with the Parr reactor, design C4. Parr reactor with the heating device (B) or without it (C).

4.1.3 NaOH desorption of remaining VFA

NaOH desorption: design A

Any residual adsorbed VFA on the resin was desorbed with a 1M NaOH solution for further quantification. In the first experiments (figure 4-8A), washing was done by recirculating a solution of 100 mL of 1M NaOH at 0.4 mL/s.

NaOH desorption: design B

Experiments indicated that desorption by elution was more efficient for recovery of any residual VFA. Desorption was then performed by passing 100 mL of 1M NaOH at a flow of 0.1 mL/s (figure 4-8B).

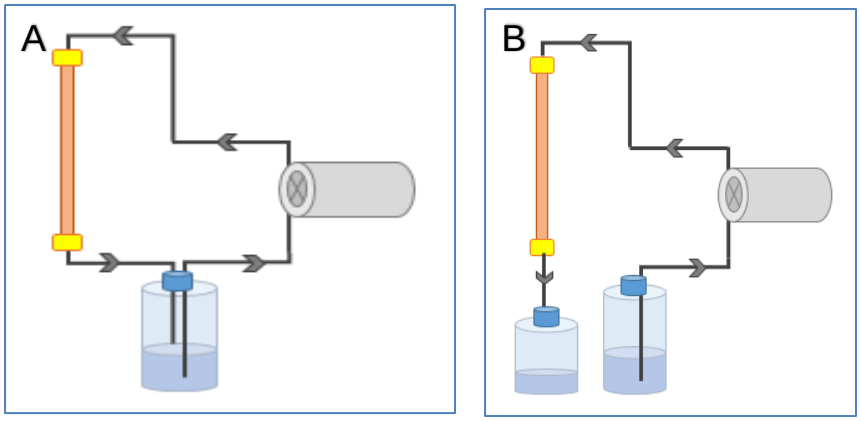

Figure 4-8: Resin washing using a recirculating flow (A) and elution (B).

4.3 VFA analysis

4.3.1 Analytical samples preparation

Analytical samples used for HPLC analysis were prepared in a 2 mL eppendorf by adding 150 µL of H_2SO_4 0.6M, 250 µL of sample to be analyzed, 200 µL of 4-methylvaleric acid used as intern standard and 650 µL of water.

4.3.2 Volatile fatty acids

Concentration of the volatile fatty acids was determined with a high-performance liquid chromatograph (Agilent 1200 series, Agilent technologies, Belgium). The chromatograph was equipped with a storage bottle of eluent, a degasser, a quaternary pump to insure the eluent flow, an automatic injector, a Micro-Guard Cation H pre-column (30 mm x 4.6 mm, Bio-Rad, USA) and an Aminex HPX-87H column (300 mm x 7.8 mm, Bio-Rad, United States). 50 µL of the analytical samples were injected and eluted with a 5mM H_2SO_4 aqueous mobile phase in milli-Q water with a constant rate flow of 0.6 mL/min. The temperature in the column was set to 65°C. Two detectors were placed in series after the column. The first detector was a UV-Visible diode array detector (DAD) and the second detector was a refractive index detector (RID).

Before launching a sample analysis, the purge valve was opened so that canals could be purged for 5 minutes at 3 mL/min. Next, the column was replaced by a connector,

the purge valve was closed and tubes were then further purged during 3 minutes at 2 mL/min. The connector was then removed and the inlet of column was connected while the outlet was kept disconnected. The flow was set to 0.1 mL/min until the first drops could be observed at the outlet of the column. At that point, the outlet was connected to the tube that leads to the detectors. The flow was risen progressively until reaching 0.6mL/min. Once the desired temperature of the column was reached and the UV signal was stabilized, analysis could be launched.

4.3.3 Calibration

For each analysis cycle, calibration lines (R^2 > 99%) were obtained with 0.2, 0.1, 0.02, 0.01 g/L of lactic acid, acetic acid and butyric acid calibration solutions, and with 0.05, 0.1, 0.5, 1.0 g/L of propionic acid, valeric acid, iso-valeric acid, iso-butyric acid and acid caproïc acid calibration solutions.

4.3.4 Calculation

Acetic and butyric acid concentrations in samples were calculated by measuring the peak areas obtained during HPLC analysis and by using a calibration line.

$$[\text{Volatile fatty acid}] = \frac{\text{Area}_{\text{compound}}}{\text{Area}_{4-\text{MV}}} * \text{slope}_{\text{compound}}$$

With:

$[\text{Volatile fatty acid}]$	Compound (acetic or butyric acid) concentration (ppm)
$\text{Area}_{\text{compound}}$	Peak area of a given compound (internal standard, VFAs)
$\text{slope}_{\text{compound}_{\text{DAD}}}$	Slope of the calibration line of the compound (acetic or butyric acid)

4.4 Mass balance in the adsorption-desorption experiments

4.4.1 Initial amount of VFA

The initial amount of VFA introduced in the 100 mL vial, $VFA_{initial,}$ is initially controlled by injecting the desired volume of VFA with a micropipette in a 100 mL volumetric flask. The quantity of VFA is verified by taking the weight after injecting the volume on

an analytical weight scale, and 1 mL of the 100 mL solution is then taken for HPLC analysis.

4.4.2 Amount of VFA adsorbed on the resin

The quantity of VFAs adsorbed during the adsorption step is measured by subtracting the remaining number of moles in solution after the adsorption step ($VFA_{not\ adsorbed}$) plus the VFAs that were present in the rinsing waters (VFA_{rinsed}) from the initial number of moles.

$$VFA_{adsorbed} = VFA_{initial} - VFA_{not\ adsorbed} - VFA_{rinsed}$$

4.4.3 Amount of VFA desorbed

The number of moles desorbed, $VFA_{desorbed,}$ is calculated directly from the solution containing the desorbed VFAs.

4.4.4 Amount of residual VFA

During the NaOH desorption step for measuring residual VFAs, the number of moles desorbed, $VFA_{desorbed\text{-}NaOH,}$ is calculated directly from the solution containing the NaOH-desorbed VFAs.

4.4.5 Amount of unrecovered VFA

The amount of VFA unrecovered during the process is calculated by subtracting the amount adsorbed by the amount recovered in the desorbed solutions.

$$VFA_{lost} = VFA_{adsorbed} - VFA_{desorbed} - VFA_{desorbed\text{-}NaOH}$$

5. Results

All experiments were performed in the framework of an exploratory approach and were performed only once. No error bars are presented with the results. Nevertheless, analytical reproducibility was usually better than 5%.

5.1 VFA adsorption on resins

The first step was to characterize the **kinetics of adsorption** of the two VFAs used on the three resins chosen. The purpose was to measure after how much time an equilibrium would be reached between the VFAs present in the solution and the ones adsorbed, to know what adsorption time is needed for the further experiments. After conditioning the resin, adsorption was performed for one hour and a 1 mL sample of the model solution (MS) was taken every 15 minutes. It was also possible to calculate **resin capacity** after the equilibrium was reached.

The 100 mL model solution contained 8mmol of acetic acid (HAc) and 8mmol of butyric acid (HBu). To measure the impact of the pH on the capacity of the resins, the MS was prepared with three different pH values. pH was unchanged (pH 3), adjusted to 4.8 or 6. To basify the pH of the MS, sodium hydroxide was added. The value 4.8 corresponds to a value close to the HBu and HAc pK_a, since the pK_a of HBu is 4.81 and HAc is 4.75 (López-Garzón and Straathof, 2014). The pH value 6 is close to the pH of a representative fermentation broth.

The kinetics of adsorption for the weak base resin (Purolite A103Splus, tertiary amine) (Figure 5-1) shows that equilibrium is not completely reached after 15 minutes and the adsorption only seem to stabilize between 45 and 60 minutes. The strongest adsorbed molar fraction was observed after one hour with the MS of pH=3, with molar fractions of 0.93 and 0.96 for acetic and butyric acid respectively. Concerning the MS of pH=4.8, adsorbed molar fractions reached 0.48 and 0.69 for HAc and HBu respectively, indicating a decrease in the adsorption of VFAs when initial pH is increased. This was further confirmed by the pH6-MS, which showed low VFA adsorption. Altogether, the data indicate that 60 minutes of recirculation are necessary for maximized adsorption on the resin, and the initial pH strongly influences the adsorption equilibrium, as adsorption is enhanced with low pH values.

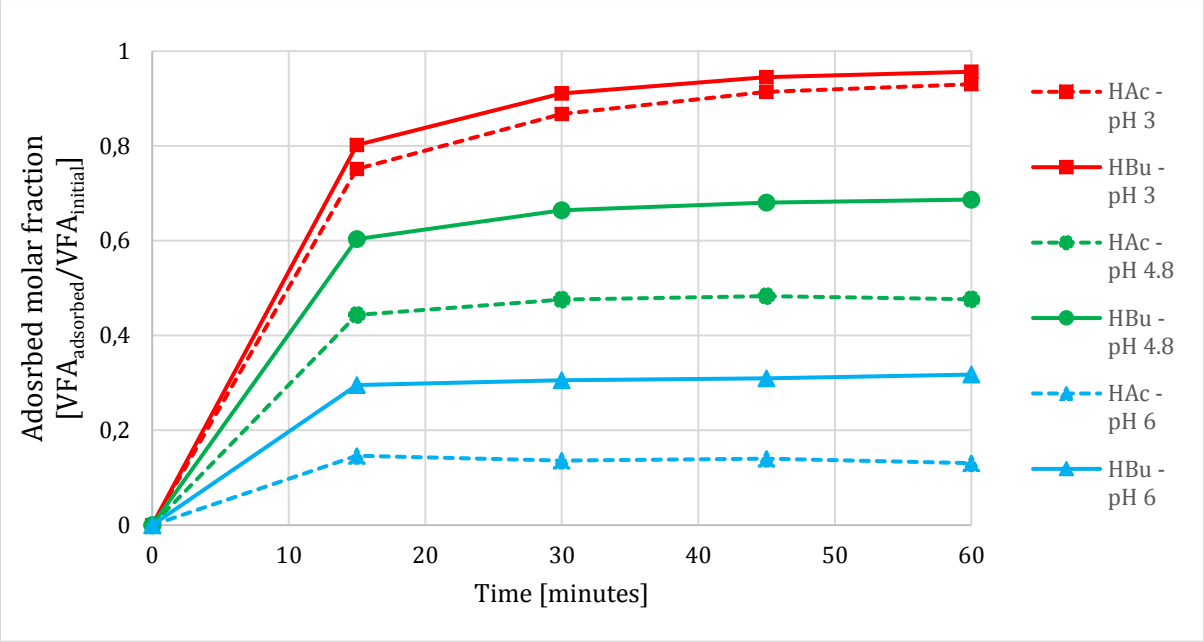

Figure 5-1: Kinetics of VFA adsorption on the weak base resin (tertiary amine) with model solutions of different pH values.

Adsorption on the strong basic resin (Purolite SGA 550, quaternary ammonium) (Figure 5-2) shows no significant difference in the adsorbed molar fraction between 15 and 60 minutes. It can be estimated that maximized adsorption equilibrium is reached in 15 minutes or less. The adsorbed molar fraction was stronger for low MS-pH values. Molar fractions of 0.93 HAc/HAc$_{initial}$ and 0.95 HBu/ HBu$_{initial}$ could be adsorbed when the MS had a pH=3. These data indicate that low pH values enhance the adsorbed molar fraction and 15 minutes of adsorption are sufficient for equilibrium to be reached.

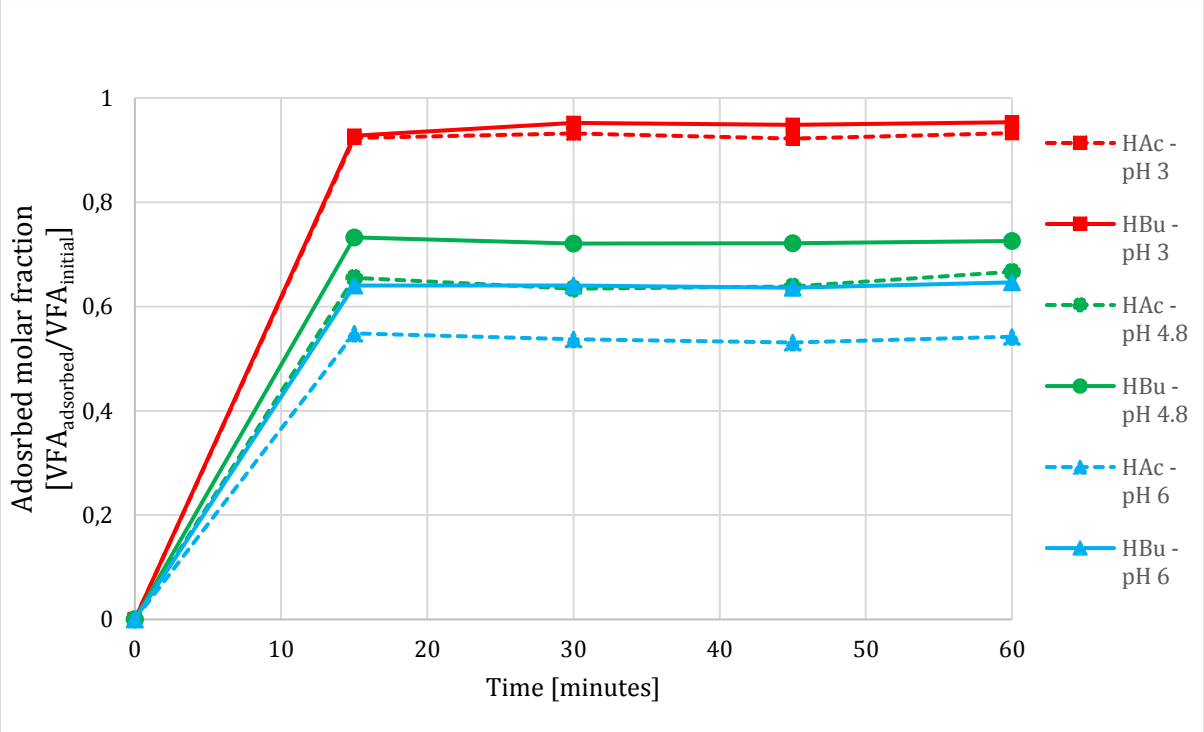

Figure 5-2: Kinetics of VFA adsorption on the strong base resin (quaternary ammonium) with model solutions of different pH values.

The comparison of the adsorption profile of the weak base resin with the strong base resin (Figure 5-1, Figure 5-2) shows that with both types of resins, adsorption is affected by the initial pH of the MS. In contrast, while the resins show similar performances at pH=3, the data show that a higher pH value affects more the weak base resin than the strong base resin.

Adsorption on the non-ionic resin (Mitsubitchi Chemical Sepabeads SP207) was very different for HAc and HBu (Figure 5-3). As HBu could be well adsorbed at pH values of 3 and 4.8, its adsorption for pH=6 was very weak. HAc was only poorly adsorbed for all pH values. Equilibrium was reached within 15 minutes of adsorption. These results indicate that the non-ionic resin adsorbs selectively HBu and weakly HAc.

The adsorption is possibly linked to the hydrophobicity of the target molecule, so it is expected that a VFA with a longer carbon chain, whose hydrophobicity is higher (Yalkowsky et al., 2010), is more adsorbed on this resin.

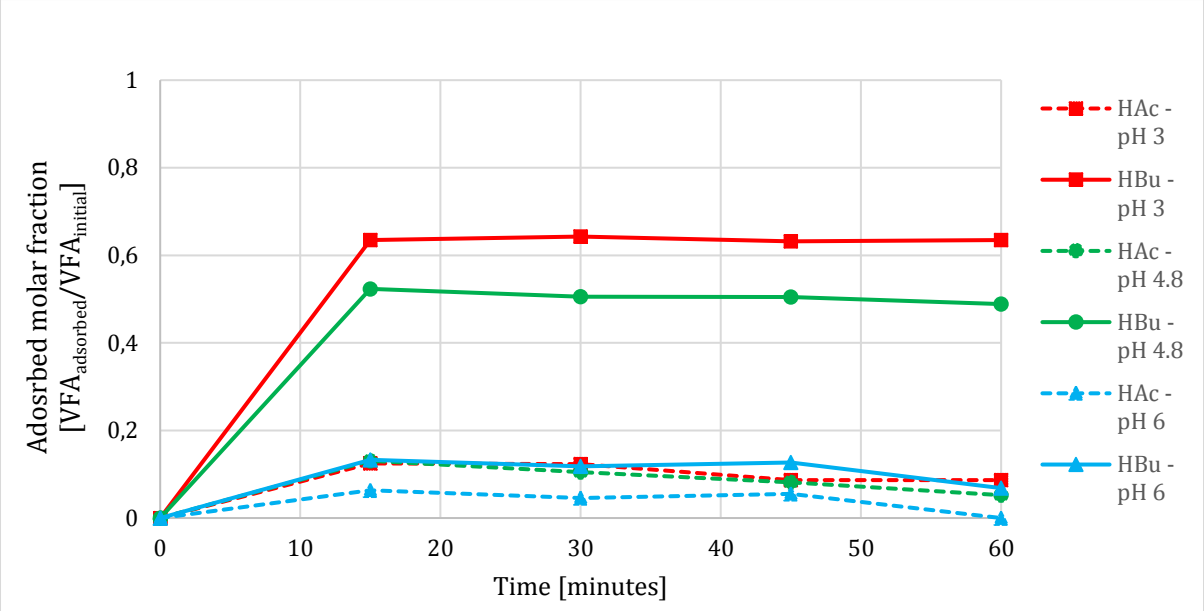

Figure 5-3: Kinetics of VFA adsorption on the non-ionic resin (bromine group) with model solutions of different pH values.

The pH of the model solutions (MS) were measured before and after adsorption (Table 5-1) because it was expected that the adsorption of acids increases the pH-value. Interestingly, the strong base caused the strongest pH increase of the MS.

Table 5-1: Measure of MS-pH before and after the adsorption step.

Initial pH	Final pH		
	Strong base	Weak base	Non-ionic
3	3.8	3.7	3.4
4.8	12.3	6.3	5.2
6	12.7	12.1	7

As seen in the theory, the mechanism of ion exchange is different for the weak base and the strong base. With the weak base resin, the VFA is adsorbed to the resin in its acid form. With the strong base resin, the carboxylate anion is adsorbed and exchanged with a hydroxide. For all initial pH values, the non-ionic resin systematically causes the weakest pH changes. This can be explained by the smaller fraction of adsorbed VFAs.

With all these results taken together, it is possible to conclude that initial pH=3 is the best from the three tested values for VFA adsorption, and at that initial acidity, the weak base and strong base resin show similar performances. Because pH=3 showed the strongest adsorption performances, the next experiments were all driven with pH=3 model solutions (except 5.2.1). At higher pH, the strong base resin is more efficient for adsorption. The non-ionic resin has some strong interest in the case of selective adsorption, as the weakly hydrophobic VFAs are expected to be weakly

adsorbed and the more hydrophobic VFAs (propionic, butyric, valeric, caproic acid) are expected to be strongly adsorbed.

5.2 CO_2-mediated VFA desorption

5.2.1 VFA desorption by volatilization in a CO_2 flow

The first design tested (C1) aimed at stripping the VFA out of the resin by a CO_2 steam. The CO_2 flow was saturated with water to keep the resin humid and allow the formation of carbonic acid to increase the volatility of VFAs. The CO_2 flow was also heated to increase the volatility of VFA. As it can be seen in Figure 5-4, the CO_2-mediated desorption was very weak. Quantification was difficult because the desorbed vapors were recovered in a 1-L solution, thus the VFAs were very diluted and close to the detection limit. Concerning the strong base desorption, when the HPLC peaks were detectable, they were too small to be quantified. CO_2-mediated desorption with the weak base resulted in some small amounts of VFAs measured for pH=4.8. It is the non-ionic resin that demonstrated the highest CO_2-desorbed molar fractions. For the pH=3, molar fractions of 0.085 HAc and 0.077 HBu were reached.

The results indicated that this design was not convenient for VFA desorption. It appeared that one of the problems with the resins contained inside the column was the humidity of the resins. After ~15 minutes, the resins took a very dry appearance, what could be explained by the hot CO_2 that flowed through the column and took the water vapor with it, supposing that it was not completely saturated with vapor when entering in contact with the resins. The results and observations during desorption indicated that the desorption process needed to be reviewed.

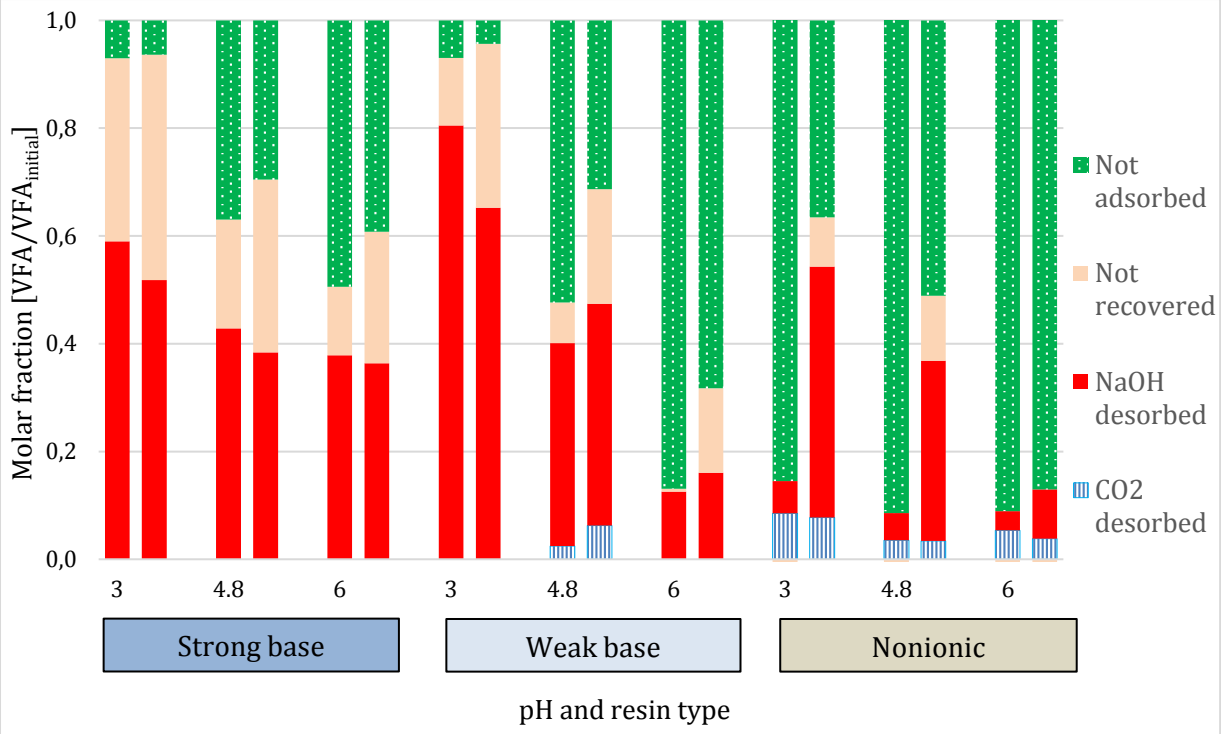

Figure 5-4: Molar fractions of VFAs. Experiments of adsorption and desorption using the 3 three types of resins and pH value 3, 4.8 and 6, with CO_2 desorption: design C1. Each pair of columns represents an experiment, where the left column is HAc and the right column is HBu.

5.2.2 VFA desorption in water under 1 bar CO_2

Due to the very weak results of experiments realized with design C1, we tried to optimize the desorption process. One of the points to improve was to maintain the resins wet. Since CO_2 needs water to form carbonic acid, and the ion exchanges take place in an aqueous phase, it is suspected that enough water can strongly enhance the CO_2-mediated desorption. A new desorption process was designed were the resin was suspended in 50 mL of water, and CO_2 sparged through the resin-water suspension. The CO_2 bubbles were also expected to agitate the resin suspension. As illustrated in Figure 5-5, the CO_2-desorbed molar fractions were still very weak, not exceeding 0.05 $VFA_{desorbed}/VFA_{initial}$. Furthermore, the recovered VFAs were found in the aqueous solution with the resins, and no VFA was detected in the NaOH trap on the gas exhaust. These results indicate that carbonic acid with a 1 atm CO_2 partial pressure is not sufficient for efficient VFA desorption.

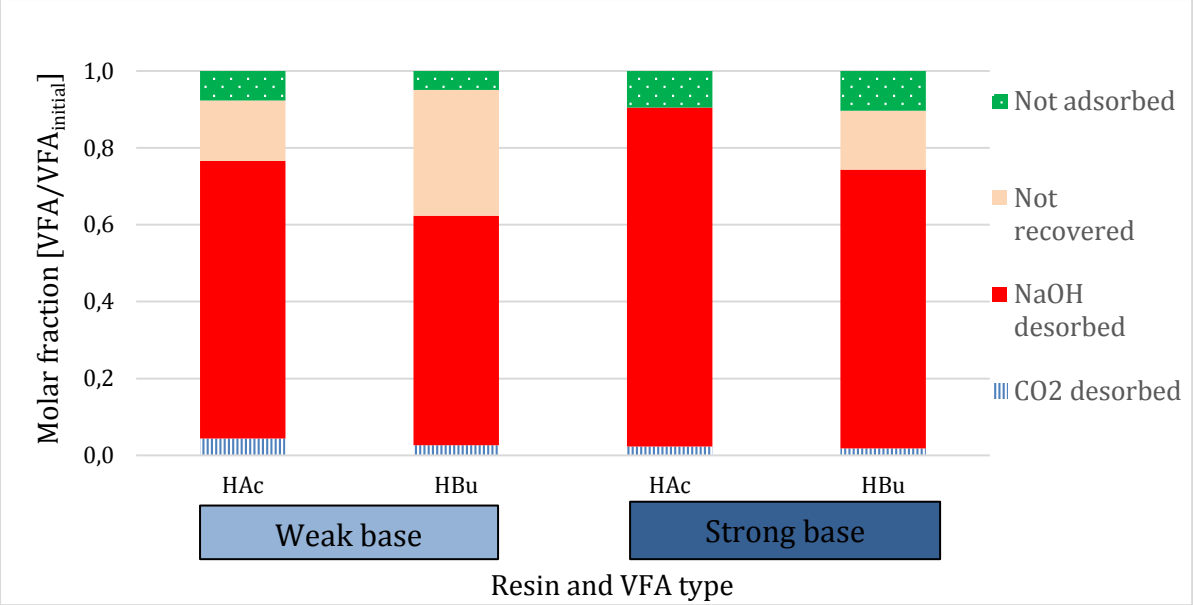

Figure 5-5: Molar fractions on VFAs. Experiments of desorption with design C3, the resins are suspended in water sparged with CO_2 at 1atm.

5.2.3 VFA desorption in water under 3 bar CO_2

We further thought that the increase in CO_2 pressure could increase the acidity of the solution and affect the VFA desorption. Here, a stainless-steel container resistant to 10 bar was used. A pressure of 3 bar was set inside the container, and it was regularly shaken to homogenize the resin in suspension. The container was maintained under pressure for 30 minutes or 24 hours. As shown in Figure 5-6, the CO_2-mediated desorption showed poor results, as the maximal molar fraction reached 0.053 $HAc_{desorbed\text{-}CO2}/HAc_{initial}$ for the 24-hour desorption. With a slightly better desorbed molar fraction as compared to the desorption using design C2, the results indicated that the process should be further optimized.

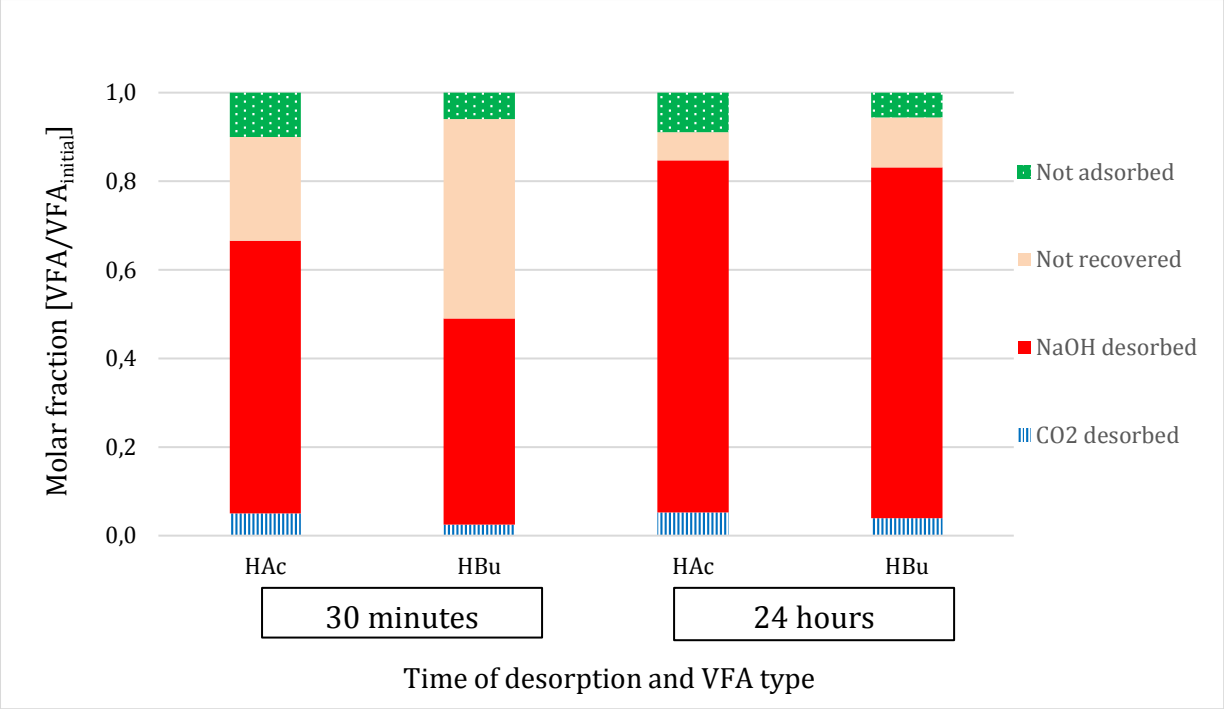

Figure 5-6: VFA desorption using design C3. Weak base resin was used and CO_2 pressure was increased to 3 bar.

Figure 5-6 also shows a decrease in the not recovered fraction for the 24hours experiment. The 30 minutes experiment was realized with a NaOH solution that was recirculating and the 24hours experiment was performed with eluted NaOH, what explains the higher NaOH desorption results for the 24 hours experiment, but that does not influence the CO_2-mediated desorption because it is a posterior step.

5.2.4 VFA desorption in water under up to 40 bar CO_2

As the design C3 was not practical to use and unsafe for higher pressures, design C4 was necessary. Design C4, using a Parr reactor, enables to reach higher pressures and easier control of parameters such as temperature and agitation.

Kinetics

It was first necessary to check the kinetics of CO_2 dissolution and VFA desorption with the Parr reactor. In these experiments, pressure was set to 20 bar. After 5 minutes, the pressure decreased slightly, enough to be observable, so the CO_2 valve was opened to readjust the CO_2 pressure to 20 bar. After this step, the pressure did not observably decrease, so it was concluded that 5 minutes are sufficient for the pressurized CO_2 to dissolve in the water.

The kinetics of desorption was tested in the Parr with the weak and strong base resin. The pressure was set to 20 bar of CO_2 and a sample was taken every 10 minutes for

one hour. Figure 5-7 shows that the desorption equilibrium is reached after 30-40 minutes for the weak base resin and after 40-60 minutes for the strong base resin.

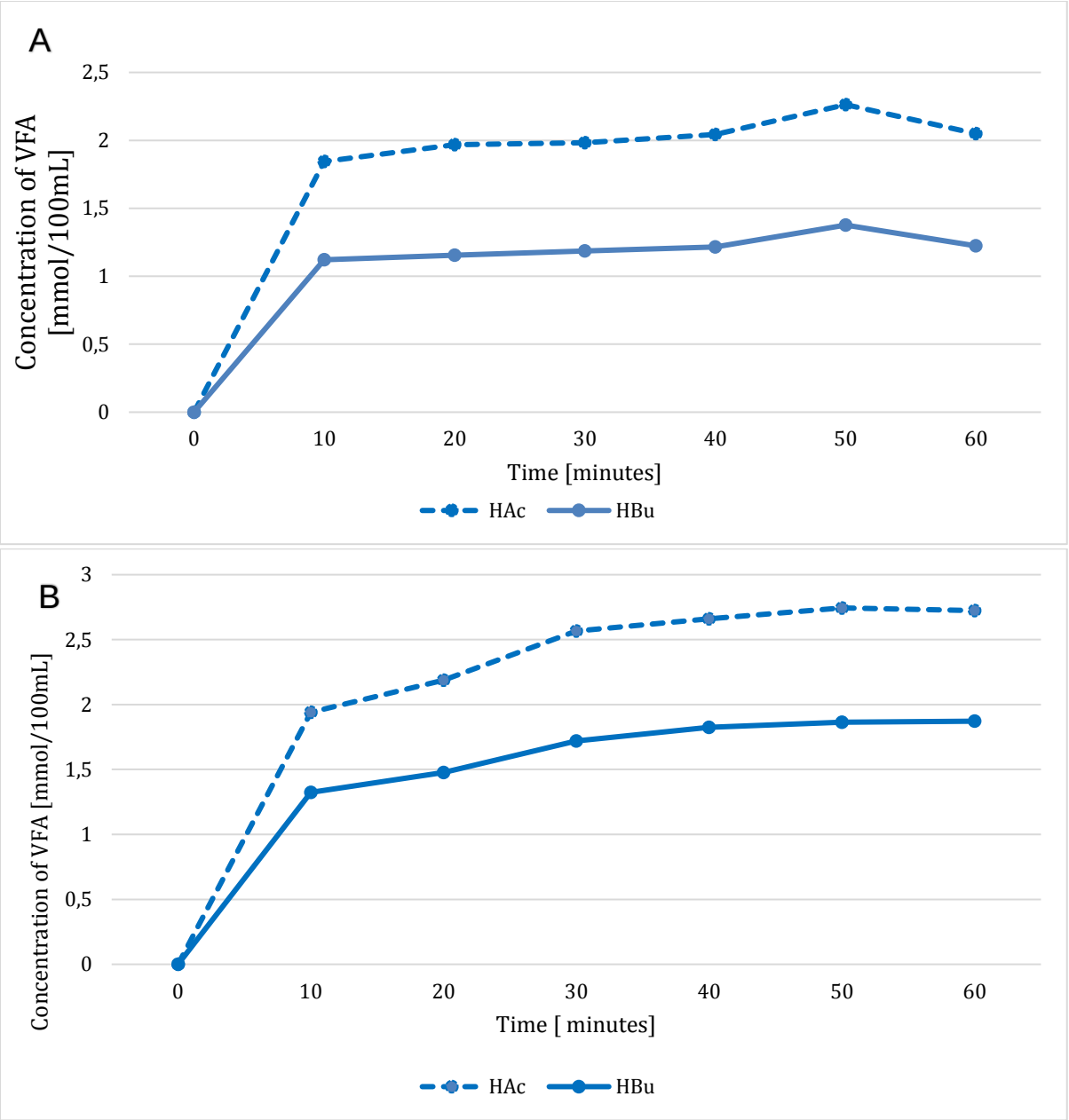

Figure 5-7: Study of desorption kinetics using a Parr reactor under 20 bar for (A) the weak base resin and (B) the strong base resin.

Influence of temperature

Three desorption temperatures were tested with the Parr reactor. A desorption time of 1 hour was selected on the basis of the previous results. Figure 5-8 shows that temperature has no strong effect on the CO_2-mediated desorption.

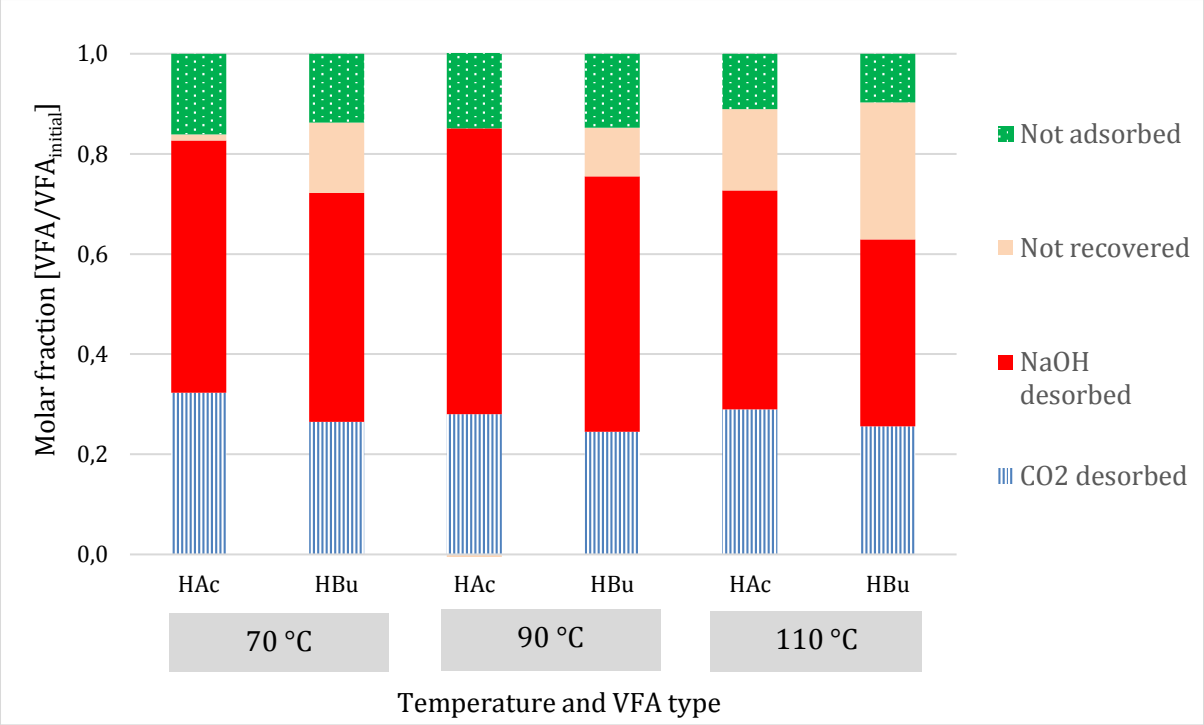

Figure 5-8: Effect of temperature on CO_2-mediated desorption in the Parr reactor. The desorption was performed with a CO_2 pressure of 40 bar and the strong base resin.

Influence of CO_2 pressure

Four CO_2 pressures (1, 5, 20, 40 bar) were applied to investigate the influence of CO_2 pressure on the efficiency of desorption. As there were no clear effects of temperature on the desorption, the experiments were performed at 20°C.

The data (Figure 5-9, Figure 5-10, Figure 5-11) shows that an increase in CO_2-pressure has a strong effect on the desorption for all the 3 types of resins tested. For the ionic resins, the CO_2-desorbed molar fractions are systematically higher for HAc compared to HBu. The highest molar fraction recovered is HAc at 40 bar with the strong base resin, reaching 0.44 $HAc_{desorbed}/HAc_{initial}$.

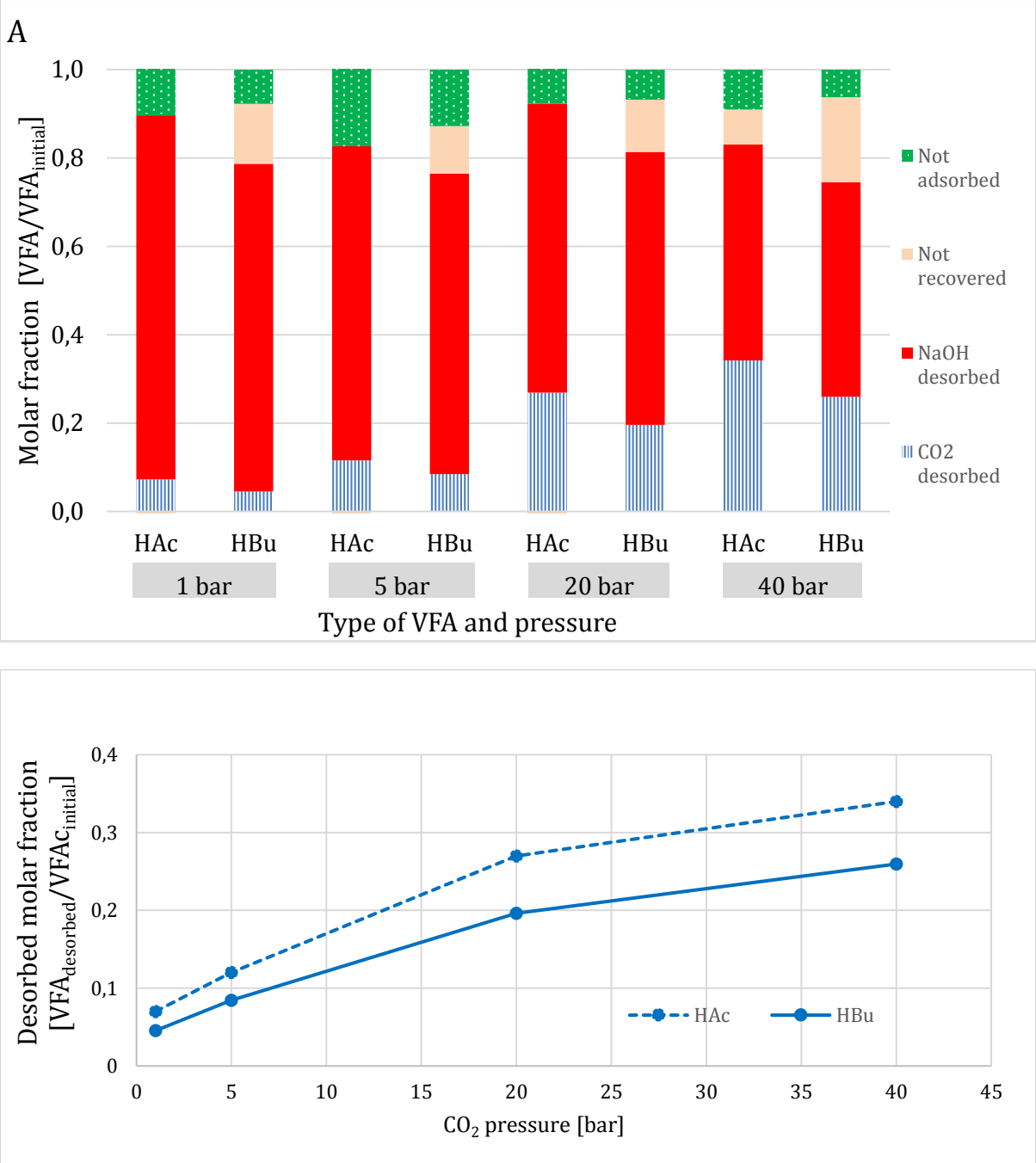

Figure 5-9: (A) Effect of CO_2 pressure on the CO_2-mediated desorption in the Parr reactor containing the weak base resin. (B) Plot of the VFA desorbed molar fraction as a function of the CO_2 pressure.

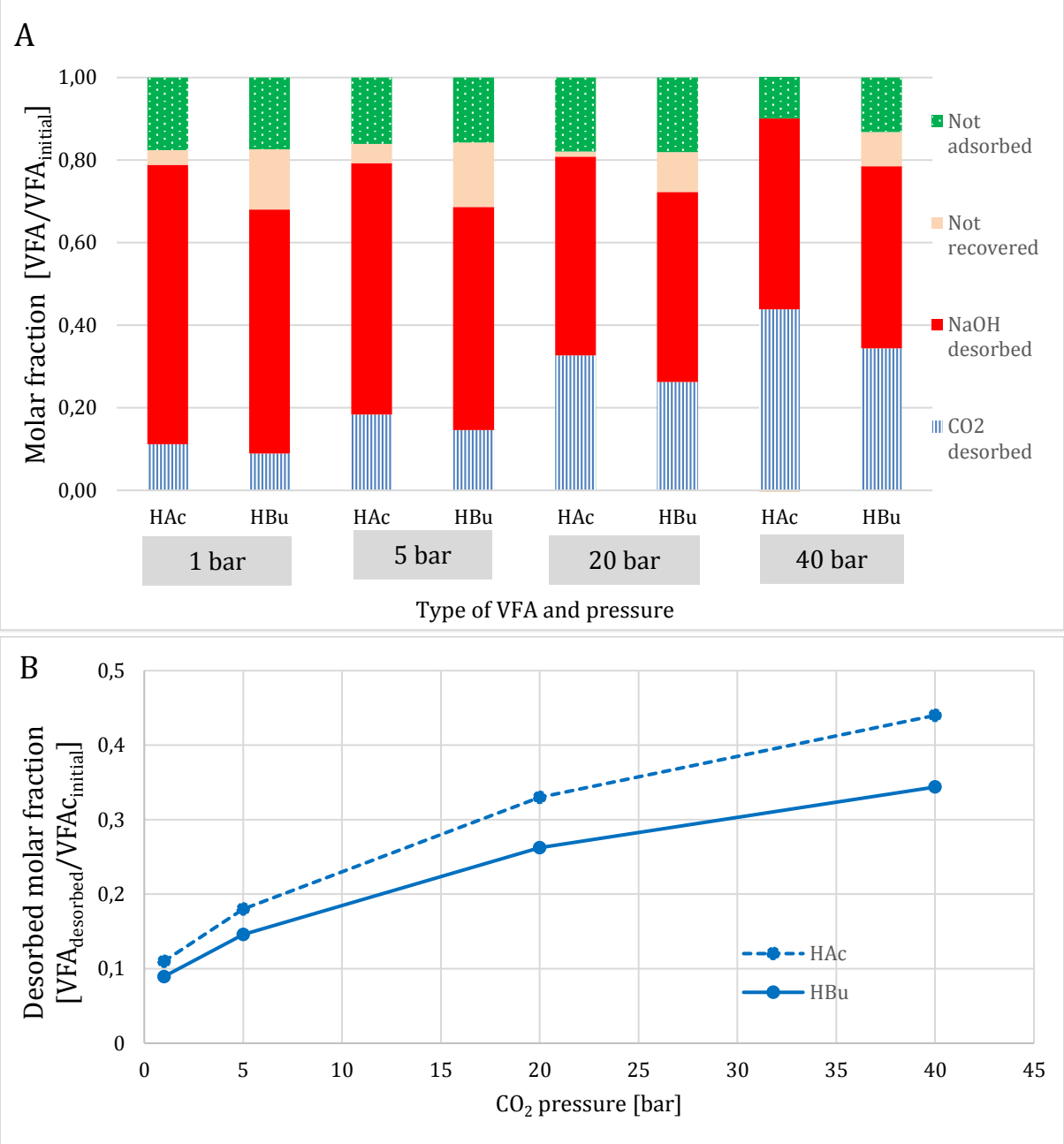

Figure 5-10: (A) Effect of CO_2 pressure on the CO_2-mediated desorption in the Parr reactor containing the strong base resin. (B) Plot of the VFA desorbed molar fraction as a function of the CO_2 pressure.

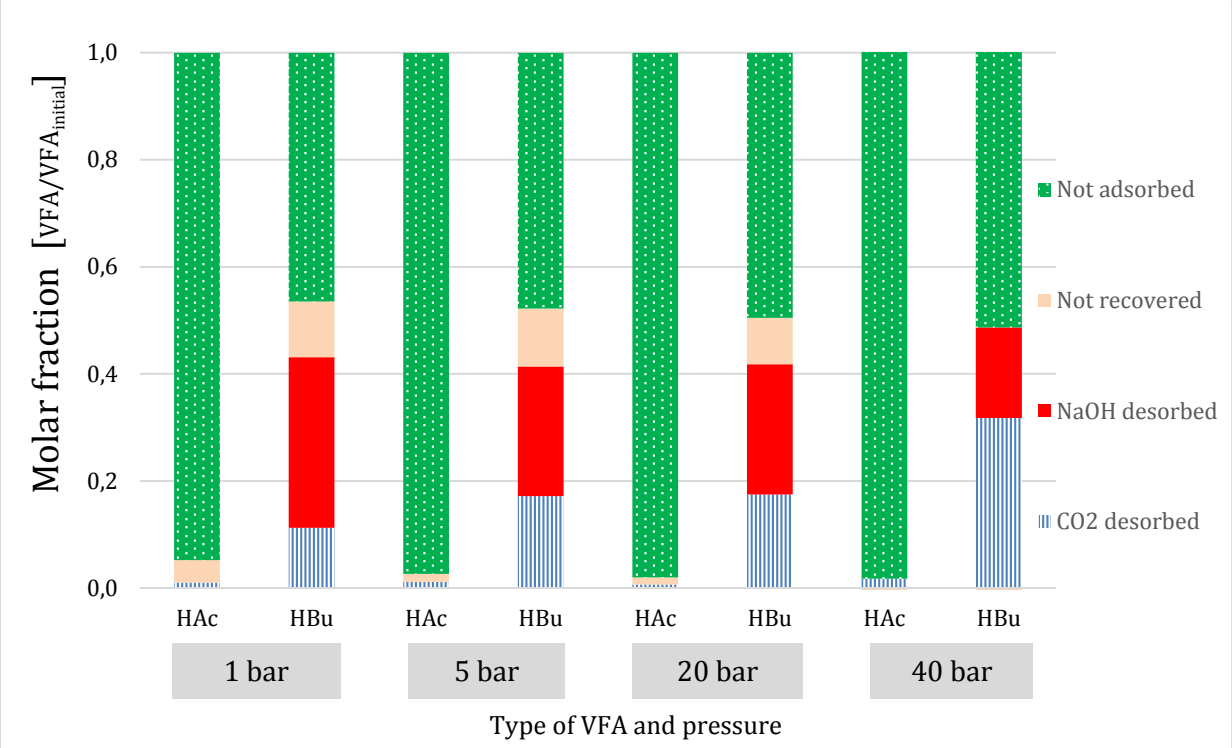

Figure 5-11: Effect of CO_2 pressure on the CO_2-mediated desorption in the Parr reactor containing the non-ionic resin.

As already mentioned, it was not surprising to see a very different profile with the non-ionic resin, as it was already noticed that HAc was very weakly adsorbed. At 40 bars, HBu was particularly well desorbed by CO_2.

Together, these results confirm that CO_2-mediated VFA desorption is possible and suggest a non-linear relation between the CO_2 pressure set inside the reactor and the desorbed fraction of VFAs. Slightly increasing the pressure is interesting for desorption but increasing the pressure more will not desorb proportionally more VFAs.

5.3 Thermal desorption

Since the non-ionic resin binds the VFAs with hydrophobic interactions, it was thought that desorption can be done with heat, so that the VFAs, in a vapor phase, can be condensed and recovered in a concentrated form.

5.3.1 Thermal desorption: design T1

We wanted to further investigate the feasibility of this process and operated with a setup similar to a distillation. The heating was maintained for 2 hours and the vapors were condensed and trapped in a sodium hydroxide solution. The results (Figure 5-12) indicate that the molar fraction desorbed is very weak, 0.075 $HBu_{desorbed-thermally}/HBu_{initial}$. During the 2 hours of desorption, the resin was suspended in a small quantity of water (not measured), and the head of the distillation pot did not reach

higher temperatures than 80°C, although the pot was plunged in oil at 120°C. Strangely, the not recovered fraction was very high. These data and observations suggest that the water present in the pot might disable an efficient thermal desorption.

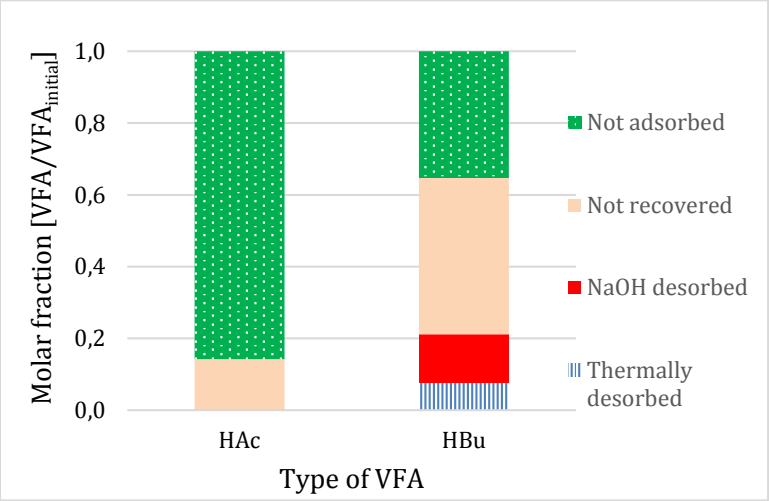

Figure 5-12: Thermal desorption using design T1.

5.3.2 Thermal desorption: VFA stripping with CO_2

The weak results of the desorption using design T1 encouraged to rethink the design of the process. We further wanted to investigate if the thermal desorption would be more efficient with a gas vector that would carry the vapors of desorbed VFA. Using directly the column for the desorption instead of transferring the resins to a pot also simplified the manipulations and allowed the resins to keep dry, since the transfer to a pot necessitates resuspending the resin in water. For this thermal desorption, the column loaded with resin was set inside an oven at 120°C, CO_2 flowed through the column, carrying the vapors of VFA to a condenser and ending in a sodium hydroxide solution as a final trap. A sample was taken every 15 minutes to study the kinetics of desorption.

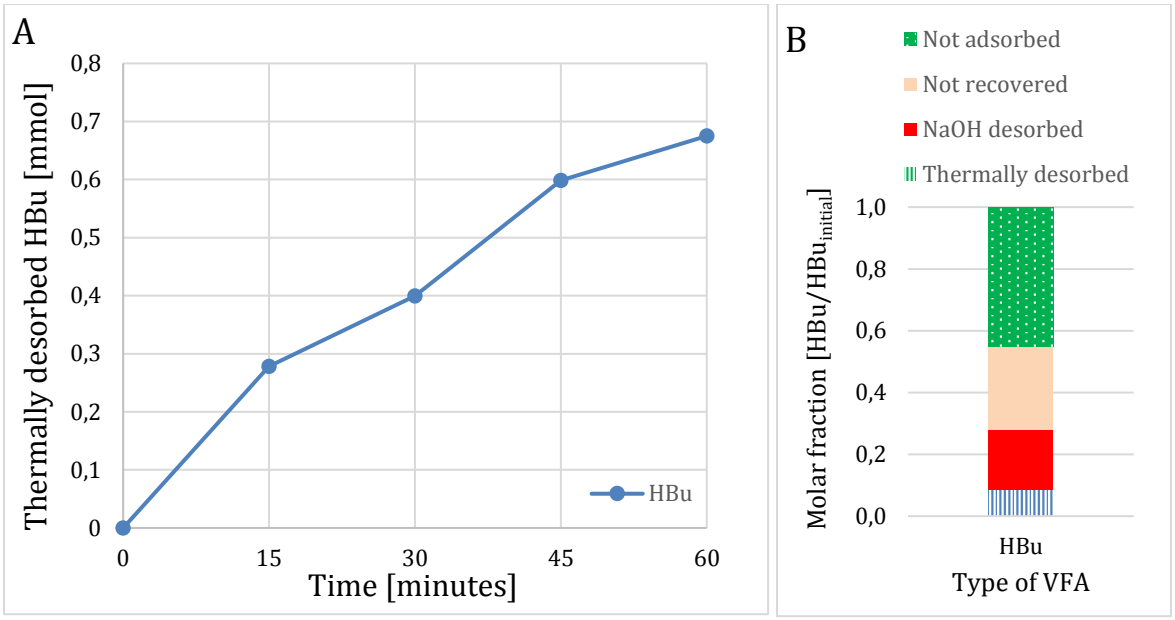

Figure 5-13: Thermal desorption using design T2. (A) Kinetics of thermal desorption, a sample is taken from the NaOH solution every 15 minutes. (B) Molar fractions after one hour of desorption.

Figure 5-13 shows that the quantity of desorbed HBu increases with time. HAc is not shown because the peaks obtained during HPLC analysis were too small to be quantified. The final desorbed quantity of HBu represents only a small molar fraction: 0.085 $HBu_{desorbed\text{-}thermally}/HBu_{initial}$. This data indicates that a prolonged desorption time can increase the quantity of desorbed HBu.

5.4 Other desorption processes

5.4.1 Desorption by NaOH and NH_4Cl

Since NaOH-desorption is considered in the experiments as a second desorption step that enables the quantification of the VFAs still adsorbed on the resin, a lot of importance was also given to find the conditions that allow a full recovery of VFA. We wanted to investigate whether equilibrium with 1M NaOH solution is enough to desorb all VFA, or whether elution is needed to get full VFA desorption. In addition, we also wanted to test whether a NH_4Cl solution would be a better exchanger than NaOH

During these experiments, the VFAs were adsorbed on resins and then directly desorbed with NaOH or NH_4Cl, without any step of CO_2-or thermal desorption. The results for the weak base (Figure 5-14A) and the strong base resins (Figure 5-14B) indicate that NaOH equilibrium is the less efficient for VFA desorption, as NaOH in elution is slightly more efficient. Desorption is complete with NH_4Cl when using the strong base resin, and with the weak base HAc is completely recovered but not HBu. Altogether, these results suggest that using eluted NH_4Cl gives the highest VFA recovery of all the three compared methods, and for maximized desorption it is more adequate to use elution than a recirculation.

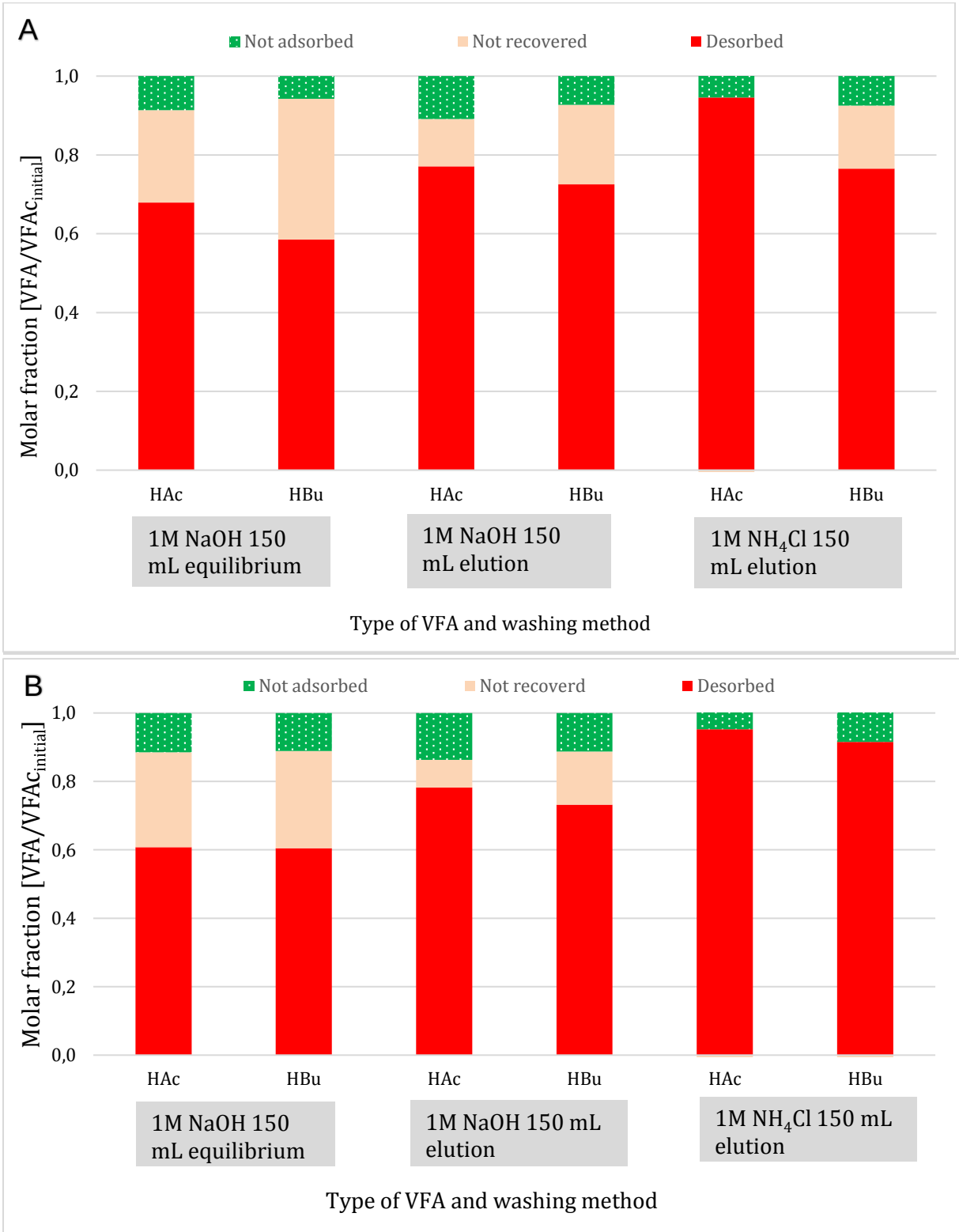

Figure 5-14: Desorption by elution or equilibrium of the VFAs using basic species with (A) is a weak base resin and (B) is a strong base resin.

5.4.2 NaOH desorption by elution

We tested the desorption profile when eluting the resin with NaOH. A desorption was realized by elution and every 20 mL of desorbed solution was taken and analyzed. The volume of NaOH was converted in amount of OH^- added divided by the amount of equivalent sites on the resin. As shown in Figure 5-15, the NaOH-mediated desorption is strong at the beginning and gradually there are less desorbed VFAs. With the weak base (Figure 5-15A), more than half of the total molar fraction of HAc and HBu is recovered with 3 mol OH^- per equivalent site on resin. With, in total 10 mol OH- per equivalent site on resin added, the last 5 mol OH^- per equivalent site only participate weakly to VFA desorption. The strong base (Figure 5-15B) shows similar results. These data indicate that for NaOH-mediated VFA desorption, the first mols OH^- per mol equivalent site added have the strongest impacts on VFA desorption.

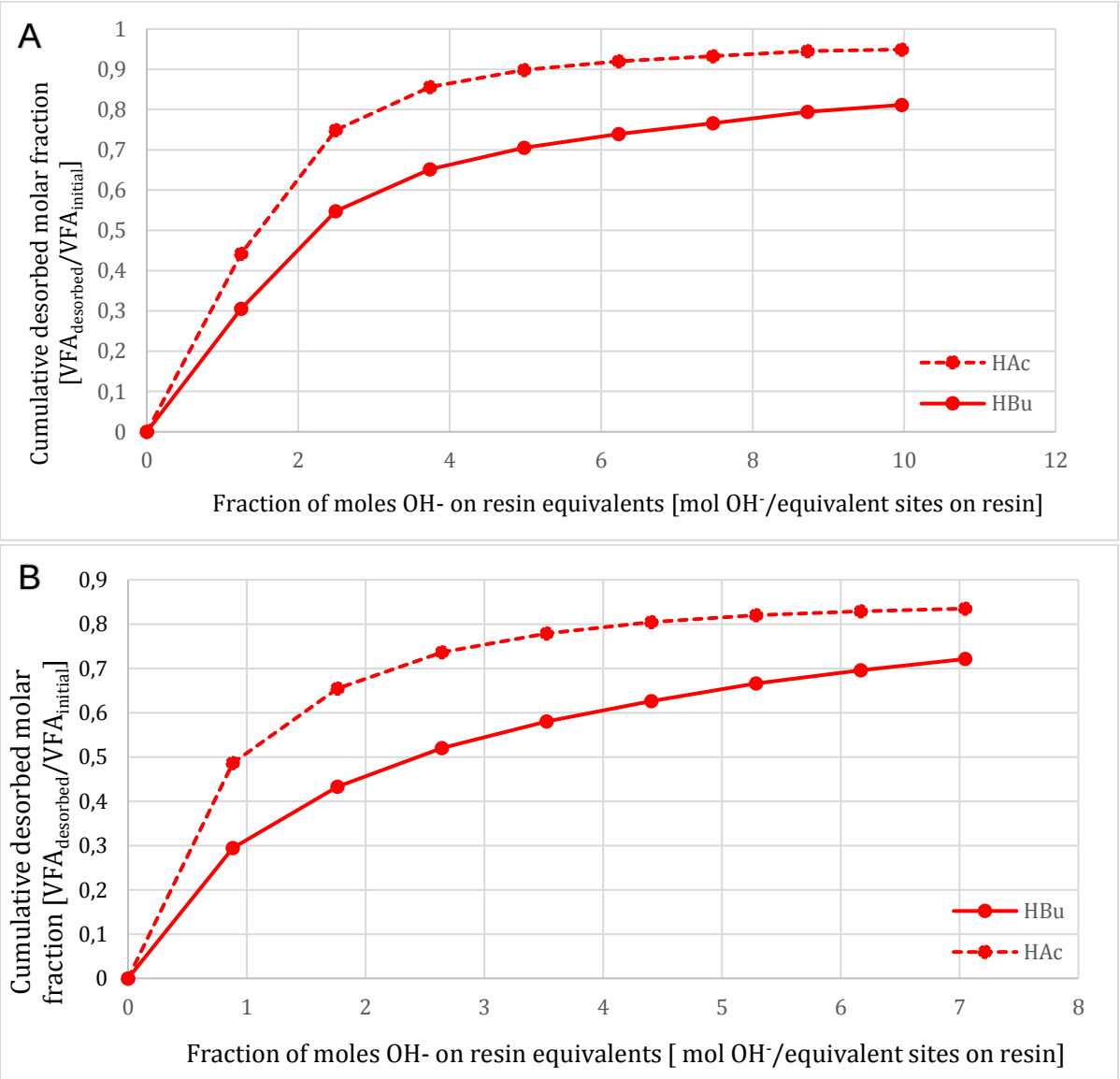

Figure 5-15: Desorption of VFAs by NaOH elution. The outgoing solution was collected by steps of 20 mL and each of them were analyzed for VFA concentration. The graph illustrates the cumulated molar fraction recovered with (A) the weak base resin and (B) the strong base resin.

6. Discussion

6.1 Adsorption of VFAs on the resins

6.1.1 Efficiency of the resins

The adsorption efficiency of the resins, which can be defined as the total amount of VFAs adsorbed per gram wet resin, is strongly influenced by the initial pH of the model solution, who in turn contributes to the equilibrium pH (see Table 5-1, p48). Our experiments show that adsorption with initial acidic conditions (pH=3) lead to a slight neutralization of the solution for all three resins used. In these conditions, the strong base and the weak base showed similar performances in terms of adsorbed VFA molar fractions, so one cannot be considered more efficient. In conditions of less acidic initial pH (pH=6), the adsorption process leads to a strongly basified solution (pH 12 – 13). The adsorbed molar fractions are also smaller and, in these conditions, the strong base is more efficient, followed by the weak base. These observations agree with the theories that consider that adsorption capacity of weak base resins is strongly influenced by the pH since a decrease in pH increases the protons available to enable ion pairing between the soluble acid and the amine (López-Garzón and Straathof, 2014).

6.1.2 Adsorption capacity of the resins

With the information provided by the ion exchange resin furnishers, the capacity can be determined in terms of equivalents (Table 6-1). This capacity determination is only possible for the ion exchange resins, the non-ionic resin does not carry any functional ion exchange group, so it does not have a determined capacity. The choice of the amount of VFA introduced in the model solution, 8 mmol of HAc and 8mmol of HBu, was calculated to correspond to the maximal capacity of the strong base resin. As can be seen in the Table 6-1, the weak base resin has a higher capacity, increased by more than 40% equivalents per gram wet resin.

Table 6-1: Ion exchange resin capacity characteristics.

Type of resin	Adsorption capacity (Eq/L_{resin})	Apparent density (g/L)	Milliequivalents for 10 grams wet resin	Total adsorbed VFAs with pH3-MS (mmol)
Weak base	1.5	645 – 675	22.73	15.24
Strong base	1.1	670 - 700	16.06	15.04

This means that, for the adsorption observed on the strong base resin, 15.24 mmol were adsorbed on a maximum of 16.06 that could have been adsorbed. In the case of the weak base resin, 15.04 mmol were adsorbed on a maximum of 22.73 mmol that

can be adsorbed (values from Figure 5-4). This further lets us think that while maximal capacity is almost reached for the strong base, the weak base could be charged with more VFAs if the MS was more concentrated. This further suggests that, in the optimal acidity conditions, the weak base resin would be more efficient for loading VFAs from a less dilute solution. This reasoning only considers the ion exchange processes, other hydrophobic forces can be responsible for adsorption.

6.2 CO_2-mediated desorption

One of the key interests in using pressurized CO_2 for desorption is that CO_2 is a costless product considered as waste during fermentation. Giving it a use is a way to recycle a waste product, even though a second adsorption cycle should release the carbonates from the resins, which means there is no net CO_2 capture during the process. If a suitable process relying on CO_2 desorption can be applied as an industrial process, this avoids the consumption of large quantities of strong base/acid. But another important advantage of using CO_2 as desorbant relies on the potential of recovering the VFAs under their protonated form, which is not the case during desorption with NaOH.

6.2.1 Ion exchange mechanism

It is thought that the CO_2-mediated desorption process happens according to these reactions:

$QH^+VFA^- + HCO_3^- + H^+ \leftrightharpoons QH^+HCO_3^- + HVFA$ For the weak base resin

$Q^+VFA^- + HCO_3^- + H^+ \leftrightharpoons Q^+HCO_3^- + HVFA$ For the strong base resin

6.2.2 Background theory

Since HCO_3^- is the key anion for the ion exchange process, it is interesting to identify the relation between the CO_2 partial pressure and the concentration of HCO_3^-. The conversion of CO_2 into HCO_3^- happens through 2 reactions and their respective equilibrium constants are function of temperature (Morse and Mackenzie, 1990). The equilibrium constants are given at 25°C and with zero ionic strength (Wang et al., 2010). When carbon dioxide is dissolved in water, it hydrates to form an acid:

$CO_{2(g)} + H_2O \leftrightharpoons H_2CO_3^*{}_{(aq)}$ $\qquad K_H = \frac{a_{H2CO3*(aq)}}{P_{CO2}} = 10^{-1.468}$

The term $H_2CO_3^*$ is referred in literature as the sum of $CO_{2(aq)}$ and H_2CO_3 (Butler, 1991). At equilibrium, $[H_2CO_3]$ is about 1000 times lower than $[CO_{2(aq)}]$. Carbonic acid deprotonates following the reaction:

$H_2CO_3^{*}{}_{(aq)} \leftrightharpoons H^+ + HCO_3^-$ $\qquad K_1 = \frac{a_{HCO3-}a_{H+}}{a_{H2CO3*(aq)}} = 10^{-6.352}$

The bicarbonate formed can undergo a second deprotonation:

$HCO_3^- \leftrightharpoons H^+ + CO_3^{2-}$ $\qquad K_2 = \frac{a_{CO3-}a_{H+}}{a_{HCO3-(aq)}} = 10^{-10.329}$

The relative proportions of the different carbonate species can be calculated using the equilibrium constants. If thermodynamic constants are used, activities must be employed instead of concentrations (Morse and Mackenzie, 1990). The activity of the i^{th} dissolved species (a_i) is related to its concentration (m_i) by an activity coefficient (y_i) so that:

$$a_i = y_i\, m_i$$

6.2.3 Ideal water-CO_2 system

In the case of a dilute ideal water-CO_2 closed system (water with a gaseous phase of CO_2), we assume that the activity coefficients are equal to unity so equilibria are defined by the molar concentrations (Peng et al., 2013). At a given temperature, the composition of the solution is completely determined by the partial pressure of carbon dioxide above the solution. By rearranging the constants of equilibrium, we find:

$$[HCO_3^-].[H^+] = K_1.[H_2CO_3^{*}{}_{(aq)}]$$
$$= K_1.K_H.P_{CO2} \qquad \text{Equation 6-1}$$

The conservation of electroneutrality gives:

$$[H^+] = [OH^-] + [HCO_3^-] + 2\,[CO_3^{2-}]$$

Since we are in acidic conditions, $[OH^-]$ can be neglected. The pH is always largely lower than pK_{a2} so that $[CO_3^{2-}]$ is always negligible with respect to $[HCO_3^-]$. With these assumptions, the previous equation can be simplified:

$$[H^+] = [HCO_3^-]$$

And the equation 6-1 can be further developed in a relation that directly links the CO_2 partial pressure to the concentration of the ion HCO_3^-:

$$[HCO_3^-]^2 = K_1.K_H.P_{CO2}$$
$$[HCO_3^-] = [H^+] = \sqrt{K_1.K_H.P_{CO2}} \qquad \text{Equation 6-2}$$

Figure 6-1 illustrates the predicted $[HCO_3^-]$ in solution as a function of the pressure, using equation 6-2. In this model, increasing the pressure from 1 to 10 bar only increase the $[HCO_3^-]$ from 0.12 to 0.38 mM, which is a multiplication factor of 3.16 (equal to $\sqrt{10}$).

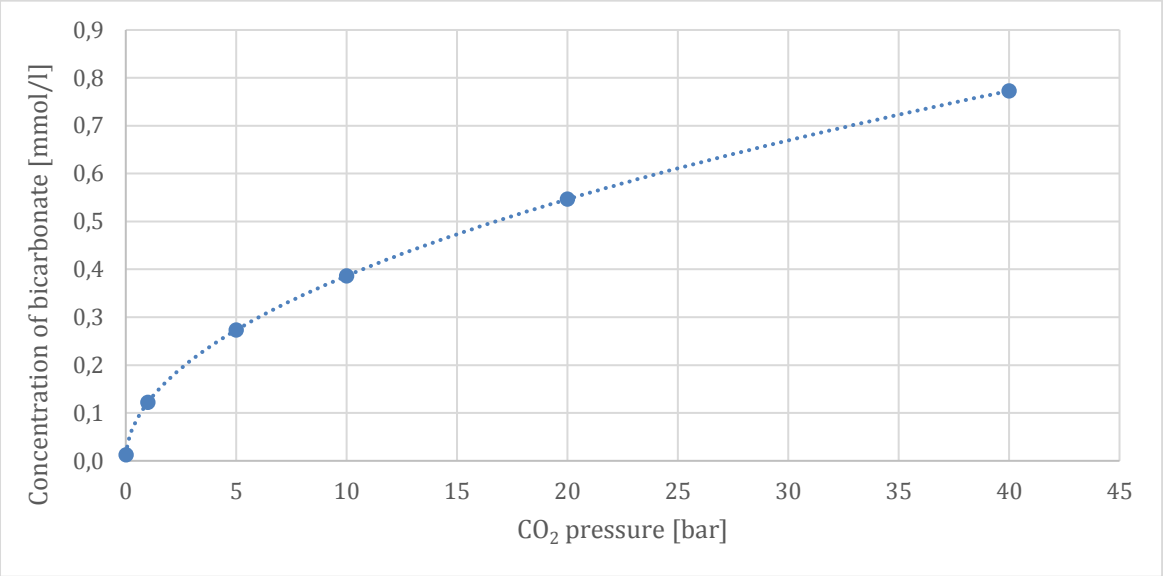

Figure 6-1: Predicted concentration of bicarbonate as a function of the CO_2 pressure in an ideal system at 25°C.

The equation 6-2 can be further developed to estimate the pH of the ideal aqueous system, by applicating a logarithmic relation on the concentration of bicarbonate, equivalent to concentration in protons:

$$pH = -\log(\sqrt{K_1 . K_H . P_{CO2}}) \qquad \text{Equation 6-3}$$

The Figure 6-2 illustrates that predictive model. The first point of the graph corresponds to a CO_2 pressure of 0.00035 bar, a value of the actual CO_2 concentration in the atmosphere (Collatz et al., 1998). It is expected that for a saturated distilled water, reflecting the idealized system, the pH is around 5.5 (Youmans, 1972). Using equation 6-3 to estimate pH at atmospheric CO_2 partial pressure, we find that pH = 5.64, in agreement with the expected value.

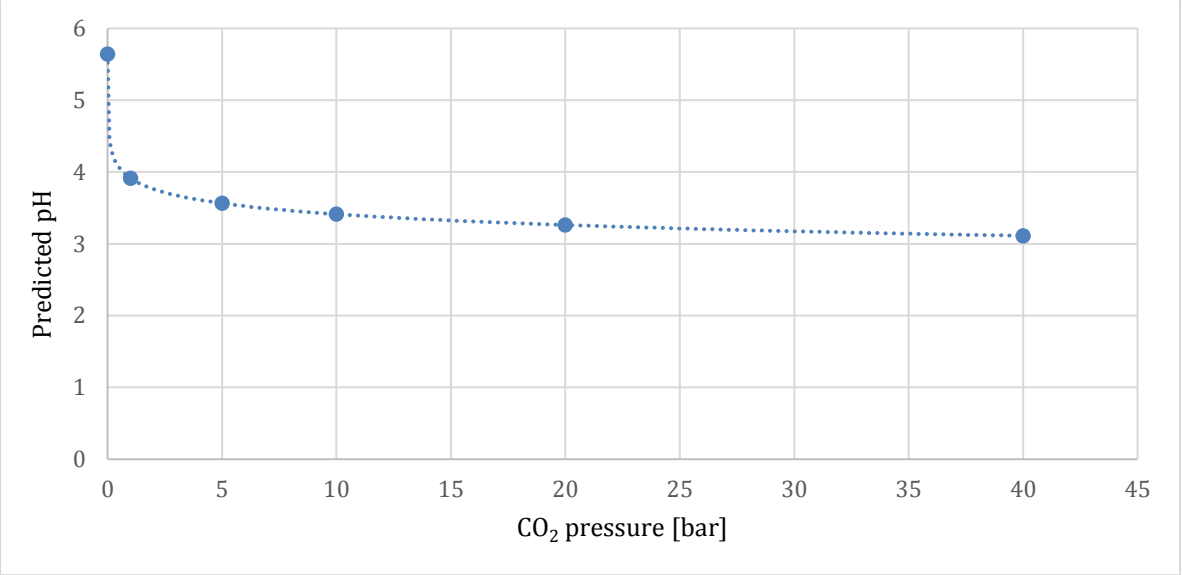

Figure 6-2: Predicted pH of an aqueous solution as a function of the CO_2 pressure in an ideal system at 25°C.

6.2.4 Thermodynamics of ion exchange

For the sake of simplification, as HBu and HAc have similar pK_a, adsorption and desorption profiles, they can be considered as one molecule for the relation of selectivity: $[Ac^-] + [Bu^-] = [VFA^-]$. The selectivity coefficient is given by:

$$K_{HCO3-}^{VFA-} = \frac{[\overline{VFA^-}]}{[\overline{HCO3^-}]} \frac{[HCO3^-]}{[VFA^-]} \qquad \text{Equation 6-4}$$

Where K_{VFA-}^{HCO3-} is the selectivity coefficient for the exchange between the two anions, the terms with a bar are adsorbed on the resin and the terms without bar are in the solution. This relation gives a preview of the effect of HCO_3^- on the desorption. We also know the relative selectivity of the anions for the strong base resin (Table 6-2).

Table 6-2: Relative selectivity of anions for resin with type 1 quaternary ammonium (De Dardel, 2015).

Anion	Relative selectivity
OH^- (reference)	1
HCO_3^-	6
CH_3COO^-	3.2

As a consequence, $K_{HCO3-}^{CH3COO-}$ = 3.2/6 = 0.53

Assuming that VFAs, including butyrate, have the same relative selectivity as acetate, the selectivity coefficient can be extended to VFAs as term K_{HCO3-}^{VFA-} =0.53.

This selectivity is not in favor of VFA desorption by HCO_3^- under equimolar conditions. However, equation 6-4 can be further developed in a relation where the real concentrations are taken into account. The formula is developed in Annex 3 to isolate as only variables [HVFA] and the CO_2 pressure. The final relation is:

$$\frac{K_{HCO3-}^{VFA-}.K_a}{K_H K_1 P_{CO2}}[HVFA]^2 + [HVFA] - VFA_T = 0$$

This second-degree equation is solved like:

$$[HVFA] = \frac{-1 \pm \sqrt{1 - 4.a.VFA_T}}{2a}$$

Where "a" represents the coefficient of the term $[HVFA]^2$. This relation is used to predict the molar concentration of HVFA desorbed in the Parr under a CO_2 pressure (all VFAs in solution are protonated, see Annex 3 for explanation). The predicted results are compared with the results obtained during the experiments in Figure 6-3.

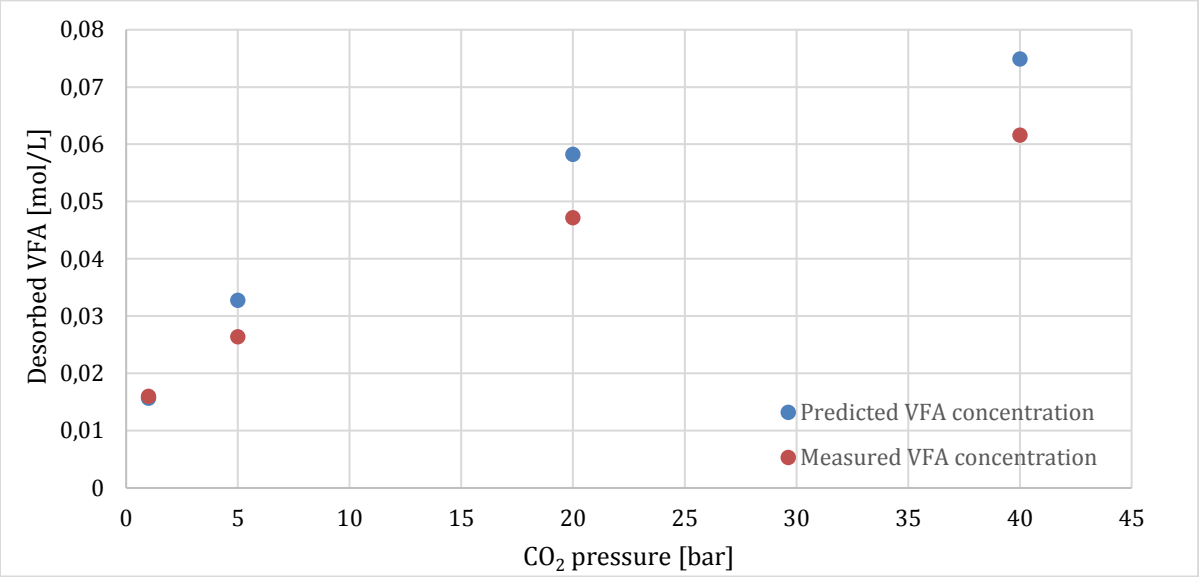

Figure 6-3: Plot of the measured and predicted CO_2-mediated VFA desorption with a strong base resin.

Figure 6.3 shows a good consistency between predicted and observed trends. The slight difference in absolute values can be attributed to uncertainties in the values used, especially the selectivity coefficient that was taken from the literature for another resin. Selectivity for the anions is function of the reticulation of the resin (De Dardel, 2015). Both the model and the data suggest that the desorbed molar fraction is proportional to the square root of the CO_2 pressure.

6.2.5 Influence of temperature

In our experiments (Figure 5-8), we observe no significant influence of temperature on the VFA desorption by CO_2. However, the equilibrium constants mentioned before are all dependent of temperature, so we could expect to observe a different desorption profile between the 70°C experiment and the 110°C experiment. One of the possible reasons why there is no observable effect is that temperature has opposite effects on the formation of HCO_3^-. The influence of temperature was further analyzed.

As shown in Figure 6-4, the equilibrium constant K_1 increases marginally from 0°C until reaching 50°C, and from 50°C K_1 starts to decrease. In other words, 50°C is the ideal value for the deprotonation of carbonic acid. Higher or smaller temperatures lead to a smaller equilibrium constant.

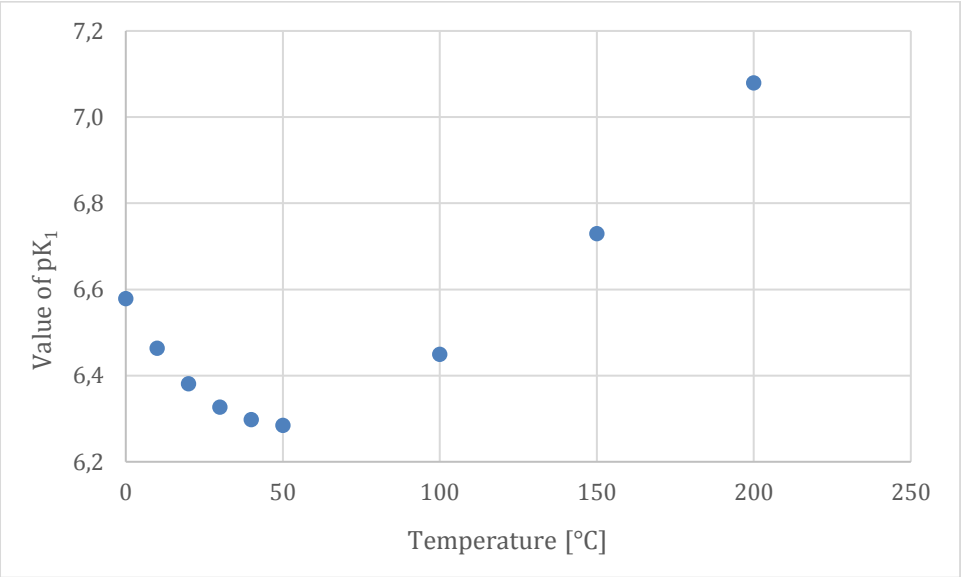

Figure 6-4: Plot of the pK_1 in function of temperature. Values from Butler (1991) are in Annex 2.

The constant K_H decreases with temperature, thus the solubility of CO_2 in water decreases when temperature increases *(*Aissa et al., 2015*)*. K_H decreases from $10^{-1.41}$ at 20°C to $10^{-1.99}$ at 100°C *(*Butler, 1991*)*. The equation that estimates $[HCO_3^-]$ as a function of P_{CO2} can be used for 20°C and 100°C in an ideal system at 40 bar, which equals 39.477atm, and we obtain (for values, see annex 2):

For 20°C: $[HCO_3^-] = \sqrt{10^{-1.41} * 10^{-6.381} * 39{,}477} = 8.045 * 10^{-4}\ \mathrm{mol/L}$

For 100°C: $[HCO_3^-] = \sqrt{10^{-1.99} * 10^{-6.45} * 39{,}477} = 3.81 * 10^{-4}\ \mathrm{mol/L}$

The Figure 6-5 further indicates the relation between bicarbonate concentration and temperature between 0 and 200°C using equation 6-2.

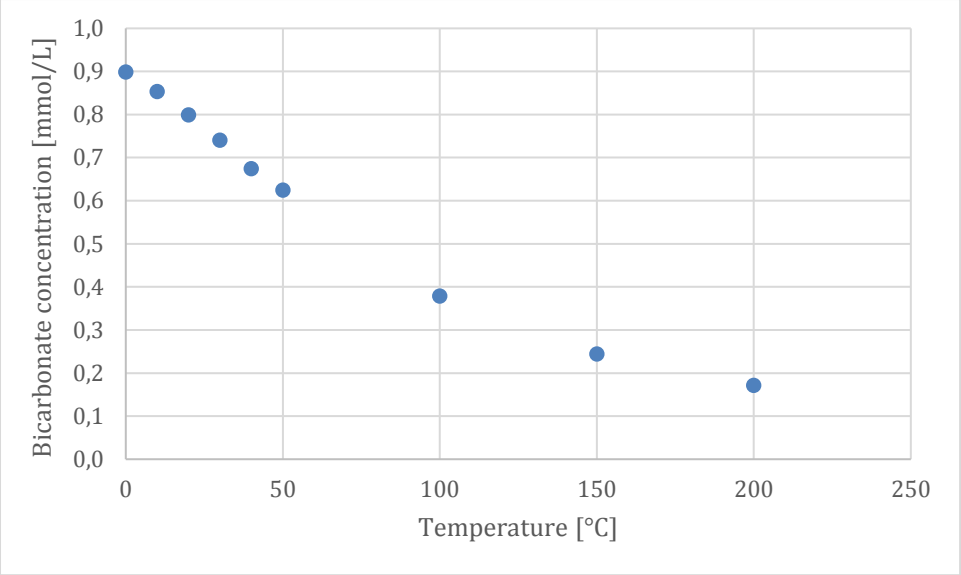

Figure 6-5: Plot of the predicted bicarbonate concentration in function of the temperature at 40 bar in an ideal system.

Unfortunately, we don't have the information on the evolution of the selectivity coefficients with temperature. Changes in selectivity coefficient with temperature can potentially have an opposite effect to the decrease of bicarbonate concentration with increasing temperature (Figure 6-5) and explain why temperature changes in the tested range (70 – 110°C) had no observable influence on desorption.

6.2.6 Possibility of using a carbonate salt

Since the key anion for the VFA desorption is considered to be HCO_3^-, it is interesting to investigate all the possibilities for obtaining this anion in solution. Setting a high CO_2 pressure in the system is not the only way to produce a carbonate-rich solution. Very few information is available in literature on the desorption of carboxylic acids with carbonate salts, but it can be supposed that these salts, such as $NaHCO_3$, $CaCO_3$ or K_2CO_3 behave very differently, and if their use for desorption was effective, it would probably result in the formation of carboxylate salts, that are much less interesting than carboxylic acids.

6.3 Thermal desorption

Even if the fraction of HBu recovered during thermal desorption, 0.085 $HBu_{desorbed-thermally}/HBu_{initial}$ (Figure 5-13, p59) was small, the results also suggest that a prolonged desorption time could lead in enhanced recovery. The experimental setup that we have built is a setup where the equilibrium is continuously shifted towards the vaporization of VFAs, because the VFA vapors are continuously flushed out of the system.

Despite the weak results obtained, the process still has some very strong advantages. The thermal desorption was already investigated by Reyhanitash et al (2017). According to them, under normal fermentation conditions the only nitrogen-based adsorbents capable of recovering carboxylate anions through anion exchange are the quaternary ammonium-based adsorbents, but the ion exchange makes regeneration of the adsorbent impossible without another ion exchange with the mineral acid of the replaced anion of the ammonium. This requires an extra process with the use of a chemical and the VFA obtained after adsorbent regeneration is not pure, but in an aqueous solution containing a significant mineral impurity. It is the reason why they performed experiments with a non-ionic resin. VFA adsorption is still possible because the molecules interact with the non-ionic adsorbent through the hydrogen bond−π interactions between their carboxyl groups and the adsorbent aromatic rings, and the hydrophobic interactions between the hydrocarbon chain and the adsorbent surface. Thus, the main idea was that direct desorption of the adsorbed VFAs by nitrogen-stripping could be an alternative regeneration method, and after condensation of the desorbed VFAs, it may yield highly concentrated VFAs. They used a non-ionic resin that was polystyrene-divinylbenzene-based, and observed a very high selectivity for the VFAs from a complex model solution that also contained chloride, sulfate, and phosphate salts. They found that regeneration of the non-ionic resin with a short water-wash stage followed by a temperature-profiled evaporation enabled fractionation of VFAs, and butyric acid was obtained with purities of up to 91 wt % starting with a feed concentration of only 0.25 wt %. The weakness of this study relies on the temperature profiles that they used. Because the temperatures reached are 200°C for the mentioned butyric acid recovery, there is a risk that the resin degrades.

A study (Li et al., 2001) observed that there is a linear relationship between the peak temperature of thermal decomposition and crosslinking degree of the copolymer matrix. According to them, if the crosslinking degree is less than 15%, porous polystyrene-type beads show a glass transition[2] at a temperature higher than 120°C and melting at a temperature higher than 270°C so that their physical structure is not stable above 120°C. When the crosslinking degree is higher than 30%, the beads undergo two chemical reactions respectively at the temperature of above 120 and of 200 - 300°C owing to the presence of double bonds so that their chemical structure is not stable above 120°C. Consequently, only 30% crosslinked polystyrene beads demonstrated perfect physical and chemical stability at high temperature before the thermal decomposition took place above 350°C.

Reyhanitash et al. (2017) used the Lewatit (VP OC 1064 MD PH), and according to the furnisher, the temperature of application is situated between -20 and 120°C. The degree of crosslinking is not specified but there are two situations: or the beads are 30% crosslinked polystyrene, or they are not, what would be the privileged situation

[2] Temperature region where the polymer transitions from a hard, glassy material to a soft, rubbery material (Li et al., 2001).

since an operating temperature lower than 120°C is recommended. Thus, it is possible that the resin after prolonged exposition to high temperatures, becomes degraded thermally, what seriously complicates the industrial applications of the process.

Besides the fact that the resin used in our experiments is different (Sepabeads SP207), one of the major changes is that we did not exceed the maximum recommended operating temperature, which was 130°C.

6.4 Lost fraction

It was surprising to observe that in some experiments, the “not recovered fraction” reached significant values. Since the primary purpose of most experiments was to test the desorption processes, it was not a real problem. The origin of the not recovered fraction can be explained by two hypotheses:

1. Some part of the lost fractions is considered to be a “real loss”. During the first experiments, it is highly suspected that some VFAs desorbed with CO_2 or with a thermal method have not been recovered correctly. Indeed, when sparging the VFA vapors in a NaOH solution, it is possible that a part of these vapors did not have time for the acid-base reaction to be complete (HAc +NaOH → NaAc + H_2O), what means that a part of the VFAs could have reached the air of the laboratory without being reacted in there salt form in the NaOH solution. Later experiments have been conducted with designs where the possible origins of real loss were reduced. The not recovered fraction was diminished but not totally.

2. As we used new resins, some functional sites could adsorb the VFAs more strongly than others, in a way that a small fraction of the VFAs would be irreversibly adsorbed. This hypothesis can be further verified by repeating cycles of adsorption/desorption on the same resin sample. If our hypothesis is correct, the “not recovered fraction” should be only observable for the first adsorption/desorption, and not for the following cycles.

6.5 Integration of resins with an acidogenic fermentation process

6.5.1 Acidity of fermentation broth

Acetic and butyric acid have low pK_a values (4.75 and 4.81 respectively), as well as much of the other VFAs produced during fermentation (López-Garzón and Straathof, 2014). During their production, the medium is thus progressively acidified and that can be a reason for decreased VFA production. Three classical solutions exist:

- Use an acid-tolerant producing strain that will continue to produce VFAs until the acid stress is too strong. In the context of a mixed bacterial fermentation, this solution is not applicable.

- Use of a base to maintain a neutral pH. This has as consequence to transform the carboxylic acids into carboxylate salts.
- Remove the carboxylic acid in-situ by a physical method with the result that acid stress diminishes and that fermentation can continue.

Unless exploiting the first solution, the recovery is performed by using a fermentation broth with a pH that is not strongly acid. This means that the acidic conditions, that have been demonstrated to cause better adsorption on the anion exchange resins, are not met in fermentation broths with maximized VFA production. As mentioned by Roque (1994), to maximize the adsorption capacity of a weak-base sorbant, the feed stream must be acidified first. But acidification by adding a mineral acid to the broth is not desirable because the mineral acid competes with lactic acid for the sorption sites. One solution to this problem is using a cation exchange resin loaded with H^+, it will acidify the broth without inducing competing acids.

6.5.2 Competitive adsorption on resins

Real fermentation broths contain a large number of compounds, including sugars and salts remaining from the fermentation feed, fermentation by-products such as proteins and undesired carboxylic acids, and debris derived from the cell lysis and/or decay (López-Garzón and Straathof, 2014). A synthetic solution containing mineral acids and VFAs mimicking fermented wastewater (Reyhanitash et al., 2017) showed that chloride, sulfate, and phosphate adsorption on the amine-functionalized adsorbents were very high, even exceeding capacities of 200 g/kg dry adsorbent for H_3PO_4. The major drawback of mineral acid coadsorption was the remarkably lower capacity of the amine-based adsorbents for the VFAs. According to them, the mineral acid coadsorption by the amine-based adsorbents was so large that using idealized model solutions solely containing the VFAs may well lead to completely different findings. Besides losing capacity for the VFAs, mineral acid coadsorption may result in problematic adsorbent regeneration, and, if not removed, the mineral acids may accumulate on the adsorbent over time leading to a reduced adsorbent lifetime.

6.6 Coupling CO_2 desorption with esterification

Similar to the idea of desorbing VFAs with CO_2, Cabrera-Rodríguez et al. (2017) focused on the possibility of desorbing carboxylates including acetate with CO_2 and methanol. In their study, they used an anion exchange resin (strong base resin, type 1) and searched to produce a methyl ester. The alcohol-CO_2 system is thought to cause this reaction:

$$Q^+Ac^- + MeOH + CO_2 \rightarrow Q^+HCO_3^- + MeAc$$

A major advantage of coupling the CO_2 desorption with an esterification is that equilibrium is shifted during the desorption step to the product side by the consumption of acetic acid during esterification.

They succeeded at producing 1.03 ± 0.07 mol methyl acetate/ mol of $acetate_{adsorbed}$, corresponding to a complete conversion. The conditions were 5 bar of CO_2 and 60 °C, with 1.7 %w/w dry resin Dowex MSA/ methanol, methanol being in large excess. The excess of methanol improves the reaction. However, it decreases the overall productivity of the process and increases costs of ester recovery by methods such as distillation. This might compromise the process feasibility, especially for low-priced products such as methyl acetate.

The proposed process works, with a lower yield, for other carboxylates (lactate and succinate) and alcohols (ethanol).

Unfortunately, the proposed process produces a binary mixture of methanol and methyl acetate (considering only acetic acid was adsorbed). By distillation, methyl acetate (boiling point = 56.3°C) and methanol (boiling point = 64.5°C) form a binary azeotrope boiling at 54°C and containing 81.3 wt % methyl acetate, 18.7 wt % methanol (Berg and Yeh, 1984). Instead, methyl acetate can be readily removed as overhead product from mixtures containing it and methanol by using extractive distillation in which the extractive distillation agent is a higher boiling oxygenated, nitrogenous and/or sulfur containing organic compound or a mixture of these. Still, the problem of an easy purification remains.

7. Conclusion and perspectives

In this research, we used amine-functionalized polystyrene-divinylbenzene-based exchangers, and a non-ionic bromine-functionalized material to investigate the adsorption/desorption cycle of VFAs as a process for recovery from fermentation broths.

For adsorption of VFAs with our experimental setup, kinetics studies showed that equilibrium was reached between the VFAs in solution and adsorbed on the resin within 15 minutes for the strongly basic resin and the nonionic resin, whereas the weakly basic resin necessitated one hour for equilibrium to be reached.

We demonstrated that, from the three initial pH values of model solutions, the most acidic, at pH=3 is the one whose VFAs show the highest adsorbed molar fraction for all resins tested. The pH has a strong impact on the adsorption of the VFAs.

Using the nonionic material, it was possible to adsorb preferentially butyric acid and to a lesser extent acetic acid. The adsorbed butyric acid could be partially desorbed by thermal desorption in an oven by stripping with CO_2. Desorption was directly linked to desorption time and after one hour no plateau was reached, signifying that a greater desorption time could yield in higher desorbed molar fractions of butyric acid.

CO_2-mediated desorption of VFA adsorbed on anion exchange resins was partially achieved by using pressures up to 40 bars in a closed system containing resins suspended in water. We studied the relation between the CO_2 pressure and the molar fraction desorbed, and we concluded that the VFA desorption is proportional to the square root of the CO_2 pressure. Acetic acid was systematically desorbed with a higher molar fraction than butyric acid. At 40 bar and with a strong anion exchanger, a fraction of 0.44 $HAc_{desorbed}/HAc_{initial}$ was reached.

Further experiments could be realized on CO_2-mediated desorption to investigate the possibility of applicating a second adsorption/desorption cycle on the resins, as one of the important points is to know if the resin will show the same performances after repeated cycles.

It will also be interesting to perform an adsorption/desorption cycle with a real fermentation broth, as one of the crucial questions is the amount of molecules that will be adsorbed and that are not targeted, since it is expected that other organic acids will interfere with the optimal adsorption of the VFAs.

8. Bibliography

Aissa, M.F.B., Bahloul, S., Monteau, J.-Y., Le-Bail, A., 2015. Effect of Temperature on the Solubility of CO_2 in Bread Dough. Int. J. Food Prop. 18, 1097–1109. https://doi.org/10.1080/10942910903176360

Andersen, S.J., Berton, J.K.E.T., Naert, P., Gildemyn, S., Rabaey, K., Stevens, C.V., 2016. Extraction and Esterification of Low-Titer Short-Chain Volatile Fatty Acids from Anaerobic Fermentation with Ionic Liquids. ChemSusChem 9, 2059–2063. https://doi.org/10.1002/cssc.201600473

Anonymous, 2017. Acetic Acid Production from Methanol - Cost Analysis - Acetic Acid E21A. Intratec Solutions. https://www.intratec.us/analysis/acetic-acid-e21a.

Baumann, I., Westermann, P., 2016. Microbial Production of Short Chain Fatty Acids from Lignocellulosic Biomass: Current Processes and Market. BioMed Res. Int. 2016, 1–15. https://doi.org/10.1155/2016/8469357

Bengtsson, S., Hallquist, J., Werker, A., Welander, T., 2008. Acidogenic fermentation of industrial wastewaters: Effects of chemostat retention time and pH on volatile fatty acids production. Biochem. Eng. J. 40, 492–499. https://doi.org/10.1016/j.bej.2008.02.004

Berg, L., Yeh, A.-I., 1987. Dehydration of propanoic acid by extractive distillation. US patent n° 4670105A.

Berg, L., Yeh, A.-I., 1984. The separation of methyl acetate from methanol by extractive distillation. Chem. Eng. Commun. 30, 113–117. https://doi.org/10.1080/00986448408911119

Bhatia, S.K., Yang, Y.-H., 2017. Microbial production of volatile fatty acids: current status and future perspectives. Rev. Environ. Sci. Biotechnol. 16, 327–345. https://doi.org/10.1007/s11157-017-9431-4

Burdock, G.A., 1997. Encyclopedia of food and color additives. CRC Press, Boca Raton. Pp 13, 359.

Butler, J.N., 1991. Carbon dioxide equilibria and their applications. Lewis Publ, Chelsea, Mich. Pp 15-20.

Cabrera-Rodríguez, C.I., Paltrinieri, L., de Smet, L.C.P.M., van der Wielen, L.A.M., Straathof, A.J.J., 2017. Recovery and esterification of aqueous carboxylates by using CO_2 -expanded alcohols with anion exchange. Green Chem. 19, 729–738. https://doi.org/10.1039/C6GC01391K

Cheryan, M., Parekh, S., Shah, M., Witjitra, K., 1997. Production of Acetic Acid by Clostridium thermoaceticum, in: Advances in Applied Microbiology. Elsevier, pp. 1–33. https://doi.org/10.1016/S0065-2164(08)70221-1

Collatz, G.J., Berry, J.A., Clark, J.S., 1998. Effects of climate and atmospheric CO 2 partial pressure on the global distribution of C 4 grasses: present, past, and future. Oecologia 114, 441–454. https://doi.org/10.1007/s004420050468

Coma, M., Martinez-Hernandez, E., Abeln, F., Raikova, S., Donnelly, J., Arnot, T.C., Allen, M.J., Hong, D.D., Chuck, C.J., 2017. Organic waste as a sustainable feedstock for platform chemicals. Faraday Discuss. 202, 175–195. https://doi.org/10.1039/C7FD00070G

de Bruyn, H., 1999. The emulsion polymerization of vinyl acetate. PhD Thesis. University of Sydney. Pp 1. https://ses.library.usyd.edu.au/bitstream/2123/381/3/.

De Dardel, F., 2015. Échange d'ions- Principes de base. Techniques de l'ingénieur. Vol J2783, 1-19.

Dwidar, M., Park, J.-Y., Mitchell, R.J., Sang, B.-I., 2012. The Future of Butyric Acid in Industry. Sci. World J. 2012, 1–10. https://doi.org/10.1100/2012/471417

Eda, S., Kumari, A., Thella, P.K., Satyavathi, B., Rajarathinam, P., 2017. Recovery of volatile fatty acids by reactive extraction using tri- *n* -octylamine and tri-butyl phosphate in different solvents: Equilibrium studies, pH and temperature effect, and optimization

using multivariate taguchi approach. Can. J. Chem. Eng. 95, 1373–1387. https://doi.org/10.1002/cjce.22803
Eggeman, T., Verser, D., 2005. Recovery of Organic Acids from Fermentation Broths, in: Davison, B.H., Evans, B.R., Finkelstein, M., McMillan, J.D. (Eds.), Twenty-Sixth Symposium on Biotechnology for Fuels and Chemicals. Humana Press, Totowa, NJ, pp. 605–618. https://doi.org/10.1007/978-1-59259-991-2_52
Ehsanipour, M., Suko, A.V., Bura, R., 2016. Fermentation of lignocellulosic sugars to acetic acid by Moorella thermoacetica. J. Ind. Microbiol. Biotechnol. 43, 807–816. https://doi.org/10.1007/s10295-016-1756-4
Gangadwala, J., Radulescu, G., Kienle, A., Steyer, F., Sundmacher, K., 2008. New processes for recovery of acetic acid from waste water. Clean Technol. Environ. Policy 10, 245–254. https://doi.org/10.1007/s10098-007-0101-z
Hábová, V., Melzoch, K., Rychtera, M., Sekavová, B., 2004. Electrodialysis as a useful technique for lactic acid separation from a model solution and a fermentation broth. Desalination 162, 361–372. https://doi.org/10.1016/S0011-9164(04)00070-0
Harland, C.E., 1994. Ion-exchange: theory and practice, 2nd ed. ed. Royal Society of Chemistry, London. Pp 39-48.
Jang, Y.-S., Im, J.A., Choi, S.Y., Lee, J.I., Lee, S.Y., 2014. Metabolic engineering of Clostridium acetobutylicum for butyric acid production with high butyric acid selectivity. Metab. Eng. 23, 165–174. https://doi.org/10.1016/j.ymben.2014.03.004
Jantasee, S., Kienberger, M., Mungma, N., Siebenhofer, M., 2017. Potential and assessment of lactic acid production and isolation - a review: Potential and assessment of lactic acid production. J. Chem. Technol. Biotechnol. 92, 2885–2893. https://doi.org/10.1002/jctb.5237
Jha, ajay kumar, Li, J., Yuan, Y., Baral, N., Ai, B., 2014. A Review on Bio-butyric Acid Production and its Optimization. Int. J. Agric. Biol. 1019–1024.
Jones, R.J., Massanet-Nicolau, J., Guwy, A., Premier, G.C., Dinsdale, R.M., Reilly, M., 2015. Removal and recovery of inhibitory volatile fatty acids from mixed acid fermentations by conventional electrodialysis. Bioresour. Technol. 189, 279–284. https://doi.org/10.1016/j.biortech.2015.04.001
Komesu, A., Wolf Maciel, M.R., Maciel Filho, R., 2017a. Separation and Purification Technologies for Lactic Acid – A Brief Review. BioResources 12. https://doi.org/10.15376/biores.12.3.6885-6901
Komesu, A., Wolf Maciel, M.R., Rocha de Oliveira, J.A., da Silva Martins, L.H., Maciel Filho, R., 2017b. Purification of Lactic Acid Produced by Fermentation: Focus on Non-traditional Distillation Processes. Sep. Purif. Rev. 46, 241–254. https://doi.org/10.1080/15422119.2016.1260034
Kun, K.A., Kunin, R., 1967. The pore structure of macroreticular ion exchange resins. J. Polym. Sci. Part C Polym. Symp. 16, 1457–1469. https://doi.org/10.1002/polc.5070160323
Li, Q.-Z., Jiang, X.-L., Feng, X.-J., Wang, J.-M., Sun, C., Zhang, H.-B., Xian, M., Liu, H.-Z., 2016. Recovery Processes of Organic Acids from Fermentation Broths in the Biomass-Based Industry. J. Microbiol. Biotechnol. 26, 1–8. https://doi.org/10.4014/jmb.1505.05049
Li, Y., Fan, Y., Ma, J., 2001. Thermal, physical and chemical stability of porous polystyrene-type beads with different degrees of crosslinking. Polym. Degrad. Stab. 73, 163–167. https://doi.org/10.1016/S0141-3910(01)00083-0
López-Garzón, C.S., Straathof, A.J.J., 2014. Recovery of carboxylic acids produced by fermentation. Biotechnol. Adv. 32, 873–904. https://doi.org/10.1016/j.biotechadv.2014.04.002
Miller, C., Fosmer, A., Rush, B., McMullin, T., Beacom, D., Suominen, P., 2011. Industrial Production of Lactic Acid, in: Comprehensive Biotechnology. Elsevier, pp. 179–188. https://doi.org/10.1016/B978-0-08-088504-9.00177-X

Morse, J.W., Mackenzie, F.T. (Eds.), 1990. Chapter 1 The CO2-Carbonic Acid System and Solution Chemistry, in: Geochemistry of Sedimentary Carbonates, Developments in Sedimentology. Elsevier, pp. 1–38. https://doi.org/10.1016/S0070-4571(08)70330-3
Murali, N., Srinivas, K., Ahring, B.K., 2017. Biochemical Production and Separation of Carboxylic Acids for Biorefinery Applications. Fermentation 3, 22. https://doi.org/10.3390/fermentation3020022
Ndaba, B., Chiyanzu, I., Marx, S., 2015. n-Butanol derived from biochemical and chemical routes: A review. Biotechnol. Rep. 8, 1–9. https://doi.org/10.1016/j.btre.2015.08.001
Oliveira, F.S., Araújo, J.M.M., Ferreira, R., Rebelo, L.P.N., Marrucho, I.M., 2012. Extraction of l-lactic, l-malic, and succinic acids using phosphonium-based ionic liquids. Sep. Purif. Technol. 85, 137–146. https://doi.org/10.1016/j.seppur.2011.10.002
Padhiyar, T., Thakore, S., 2013. Recovery of Acetic Acid From Effluent via Freeze Crystallization. Int. J. Sci. Eng. Technol. Vol. 2 Issue 4 PP 211-215.
Pal, P., Nayak, J., 2017. Acetic Acid Production and Purification: Critical Review Towards Process Intensification. Sep. Purif. Rev. 46, 44–61. https://doi.org/10.1080/15422119.2016.1185017
Patil, D.K., Kulkarni, B., 2014. Review of Recovery Methods for Acetic Acid from Industrial Waste Streams by Reactive Distillation. J. Water Pollut. Purif. Res. 1, 1–6.
Paudel, A., 2015. Liquid CO2 and CO2-expanded methanol for lipid extraction from microalgae. Thesis. Queen's University Kingston, Ontario, Canada.
Peng, C., Crawshaw, J.P., Maitland, G.C., Martin Trusler, J.P., Vega-Maza, D., 2013. The pH of CO2-saturated water at temperatures between 308K and 423K at pressures up to 15MPa. J. Supercrit. Fluids 82, 129–137. https://doi.org/10.1016/j.supflu.2013.07.001
Ponnampalam, E., 1999. Purification of organic acids using anion exchange chromatography. Patent US09623253.
Raspor, P., Goranovič, D., 2008. Biotechnological Applications of Acetic Acid Bacteria. Crit. Rev. Biotechnol. 28, 101–124. https://doi.org/10.1080/07388550802046749
Rebecchi, S., Pinelli, D., Bertin, L., Zama, F., Fava, F., Frascari, D., 2016. Volatile fatty acids recovery from the effluent of an acidogenic digestion process fed with grape pomace by adsorption on ion exchange resins. Chem. Eng. J. 306, 629–639. https://doi.org/10.1016/j.cej.2016.07.101
Reyhanitash, E., Kersten, S.R.A., Schuur, B., 2017. Recovery of Volatile Fatty Acids from Fermented Wastewater by Adsorption. ACS Sustain. Chem. Eng. 5, 9176–9184. https://doi.org/10.1021/acssuschemeng.7b02095
Reyhanitash, E., Zaalberg, B., IJmker, H.M., Kersten, S.R.A., Schuur, B., 2015. CO2-enhanced extraction of acetic acid from fermented wastewater. Green Chem. 17, 4393–4400. https://doi.org/10.1039/C5GC01061F
Reyhanitash, E., Zaalberg, B., Kersten, S.R.A., Schuur, B., 2016. Extraction of volatile fatty acids from fermented wastewater. Sep. Purif. Technol. 161, 61–68. https://doi.org/10.1016/j.seppur.2016.01.037
Rocha, M.A.A., Raeissi, S., Hage, P., Weggemans, W.M.A., van Spronsen, J., Peters, C.J., Kroon, M.C., 2017. Recovery of volatile fatty acids from water using medium-chain fatty acids and a cosolvent. Chem. Eng. Sci. 165, 74–80. https://doi.org/10.1016/j.ces.2017.02.014
Roque Lagman, E., 1994. Recovery and purification of lactic acid from fermentation broth by adsorption. PhD thesis. Iowa State University. Ames, Iowa. Pp 66-76.
Schuchmann, K., Müller, V., 2016. Energetics and Application of Heterotrophy in Acetogenic Bacteria. Appl. Environ. Microbiol. 82, 4056–4069. https://doi.org/10.1128/AEM.00882-16
Serras-Pereira, J., Aleiferis, P.G., Richardson, D., 2013. An Analysis of the Combustion Behavior of Ethanol, Butanol, *Iso* -Octane, Gasoline, and Methane in a Direct-Injection Spark-Ignition Research Engine. Combust. Sci. Technol. 185, 484–513. https://doi.org/10.1080/00102202.2012.728650

Silva, F., Serafim, L., Nadais, M., Arroja, L., Capela, I., 2013. Acidogenic Fermentation Towards Valorisation of Organic Waste Streams into Volatile Fatty Acids. Chem. Biochem. Eng. Q., 27 (4) 467–476. https://hrcak.srce.hr/112368.
Stefánsson, A., Bénézeth, P., Schott, J., 2013. Carbonic acid ionization and the stability of sodium bicarbonate and carbonate ion pairs to 200°C – A potentiometric and spectrophotometric study. Geochim. Cosmochim. Acta 120, 600–611. https://doi.org/10.1016/j.gca.2013.04.023
Sun, X., Wang, Q., Zhao, W., Ma, H., Sakata, K., 2006. Extraction and purification of lactic acid from fermentation broth by esterification and hydrolysis method. Sep. Purif. Technol. 49, 43–48. https://doi.org/10.1016/j.seppur.2005.08.005
Tonova, K., 2017. State-of-the-Art Recovery of Fermentative Organic Acids by Ionic Liquids: An Overview. Hung. J. Ind. Chem. 45. https://doi.org/10.1515/hjic-2017-0019
Vaccari, G., y González-Vara, A.R., Campi, A.L., Dosi, E., Brigidi, P., Matteuzzi, D., 1993. Fermentative production of l-lactic acid by Lactobacillus casei DSM 20011 and product recovery using ion exchange resins. Appl. Microbiol. Biotechnol. 40, 23–27. https://doi.org/10.1007/BF00170423
Vidra, A., Németh, Á., 2017. Bio-produced Acetic Acid: A Review. Period. Polytech. Chem. Eng. https://doi.org/10.3311/PPch.11004
Volynets, B., Ein-Mozaffari, F., Dahman, Y., 2017. Biomass processing into ethanol: pretreatment, enzymatic hydrolysis, fermentation, rheology, and mixing. Green Process. Synth. 6, 1–22. https://doi.org/10.1515/gps-2016-0017
Wang, X., Conway, W., Burns, R., McCann, N., Maeder, M., 2010. Comprehensive Study of the Hydration and Dehydration Reactions of Carbon Dioxide in Aqueous Solution. J. Phys. Chem. A 114, 1734–1740. https://doi.org/10.1021/jp909019u
Wang, Y., Tashiro, Y., Sonomoto, K., 2015. Fermentative production of lactic acid from renewable materials: Recent achievements, prospects, and limits. J. Biosci. Bioeng. 119, 10–18. https://doi.org/10.1016/j.jbiosc.2014.06.003
Wheaton, R.M., Lefevre, L.J., 2000. Fundaments of ion exchange. Dowex ion exchange resins. Dow Chemical U.S.A. http://msdssearch.dow.com/PublishedLiteratureDOWCOM/dh_0032/0901b803800326ca.pdf
Yalkowsky, S.H., He, Y., Jain, P., 2010. Handbook of aqueous solubility data. CRC Press, Boca Raton. Pp 32, 118.
Youmans, H.L., 1972. Measurement of pH of distilled water. J. Chem. Educ. 49, 429. https://doi.org/10.1021/ed049p429
Yousuf, A., Bonk, F., Bastidas-Oyanedel, J.-R., Schmidt, J.E., 2016. Recovery of carboxylic acids produced during dark fermentation of food waste by adsorption on Amberlite IRA-67 and activated carbon. Bioresour. Technol. 217, 137–140. https://doi.org/10.1016/j.biortech.2016.02.035
Zaganiaris, E., 2011. Ion exchange resins and synthetic adsorbents. Books on Demand. Ion Exchange Resins and Synthetic Adsorbents in Food Processing. Pp 22-37.
Zeitsch, K.J., 2000. The chemistry and technology of furfural and its many by-products, Sugar series. Elsevier, Amsterdam ; New York.
Zhu, Y., Yang, S.-T., 2004. Effect of pH on metabolic pathway shift in fermentation of xylose by Clostridium tyrobutyricum. J. Biotechnol. 110, 143–157. https://doi.org/10.1016/j.jbiotec.2004.02.006

9. Annex

Annex 1: Name of various enzymes implicated in the metabolic pathways for VFAs (Bhatia and Yang, 2017).

Acetolactate synthase (alsS), keto-acid reductoisomerase (ilvc), dihydroxy acid dehydratase (ilvD), 2-keto acid decarboxylase (kivD), alcohol dehydrogenase (adh), 2-isopropylmalate synthase (leuA), isopropylmalate isomerase complex (leuCD), isopropylmalate dehydrogenase (leuB), aldehyde dehydrogenase (ald), aldehyde oxidoreductase (aor), phosphotransacetylase (pta), acetate kinase (ack), thiolase (thl), hydroxybutyryl-CoA dehydrogenase (hbd), crotonase (crt), butyryl-CoA dehydrogenase (bcd), phosphotransbutyrylase (ptb), butyrate kinase (bk), propionylCoA transferase (pct), lactate dehydrogenase (ldh), lactoyl-CoA dehydratase (lcdA), and acrylyl-CoA reductase (acul).

Annex 2: Equilibrium constants for CO_2 -carbonic acid system extrapolated to zero ionic strengh (Butler, 1991).

Temperature (°C)	pK_H^0 (mole/L·atm)	pK_{a1}^0 (mole/L)	pK_{a2}^0 (mole/L)	pK_w^0 $(mole/L)^2$
0	1.11	6.579	10.625	14.955
5	1.19	6.517	10.557	14.734
10	1.27	6.464	10.490	14.534
15	1.33	6.419	10.430	14.337
20	1.41	6.381	10.377	14.161
25	1.47	6.352	10.329	13.999
30	1.53	6.327	10.290	13.833
35	1.59	6.309	10.250	13.676
40	1.64	6.298	10.220	13.533
45	1.68	6.290	10.195	13.394
50	1.72	6.285	10.172	13.263
100	1.99	6.45	10.16	12.27
150	2.07	6.73	10.33	11.64
200	2.05	7.08	10.71	11.28

Annex 3: Development of the relation linking the CO_2 pressure to desorbed VFA.

The initial relation is the equilibrium between the species adsorbed and species in solution:

$$K_{HCO3-}^{VFA-} = \frac{[\overline{VFA^-}]}{[\overline{HCO3^-}]} \frac{[HCO3^-]}{[VFA^-]}$$ Equation A-1

The term $[HCO3^-]$ can be linked to the CO_2 pressure by:

$CO_2 + H_2O \leftrightharpoons H_2CO_3^*$ K_H

$H_2CO_3^* \leftrightharpoons H^+ + HCO_3^-$ K_1

$[HCO3^-] = (K_H.K_1.P_{CO2})/[H^+]$ Equation A-2

The term $[VFA^-]$ is linked to HVFA by the dissociation constant of the acid:

$HVFA \leftrightharpoons H^+ + VFA^-$ K_a

$[VFA^-] = (K_a.[HVFA])/[H^+]$ Equation A-3

The equations A-2 and A-3 can be inserted in equation A-1, resulting in:

$$K_{HCO3-}^{VFA-} = \frac{[\overline{VFA^-}]}{[\overline{HCO3^-}]} \frac{K_1 K_H P_{CO2}}{K_a [HVFA]}$$

After desorption, the pH was measured and situated between 3 and 3.6 for the experiments. In these acidic conditions, we can consider that $pH << pK_a$ of the VFAs. The only cations available for electroneutrality with the VFA^- are protons, no other cation is existent in solution. In such conditions, we consider that all VFAs in solution are protonated. This further leads to the simplification that, per liter, the amount of VFA adsorbed on the resins is equal to the total amount of VFAs ($[VFA_T]$, measured by the adsorption step) subtracted by the amount of VFAs in solution, protonated and noted [HVFA]:

$$[\overline{VFA^-}] = [VFA_T] - [HVFA]$$

And since we are in an ion exchange process, all the VFAs in solution have been exchanged with a bicarbonate. Theoretically, bicarbonate ions can also be adsorbed on functional sites where no VFA was bonded, but this case represents a small fraction of the total functional sites, as we discussed that maximum capacity is almost reached (6.1.2 Adsorption capacity of the resins). This leads to:

$$[\overline{HCO3^-}] = [HVFA]$$

We also know that the relative selectivity of the strong base resin is 6 for the species bicarbonate and 3.2 for the acetate. Assuming that butyrate has the same relative selectivity as acetate, the term K_{HCO3-}^{VFA-} can be calculated as:

$$K_{HCO3-}^{VFA-} = \frac{3,2}{6} = 0,53$$

The equilibrium relation can be written as:

$$K_{HCO3-}^{VFA-} = \frac{[VFA_T] - [HVFA]}{[HVFA]} \frac{K_1 K_H P_{CO2}}{K_a [HVFA]}$$

Re-arranging the terms leads to a second-degree equation:

$$\frac{K_{HCO3-}^{VFA-} . K_a}{K_H K_1 P_{CO2}} [HVFA]^2 + [HVFA] - VFA_T = 0$$

Annex 4: K_1 in function of temperature (Stefánsson et al., 2013).

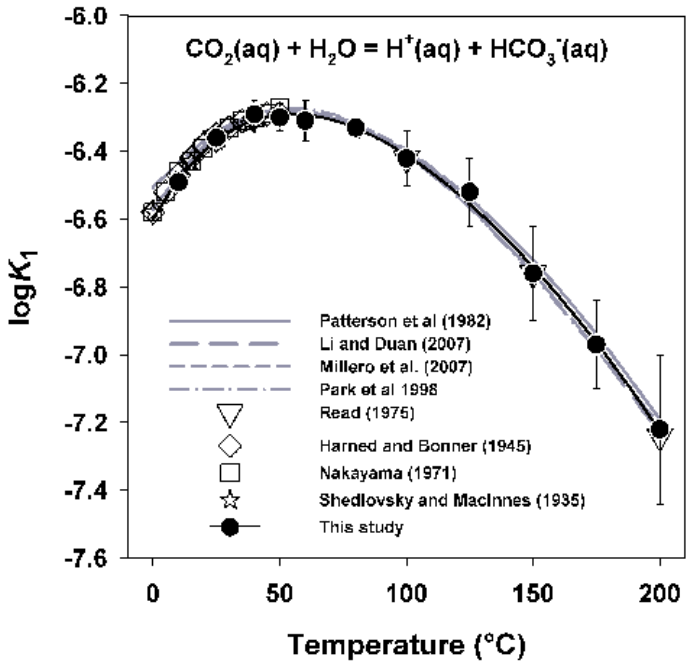

Extraction and purification of volatile fatty acids

Présenté par Alexis Struyf

Résumé This master thesis was realized in the Earth and Life Institute (ELI) in the cluster of Applied Microbiology. The aim of this research was to contribute to the development of a new process for the extraction and purification of volatile fatty acids, short-chain carboxylic acids that are produced during acidogenic fermentation. Volatile fatty acids find numerous uses in green chemistry, food and pharmaceutical industry. VFAs are conventionally produced by petrochemical pathways not sustainable nor environmental-friendly. Therefore, increasing attention has been given in the recovery of VFAs from microbial origin.

We investigated the potential of adsorption and desorption on ion exchange resins and non-ionic resin for the extraction and purification of VFAs from fermentation liquor. Our experiments were performed with model acetic and butyric acids aqueous solutions. One focus was to investigate CO_2-mediated desorption of VFAs, since CO_2 is cheap and available at production sites, and can be converted into carbonic acid, an interesting candidate for VFA desorption.

The VFAs from initially acidic solutions were more adsorbed than from more alkaline solutions, on all resins tested. Considering the initial amount of VFA in the model solution, fractions of more than 0.9 VFAs were adsorbed on the ion exchange resins in acidic conditions. Adsorption on the non-ionic resin was more selective for butyric acid. Adsorption equilibrium was reached within the first 15 minutes for the macroporous strong base ion exchange resin and nonionic resin, while it was reached within 60 minutes for the gel weak base exchange resin.

CO_2-mediated desorption was tested by using a reactor containing the resins suspended in water under a CO_2-pressure. Under 40 bars of CO_2 inside de the reactor and using a strong anion exchanger with a capacity equivalent to the VFA introduced, a molar fraction of 0.44 moles of acetic acid was desorbed by CO_2, per mole of acetic acid initially introduced. The VFAs desorption is proportional to the square root of the CO_2 pressure. Thermal desorption of the VFAs adsorbed on non-ionic resins was weak and desorbed butyric acid was proportional to the time of desorption.

The present research offers strong perspectives of CO_2-mediated desorption of VFAs, but it is too early to conclude on a possibility of large-scale application. Further investigation needs to be realized on the use of real fermentation broths and repeated adsorption/desorption cycles.

Keywords: Volatile fatty acids, recovery, ion exchange resin, carbon dioxide

Année académique 2017-2018